

**Proton Pumping in Cytochrome c Oxidase:
The Possible Role of Cu_A in
Redox Linkage**

Thesis by

Zhuyin Li

In Partial Fulfillment of the Requirements

for the Degree of

Doctor of Philosophy

California Institute of Technology
Pasadena, California

1992

(Submitted October 1, 1991)

ACKNOWLEDGEMENTS

I am very grateful to Professor Sunney Chan for his guidance and excellence in allowing me to grow at my own pace throughout the past three and half years. My appreciation is also extended to the Chan group members for their cooperation and discussion. I especially would like to thank Joel Morgan, who spent the whole day telling me the story of cytochrome c oxidase the day before his thesis examination. The story turned out to be the basis of my research at Caltech. Also I would like to thank Dr. Liang-Ping Pan for his work involved in Chapter II; Dr. Randy Larsen, Scott Ross, Siegfried Musser and Hoa Nguyen for spending their time on correcting my English; and to thank Qizhi He, Jian Lin, John Evans, Mingxing Li and Silvia Cavagnero for their friendship.

Most importantly, I thank my parents for their guidance and support, my husband for love and understanding and my son for brightening my life. I dedicate this thesis to them.

ABSTRACT

Cytochrome c oxidase is the terminal enzyme of cellular respiration. It catalyzes the reduction of dioxygen to water by ferrocycytochrome c. In addition, cytochrome c oxidase is an electrogenic proton pump capable of transporting up to four protons against the proton electrochemical gradient.

An extensive and accurate analysis of the Cu, Fe, Zn and Mg contents in bovine heart cytochrome c oxidase was carried out by direct current plasma atomic emission spectrophotometer. The results confirmed a stoichiometry of 5Cu/4Fe/2Zn/2Mg per dimer. Seven enzyme preparations treated by different methods were analyzed to examine the nature of Cu_x. The results obtained suggested that Cu_x may reside in subunit III and plays a structural role in enzyme dimerization.

*p*HMB-modification of cytochrome c oxidase and heat-treatment of the oxidase have previously been shown to have a profound effect on the dioxygen reduction and proton pumping activities of the enzyme. The intrinsic reduction potentials and the midpoint reduction potential of the "Cu_A" site in both of these modified oxidases have been measured under various conditions in order to clarify the intramolecular electron transfer pathways in these systems. The study reveals that the Cu_A intrinsic reduction potential decreases by almost

150 mV upon *p*HMB modification, whereas it increases by 100 mV upon heat treatment. In addition, the redox interactions between Cu_A and the remaining metal centers are perturbed upon Cu_A modification.

DCCD-modification and subunit III-depletion of cytochrome c oxidase decreased the observed H^+/e^- stoichiometry in proton pumping to 0.5 during enzyme turnover under coupled conditions. The effects of these treatments on the optical and EPR spectra, and the reduction potentials of Cu_A , have been examined. DCCD-modification distorts the Cu_A ligand structure, while subunit III-depletion destabilizes the Cu_A structure leading ultimately to the displacement of one of the cysteine ligands. The intrinsic reduction potential of Cu_A is not significantly altered in the two modified oxidases. However, the redox interaction between Cu_A and cytochrome a becomes dramatically different: in the absence of subunit III, this redox interaction is essentially eliminated, whereas in the DCCD-modified enzyme, it becomes highly anticooperative. The results of this study implicate Cu_A as a component of the proton pumping machinery of the enzyme, and suggest that subunit III plays an important allosteric role in communicating the redox changes at the Cu_A site to the proton translocating element(s) of the proton pumping machinery during turnover.

The strong magnetic interaction between Fe_{a3} and Cu_{B} in the resting form of cytochrome c oxidase is thought to be mediated by a bridging ligand. The identity of this bridging ligand has been proposed to be an imidazole from a histidine residue, cysteine thiolate sulphur, an oxygen from hydroxide or μ -oxo anions. However, recent EXAFS experiments on a sample of oxidase isolated and purified in Cl^- -free buffer solutions revealed no (S, Cl) scattering in Fe EXAFS of the resting oxidase, thus suggesting Cl^- . To confirm this finding, we have dialyzed samples of reduced oxidase against Cl^- -free buffer in the presence of chelex resin, and have examined the spectroscopic and ligand-binding properties of the reoxidized enzyme. The dialyzed /oxygenated oxidase exhibits rapid and homogeneous binding kinetics. Upon re-addition of Cl^- to the dialyzed/oxygenated oxidase, the CN^- binding slows down and becomes heterogeneous. The anions F^- , Cl^- and Br^- all exhibit notable effects on the Soret absorption of the dialyzed/oxygenated oxidase. Similarly the EPR spectra of Cl^- or Br^- -substituted oxidase are similar to native oxidase. Both F^- -substituted oxidase and dialyzed /oxygenated oxidase exhibit complex EPR spectra. On the basis of these experiments, we conclude that the bridging ligand must be Cl^- in resting cytochrome c oxidase.

TABLE OF CONTENTS

ACKNOWLEDGEMENTS	ii
ABSTRACT	iii
TABLE OF CONTENTS	vi
LIST OF TABLES AND FIGURES	viii
CHAPTER I :	
INTRODUCTION	1
STRUCTURE	3
PROTON PUMPING	7
THE ROLE OF SUBUNIT III IN PROTON PUMPING	14
REFERENCES	18
CHAPTER II:	
THE NATURE OF CU_x IN CYTOCHROME <u>C</u> OXIDASE	21
INTRODUCTION	22
MATERIALS AND METHODS	25
RESULTS	29
DISCUSSION	38
REFERENCES	41
CHAPTER III:	
THE EFFECTS OF pHMB-MODIFICATION AND HEAT-TREATMENT ON THE CU_A REDUCTION POTENTIAL OF CYTOCHROME <u>C</u> OXIDASE	43
INTRODUCTION	44
MATERIALS AND METHODS	47
RESULTS	80
DISCUSSION	85

REFERENCES	96
CHAPTER IV: THE EFFECTS OF DCCD-MODIFICATION AND SUBUNIT III-DEPLETION ON THE PROPERTIES OF CU_A IN BOVINE CYTOCHROME C OXIDASE	98
INTRODUCTION	99
MATERIALS AND METHODS	101
RESULTS	105
DISCUSSION	120
REFERENCES	125
CHAPTER V: CHLORIDE DEPLETION OF CYTOCHROME C OXIDASE	127
INTRODUCTION	128
MATERIALS AND METHODS	130
RESULTS AND DISCUSSION	133
CONCLUSIONS	149
REFERENCES	153
CHAPTER VI: CONCLUSION	155
APPENDIX	162

LIST OF TABLES AND FIGURES

CHAPTER I

Table 1.	Cytochrome c oxidase functions are changed upon Cu_A modification	13
Table 2.	Cytochrome c oxidase functions are changed upon subunit III modification	17
Figure 1.	Chan model for redox linkage based on Cu_A	11

CHAPTER II

Table 1.	Metal contents of cytochrome c oxidase treated by different methods	30
Table 2.	Metal affinity analysis of cytochrome c oxidase	32
Table 3.	Effects of different treatments on the topology and electron transfer activity of cytochrome c oxidase	33
Figure 1.	EPR spectra of Cu_A for native (A), monomeric (B), and fully reduced (C)	37

CHAPTER III

Table 1.	Redox mediators	58
Table 2.	Reduction potentials and interaction parameters estimated from potentiometric titrations of the pHMB-modified and the heat-treated cytochrome c oxidase	81
Figure 1.	EPR signal from the Cu_A site in cytochrome c oxidase	51
Figure 2.	Visible spectra of Cu_A -modified cytochrome c oxidase	53
Figure 3.	Near-IR absorption spectra and difference spectra of cytochrome c oxidase	56
Figure 4.	Redox titration of the Cu_A site in two Cu_A -modified cytochrome c oxidase monitored by the Cu_A EPR spectra at liquid N_2 temperature	61

Figure 5.	The relationship between intrinsic, midpoint, upper asymptotic, lower asymptotic potentials in the redox titration of a system with interacting redox centers	65
Figure 6.	Simulated Nernst plots for redox titration of a redox center (observed site) in redox interaction with a redox partner (interactant)	67
Figure 7.	The influence of the asymptotic potential differences between observed site and interactant on the midpoint potential of observed site	70
Figure 8.	Simulated Nernst plots for redox titration of a redox center (observed site) in redox interaction with multiple redox partners (interactant) in cytochrome c oxidase	75
Figure 9.	The influences of interaction potential on the upper asymptotic potential and the midpoint potential of observed site	78
Figure 10.	Nernst plots for the modified Cu_A -site of Fe_a pre-reduced pHMB-modified oxidase.	84
Figure 11.	Nernst plots for the modified Cu_A -site of Fe_{a3}/Cu_B pre-reduced pHMB-modified oxidase	87
Figure 12.	Nernst plots for the modified Cu_A -site of heat treated oxidase	89
Figure 13.	Proposed interaction schemes for the two modified oxidases examined in this study	93

CHAPTER IV

Table 1.	Redox parameters estimated from potentiometric titrations of the DCCD-modified and the subunit III-depleted cytochrome c oxidase	115
Figure 1.	Effects of DCCD-incubation on the near IR absorption of bovine cytochrome c oxidase	107
Figure 2.	Effect of subunit III depletion on the Near-IR absorption spectrum of bovine cytochrome	

	c oxidase	109
Figure 3.	EPR signal from the Cu _A site of native and DCCD-modified cytochrome c oxidase	111
Figure 4.	Effect of subunit III-depletion on the Cu _A EPR signal of bovine cytochrome c oxidase	113
Figure 5.	Near-IR absorption difference spectra obtained during a potentiostatic titration of Fe _{a3} /Cu _B pre-reduced DCCD-modified cytochrome c oxidase	117
Figure 6.	Nernst plot for the Cu _A site of Fe _{a3} /Cu _B pre-reduced DCCD-modified bovine cytochrome c oxidase	119
Figure 7.	Nernst plot for the Cu _A site of Fe _{a3} /Cu _B pre-reduced subunit III-depleted bovine cytochrome c oxidase	122

CHAPTER V

Table 1.	The UV-Visible spectral properties for cytochrome c oxidase	139
Table 2.	Rate constants for reaction of cytochrome c oxidase with cyanide	146
Figure 1.	Optical difference spectra between dialyzed /oxygenated enzyme and resting enzyme	137
Figure 2.	EPR spectra of cytochrome c oxidase under different conditions	141
Figure 3.	The energy level diagrams for the Fe _{a3} -Cu _B center in cytochrome c oxidase	144
Figure 4.	Influence of Cl ⁻ concentration on the kinetics of cyanide binding to dialyzed /oxygenated oxidase	148
Figure 5.	Proposed sequence of conformations upon reduction, dialysis, reoxidation and incubation of oxidase	151

CHAPTER VI

Figure 1. Proposal for the complete turnover cycle of cytochrome c oxidase

160

CHAPTER I:
INTRODUCTION

Cytochrome c oxidase (EC 1. 9. 3. 1) is the oxygen-activating enzyme of cellular respiration both in eukaryotes and aerobic prokaryotes (Wikström et al., 1981). Digesting of food stuffs produces highly energized electrons. These electrons are transferred to the oxidative phosphorylation chain, and ultimately to cytochrome c oxidase, which catalyzes the four-electron reduction of molecular oxygen to water in the terminal step of cellular respiration. Oxidative phosphorylation occurs in the mitochondrion. The mitochondrion has two membranes, the outer membrane and the inner membrane. Hence there are two compartments: the intermembrane space often referred to as the mitochondrial cytosol, and the matrix, which is bounded by the inner membrane.

Cytochrome c oxidase catalyzes the reduction of dioxygen to water by ferrocycytochrome c:



This reaction takes place in the inner mitochondrial membrane. The four electrons necessary for the reduction of dioxygen are accepted from ferrocycytochrome c located in the cytosol of the mitochondrion one electron at a time, while the protons consumed in the reaction are taken up from the matrix. In this manner, the oxidase converts redox free energy into a proton electrochemical gradient across the inner mitochondrial membrane. In addition, cytochrome c oxidase is also an electrogenic proton pump capable of transporting up to four

protons against the proton electrochemical gradient. Since the dioxygen reduction is an energy-releasing process and the proton pumping is an energy-consuming process, the proton pumping is intimately coupled to the electron transfer activity of the oxidase, and the enzyme is thus referred to as a redox-linked proton pump. The proton electrochemical potential gradient (proton-motive force) generated by the "vectorial" proton pumping, together with the "scalar" proton consumption associated with dioxygen reduction, drives the synthesis of ATP and other energy-requiring biological processes (Krab & Wikström, 1987).

STRUCTURE:

Metal centers: Cytochrome c oxidase is a metalloprotein. Each monomer of the mitochondrial enzyme contains four redox active metal centers which may be distinguished on the basis of function. One pair, heme a and Cu_A, serves as the initial electron acceptor from ferrocycytochrome c; the other pair, heme a₃ and Cu_B, forms a binuclear center for dioxygen binding and reduction. Dioxygen only binds to the reduced binuclear center.

Heme a is a stable 6-coordinate low-spin heme complex in both oxidized and reduced forms (Babcock & Callahan, 1983, Martin et al., 1985). Heme a₃ is a 6-coordinate high-spin heme complex in the oxidized state and 5-coordinate high-spin in the reduced state

(Stevens & Chan, 1981). Cu_A is a spectroscopically unique biological metal center: the oxidized form of Cu_A has two histidine and two cysteine ligands, but a cysteine ligand is replaced by an N- or O-containing ligand upon reduction (Stevens, et al, 1982; Martin, et al., 1985; Li, et al., 1987). Cu_B is an EPR silent copper; it is known from EXAFS and ENDOR studies that Cu_B has three histidine ligands (Cline, et al, 1983; Reinhammar, et al., 1980). There is a shared bridging ligand between Cu_B and Heme a_3 . The identity of this bridging ligand has been proposed to be an imidazole nitrogen from a histidine residue, cysteine sulphur or an oxygen atom, but Fe EXAFS experiments by Scott and Chan (1988) showed that if cytochrome c oxidase is isolated and purified in Cl^- -free buffer solution, the scattering thought to originate from sulphur in the EXAFS disappears. This result suggests that Cl^- could be the bridging ligand, but more experiments are needed to settle this issue.

Recent studies of the metal contents in the enzyme revealed the existence of an additional Cu (called Cu_X) as an intrinsic component of the protein (Steffens, et al., 1987; Yewey, et al., 1988). The location, function and structure of the Cu_X center remains unknown. In addition, cytochrome c oxidase contains zinc and magnesium (Yewey, et al., 1988). The zinc has been suggested to play a structural role in the enzyme (Naqui et al., 1988). The role of the magnesium is not yet understood.

Subunits: In eukaryotes, cytochrome c oxidase is localized in the inner membrane of the mitochondrion. The three large subunits (subunit 1-3) are synthesized inside the mitochondrion (Anderson et al., 1982), and the remaining 10 smaller subunits (subunit 4-13) are synthesized in the cytoplasm. In prokaryotes, the enzyme is plugged through the plasma membrane and is comprised of only 2 or 3 subunits which are homologous to the mitochondrially coded subunit 1-3 of eukaryotes. On the basis of spectroscopic and sequence homology data, it is generally agreed that heme a , heme a₃ and Cu_B reside in subunit I, while Cu_A is associated with subunit II (Holm, et al., 1987). It has been suggested that subunit III may play an important role in redox-linked proton translocation. The remaining subunits of the eukaryotes presumably perform a regulatory function, or are involved in the assembly of the protein complex.

Reduction potential: The reduction potential of ferrocycytochrome c is about 220 mV (vs. NHE). Since the reduction potential for the reduction of dioxygen to water is about 810 mV under physiological conditions, the enzymatic reduction of dioxygen releases considerable free energy. In the native form of cytochrome c oxidase, heme a has a high reduction potential, about 350 mV, but it decreases to about 280 mV when the dioxygen binding site becomes reduced. The reduction potential of heme a also displays a pH dependence of ca. 30 mV/pH unit (Ellis, et al., 1986). The reduction potential of native Cu_A is about 240 mV (Goodman, 1984). In the absence of dioxygen, the reduction

potential of heme a_3 is around 380 mV, though it has been found to vary from batch to batch of the enzyme. The redox potential of Cu_B is about 340 mV. There are two dioxygen intermediates generated at the two- and three-electron reduced levels of dioxygen reduction. These intermediates are anchored at the binuclear center. The reduction potentials of these intermediates are 939 mV for the oxyferryl and 801 mV for the peroxo intermediate, compound C (Wikström, 1988).

Interactions among the redox active metal centers: There is evidence that all four redox active metal centers interact with each other. These interactions could be either electrostatic or magnetic. There is a strong antiferromagnetic coupling between the high spin ferric ion and the Cu_B , forming a $S=2$, EPR silent pair (Brudvig, et al., 1986). The magnetic interactions between heme a , Cu_A and the binuclear center are weak and can be treated as isolated centers.

In addition, the four redox active metal centers interact via the polypeptide chain. These conformational interactions are reflected in the redox behavior of the metal centers. The reduction potentials of the metals in cytochrome c oxidase can vary depending on whether other metal centers in the enzyme are reduced or oxidized. The outcome of these interactions is that the redox titration behavior of cytochrome c oxidase does not follow the Nernst equation. There is an anticooperative interaction of 40 mV between heme a and Cu_A , which means that when heme a is reduced, the redox potential of Cu_A is

lowered by 40 mV. In addition, there are anticooperative interactions between heme a and heme a₃ (-35 mV), heme a and Cu_B (-35 mV) and between heme a₃ and Cu_B (-35 mV) (Blair, et al., 1986a). By contrast, this type of redox interaction has not been observed between Cu_A and the binuclear center. Interaction between the metal centers in cytochrome c oxidase should play an important role in regulation of intramolecular electron transfer and redox-linked proton pumping.

PROTON PUMPING:

It is now largely accepted that cytochrome c oxidase is a redox-linked proton pump. Therefore, instead of testing the existence of the proton pumping of the enzyme, recent attention has been focused on understanding the mechanism of redox-linked proton pumping at the molecular level.

Basic requirements of redox-linked proton pumping: How does cytochrome c oxidase couple the free energy of electron transfer to translocate protons vectorially in the opposite direction to the electron transfers? In order for electron transfer to be linked to proton transfer, the first requirement is that the redox element and proton pumping element must be linked by some common intermediate. The linkage could be direct, with the redox center also being the proton translocator. Or the linkage could be indirect, with the redox element in conformational contact with the proton

translocating element(s). An eight-state cubic scheme has been proposed to link the different redox, protonation and input/output states. The second requirement is that there must be electron gating: the enzyme must be able to control the rate constants of the possible electron transfers in order to enhance the coupled process and suppress all of the leak pathways. The final requirement is: there must be proton gating, to minimize proton leaks, through the protein. Here, the electron gating is the key point: (1) the electron must enter the redox linkage site in a protein conformation different from the conformation in which electron is transferred to the dioxygen intermediates; (2) the conformational switch and subsequent electron transfer must take place faster than electron leak(s); and (3) the pump is kinetically controlled; accordingly, there must be mobile elements that can be followed in real time (Wikström, et al., 1981; Malmström, 1985; Blair, et al., 1986b).

Site of redox linkage: As discussed above, three general requirements must be met for redox-linked proton pumping. Deciphering which of the four redox centers is the redox element associated with proton pumping would be the first step towards understanding the proton pumping mechanism. It is found that the largest free energy change during enzymatic reduction of dioxygen is associated with electron transfer from the primary acceptors (Cu_A and heme a) to dioxygen reduction intermediates anchored at the dioxygen reduction site (Chan & Li, 1990). Protons are pumped only when electrons are transferred to the dioxygen reduction

intermediates; protons are not pumped when electrons are transferred to the unloaded dioxygen reduction site. The proton/electron ratio for each electron transferred in the sequence is 0.022 (Wikström & Casey, 1985). Therefore it has been argued that heme a and Cu_A are the most plausible sites of redox linkage.

Heme a has been implicated as the site of redox linkage. However, since electrons simply get in and get out of heme a without structural change, this chromophore does not satisfy the electron gating requirement. Accordingly it is less likely that heme a is the site of linkage. Cu_A is the most natural candidate for redox linkage because its ligands can be changed during enzyme turnover. Chan and coworkers have proposed that Cu_A is the site of redox linkage (Gelles, et al., 1986). The details of the Chan model are showed in Figure 1. Two proton conducting channels are implicated, one in communication with the matrix and other leading to the cytosol from the Cu_A site. In the electron input state (A in Figure 1), Cu_A is oxidized and ligated by two histidine nitrogens and two cysteine sulfurs arranged in a distorted tetrahedral geometry. Upon reduction of Cu_A (B in Figure 1), a local conformational change is triggered and the bis-dithiolate cysteine coordination is expected to become asymmetric; i. e., one of the Cu-S bonds becomes more elongated relative to the other. It has been proposed that a tyrosine or another residue with a similar pK_a in close proximity to the copper ion displaces one of the cysteine ligands. The change in pK_a of the incom-

Fig. 1 Ligand exchange proton pump. Protons move through the Cu_A site upon redox cycling by means of protonation/deprotonation of ligands as well as ligand exchange at Cu_A site.

ing tyrosine oxygen and outgoing cysteine sulfur accompany this ligand rearrangement can lead to a proton translocation from tyrosine to cysteine. In this manner, part of the redox energy of the Cu_A site is expended in translocating the proton from the matrix to the cytosolic site of the membrane, i. e., across an osmotic barrier. Following the conformational switch, the Cu_A site is now in the electron output state and poised for facile electron transfer to the dioxygen reduction site, either to the peroxo- or oxyferryl- intermediate, both with redox potentials 200- 300 mV more positive than that of Cu_A to pull the electron downhill. Upon reoxidation of the Cu_A site, a restoration of the original ligand arrangement must follow, i. e., the displaced cysteine must become coordinated with the copper ion once again, giving up its proton to the cytosol, and the associated tyrosinate must come off to be re-protonated from the matrix.

One way to test that Cu_A is the site of redox linkage is to structurally modify the Cu_A center and see if there is any functional change upon modification. Modifications on Cu_A structure which can change the proton pumping and dioxygen reduction activities of cytochrome c oxidase are *p*HMB modification and heat treatment (Table 1). These experiments do suggest a central role for Cu_A in proton pumping (Nilsson, et al., 1988; Li, et al., 1988). Also, the suggestion that a conformational transition occurs upon electron input to Cu_A is supported by the experimental evidence that large entropic change is associated with reduction of this metal center (Ellis, et al.,

Table 1 : Cytochrome c Oxidase Functions are Changed upon Cu_A Modification

Sample	Modification condition	Dioxygen reduction activity	Proton pumping activity (H^+/e^-)
Native		100%	1
pHMB-modified	Incubated with pHMB, 20 °C, 24h	20%	0
Heat-treated	40 °C, 1h, low conc. dodecyl maltoside	90%	0

1986; Wang, et al., 1986; Blair, et al., 1986). The question is whether these structural perturbations in the Cu_A cause functional change of oxidase?

THE ROLE OF SUBUNIT III IN PROTON PUMPING:

From the Chan model, we know that reduction of the Cu_A center results in one proton pumped from the matrix to the cytosol. Since mechanistically two protons are pumped for each electron transferred, the second proton translocated must be remotely coupled to the site of redox linkage within the context of the Chan model.

Over the years, subunit III has been implicated in playing a role in proton translocation (Prochaska & Fink, 1987). The most direct implication has come from covalent modification of the enzyme by dicyclohexylcarbodiimide (DCCD). DCCD modifies Glu 90 of subunit III (Prochaska, et al., 1981), and when the modified enzyme was incorporated into phospholipid vesicles and assayed for proton pumping activity, the H^+/e^- stoichiometry was observed to decrease by 50% (Brunori, et al., 1987, Prochaska, & Fink, 1987). In contrast, the electron transfer activity of the enzyme was essentially unchanged. Similar results were obtained when the subunit III-depleted enzyme was reconstituted and assayed for proton pumping (Li, et al., 1988). When the Cu_A center of subunit III-depleted enzyme is modified, there is total loss of proton pumping activity as well as curtailment of

the dioxygen reduction activity. Reconstitution of the two-subunit cytochrome c oxidase from paracoccus denitrificans into phospholipid vesicles also resulted in a H^+/e^- stoichiometry of 0.5 (Solioz, 1982) (Table 2).

Subunit III could provide the proton translocation channel itself. Alternatively, the second proton translocation is associated with one or more of the other membrane-spanning subunits, but subunit III regulates the interaction between the site of linkage and the indirectly coupled proton translocation channel. Since DCCD is a large, hydrophobic molecule, it seems rather unlikely that it covalently modified the internal hydrophilic proton translocation channel and therefore blocked proton translocation. Subunit III seems more likely to regulate the allosteric communication between various parts of the protein structure.

STUDIES DESCRIBED IN THIS THESIS:

In order to investigate the Cu_A properties of cytochrome c oxidase, metal analyses have been carried out to clarify the number of copper centers in the enzyme; the Cu_A structure has been modified, and the effects of these modifications on the reduction potential of Cu_A and on the interactions between Cu_A and other redox active metal centers have been examined. The possible role of subunit III in maintaining the Cu_A structure and in regulating the communication

between Cu_A and other elements of the proton pumping machinery has also been investigated. In addition, we try to identify the bridging ligand of binuclear center in the resting enzyme.

Table 2: Cytochrome c Oxidase Functions are Changed upon Subunit III Modification

Sample	Modification condition	Dioxygen reduction activity	Proton pumping activity (H⁺/e⁻)
Native		100%	1
DCCD-inhibited	Incubated with DCCD, 12 °C, 3h	90%	0.5
Subunit III depleted (Cu _A unmodified)	21 °C, 24h, high conc. dodecyl maltoside	90%	0.5
Subunit III depleted (Cu _A modified)	Incubation at 43 °C with the presence of Zwitterion SB-12	20%	0

REFERENCES:

- Babcock, G. T. & Callahan, P. M., (1983) *Biochemistry*, **22**, 2314-2319.
- Blair, D. F.; Ellis, W. R.; Wang, H.; Gray, H. B. & Chan, S. I., (1986a) *J. Biol. Chem.*, **261**, 11524-11537.
- Blair, D. F.; Gelles, J. & Chan, S. I., (1986b) *Biophys. J.*, **50**, 713-733.
- Brudvig, G. W., Morse, R. & Chan, S. I., (1986) *J. Magn. Reson.*, **67**, 198-201.
- Brunori, M.; Antonini, G.; Malatesta, F. & Sarti, P., (1987) *Eur. J. Biochem.*, **169**, 1-8.
- Chan, S. I. & Li, P. M., (1990) *Biochemistry*, **29**, 1-12.
- Cline, K.; Reinhammar, B.; Jensen, P.; Venters, R. & Hoffman, B. M., (1983) *J. Biol. Chem.*, **258**, 5124-5128.
- Ellis, W. R.; Wang, H.; Blair, D. F.; Gray, H. B. & Chan, S. I., (1986) *Biochemistry*, **25**, 161.
- Gelles, J.; Blair, D. F. & Chan, S. I., (1986) *Biochim. Biophys. Acta*, **853**, 205-236.
- Goodman, G., (1984) *J. Biol. Chem.*, **259**, 15094.
- Holm, L.; Saraste, M. & Wikström, M., (1987) *EMBO J.*, **6**, 2819-2823.
- Krab, K. & Wikström, M., (1987) *Biochim. Biophys. Acta*, **895**, 25-29.
- Li, P. M.; Gelles, J.; Chan, S. I.; Sullivan, R. J. & Scott, R. A., (1987) *Biochemistry*, **26**, 2091-2095.

- Li, P. M.; Morgan, J. E.; Nilsson, T.; Ma, M. & Chan, S. I., (1988) *Biochemistry*, **27**, 2091-2095.
- Malmström, B. G., (1985) *Biochim. Biophys. Acta*, **811**, 1-12.
- Martin, C. T.; Scholes, C. P. & Chan, S. I., (1985) *J. Biol. Chem.*, **260**, 2857-2861.
- Martin, C. T.; Scholes, C. P. & Chan, S. I., (1988) *J. Biol. Chem.*, **263**, 8420-8429.
- Naqui, A.; Powers, L.; Lundeen, M.; Constantinescu, A. & Chance, B., (1988) *J. Biol. Chem.*, **263**, 12342-12345.
- Nilsson, T.; Gelles, J.; Li, P. M. & Chan, S. I., (1988) *Biochemistry*, **27**, 296-301.
- Prochaska, L. J.; Bisson, R.; Capaldi, R. A.; Steffens, G. M. & Buse, G., (1981) *Biochem. Biophys. Acta*, **637**, 360-373.
- Prochaska, L. J. & Fink, P. S., (1987) *J. Bioenerg. Biomembr.*, **19**, 143-166.
- Reinhammar, B.; Maldin, R.; Jensen, P.; Karlsson, B.; Andreasson, L.-E.; Aasa, R.; Vänngård, T. & Malmström, B. G., (1980) *J. Biol. Chem.*, **255**, 5000-5004.
- Scott, R. A.; Li, P. M. & Chan, S. I., (1988) *Cytochrome oxidase structure, function, and physiopathology*, Annuals of the New York Academy of Sciences, **550**, 53-58.
- Soloz, M.; Carafoli, E. & Ludwig, B., (1982) *J. Biol. Chem.*, **257**, 1579-1582).
- Steffens, G. C. M.; Biewald, E. & Buse, G., (1987) *Eur. J. Biochem.*, **164**, 295-300.

Stevens, T. H. & Chan, S. I., (1981) *J. Biol. Chem.* , **256**, 1069-1071.

Stevens, T. H.; Martin, C. T.; Wang, H.; Brudvig, G. W.; Scholes, C. P. & Chan, S. I., (1982) *J. Biol. Chem.*, **257**, 12106-12133.

Wang, H.; Blair, D. F.; Ellis, W. R.; Gray, H. B. & Chan, S. I., (1986) *Biochemistry*, **25**, 167.

Wikström, M.; Krab, K. & Saraste, M., (1981) *Cytochrome Oxidase: A Synthesis*, Academic Press, New York.

Wikström, M. & Casey, R. P., (1985) *J. Inorg. Biochem.*, **23**, 327-334.

Wikström, M., (1988) *Chem. Scr.* , **28A**,71-74.

Yewey, G. L. & Caughey, W. S., (1988) *Biochim. Biophys. Acta*, **591**, 62-63.

CHAPTER II:

THE NATURE OF CU_x IN CYTOCHROME C OXIDASE

INTRODUCTION:

Cytochrome c oxidase is a metalloprotein that catalyzes the four-electron reduction of molecular oxygen to water and couples this reaction to the uphill movement of protons across the mitochondrial inner membrane (Wikström et al., 1981). This enzyme has a complicated composition and structure. Mammalian cytochrome c oxidases are known to consist of up to thirteen polypeptides; even the simple bacterial enzymes have two or three subunits (Kadenbach et al., 1983). In addition, the mitochondrial enzyme appears to exist as a dimer. It is generally accepted that four redox centers are associated with each monomer of the mitochondrial oxidase: two heme A's (heme a and heme a₃), and two copper ions (Cu_A and Cu_B). Available evidence suggests that heme a, heme a₃ and Cu_B reside in subunit I (Winter et al., 1980; Ludwig et al., 1980), and Cu_A is associated with subunit II (Martin et al., 1988; Hall et al., 1988).

Recent metal analyses of cytochrome c oxidase from bovine heart and certain other tissues have made it necessary to consider the presence of other metals as intrinsic components of the enzyme. Einarsdottir and Caughey (1984) first reported that zinc and additional copper (in addition to Cu_A and Cu_B) are tightly bound to cytochrome c oxidase in various preparations of the enzyme. Subsequently, they discovered that magnesium is also an integral part of the protein. On the basis of inductively coupled plasma atomic emission spectrometry (ICP-AES) measurements, a stoichiometry of

5Cu/4Fe/2Zn/2Mg was proposed for the dimer (Einarsdottir and Caughey, 1985). Following the work of Caughey et al., Bombelka et al. (1986) analyzed the metal contents of cytochrome c oxidase preparations from a variety of mammalian tissues by photon-induced X-ray emission. These workers obtained, however, a different stoichiometry of 3Cu/2Fe/1Zn for the monomer (Mg content was not measured). Steffens et al. (1987), using ICP-AES, confirmed a stoichiometry of 3Cu/2Fe/1Zn/1Mg for the monomer of bovine heart cytochrome c oxidase. In addition, they obtained the same stoichiometry for the enzyme from *Paracoccus denitrificans*. However, Yoshikawa recently supported a stoichiometry of 5Cu/4Fe/2Zn/2Mg for the dimer in crystalline preparations of bovine heart cytochrome c oxidase (Yoshikawa et al., 1988).

In order to ensure that the "extra copper" (called Cu_x), zinc and magnesium are intrinsic components rather than exogenous metal ions that are just bound to the enzyme, Yewey and Caughey (1988) dialyzed native cytochrome c oxidase against 10 mM EDTA and showed that the stoichiometry of 5Cu/4Fe/2Zn/2Mg remained unchanged. In the meantime, they examined the affinity of cytochrome c oxidase for exogenous Cu²⁺ and Zn²⁺ ions by introducing CuCl₂ or ZnCl₂ to the dialysis medium, and monitoring the effects of subsequent dialysis against metal-free buffer as well as against buffer containing EDTA. The results showed that Cu_x, Zn and Mg bind tightly to the enzyme, and that these metal ions remained associated with the enzyme even after extensive dialysis against EDTA.

Although there is no direct experimental evidence to support the possible functions of Zn^{2+} and Mg^{2+} ions in the enzyme, Yewey and Caughey (1987) have proposed that the functional role of Mg in mammalian cytochrome c oxidase is to provide an ATP binding site in association with subunit 4. Naqui et al. (1988) have suggested that the zinc ion plays a structural role in the enzyme on the basis of EXAFS results showing that the zinc ion is liganded almost exclusively by cysteine sulfurs, presumably those in subunit VIa.

The existence of Cu_x , Zn, and Mg as intrinsic metal atoms in cytochrome c oxidase seems confirmed, but there remains uncertainty about the content of Cu_x . In addition, there is no information on the binding domain of Cu_x and the possible role of Cu_x in the structure and function of the enzyme. We report here the results of further studies to classify the nature of Cu_x . Seven different preparations of cytochrome c oxidase have been obtained, and highly precise metal contents have been determined by direct current plasma atomic emission spectrometry (DCP-AES). Attempts have also been made to record the low temperature (4 K) EPR spectrum of Cu_x . On the basis of these experiments, we offer here a proposal regarding the binding domain and the structural role of Cu_x .

MATERIALS AND METHODS:

Cytochrome c Oxidase Preparation: Beef heart cytochrome c oxidase was isolated by the method of Hartzell and Beinert (1974), with special precautions to avoid contamination from exogenous metal ions during the preparation. Enzyme concentrations were determined spectrophotometrically by using $\Delta\epsilon$ (reduced minus oxidized = $27 \text{ M}^{-1} \text{ cm}^{-1}$) at 605 nm. The enzyme preparation was stored at -80°C until used.

Dialysis of Cytochrome c Oxidase: 80 μM cytochrome c oxidase in 10 mM Tris-Cl, 0.1% Triton X-100, pH 8.0 was dialyzed against 40 mM EDTA at 4°C for ten hours.

Chromatography of Cytochrome c Oxidase: Chromatography of the enzyme was performed as follows: 80 μM native enzyme in a buffer of 100 mM Tris-Cl, 0.1% sodium deoxycholate, pH 8.0 was applied to a Bio-Rad DEAE agarose 0.5 A column (1 x 20 cm) and eluted with 200 mM NaCl, 50 mM Tris-Cl, 0.1% sodium deoxycholate, pH 8.0.

Preparation of Cu_A -Depleted Cytochrome c Oxidase: Cu_A -depleted cytochrome c oxidase was prepared according to the procedure and reaction conditions outlined in Hall et al. (1988) with some modifications: 40 μM cytochrome c oxidase in 50 mM potassium

phosphate, 0.1% sodium deoxycholate, 10 mM EDTA, pH 7.4 was reduced by two electron equivalents of sodium dithionite anaerobically, the sample was then incubated with 300 mM 2-mercaptoethanol at 28 °C for 15 minutes. At this point the reaction was stopped and the excess 2-mercaptoethanol removed by passing the sample through a Bio-Rad agarose 0.5 A column (1 x 15 cm) that had previously been washed with 100 mM Tris-Cl, 0.1% sodium deoxycholate, pH 8.0.

Preparation of Subunit III-Depleted Cytochrome c Oxidase: 2 μ M cytochrome oxidase was incubated in 20 mM Tris, 0.1 M NaCl, 1 mM EDTA and 5 mg/mL dodecyl-b-D-maltoside, pH 7.8 for 24 hours at room temperature. The sample was then concentrated to 80 μ M. The removal of subunit III was performed on a Bio-Rad DEAE agarose column (1 x 15 cm), that had previously been equilibrated with a buffer of 50 mM potassium phosphate, 0.1% dodecyl-b-D-maltoside, pH 7.0. The subunit III-depleted cytochrome c oxidase was eluted from the column by 50 mM Tris-Cl, 0.1% sodium deoxycholate, 200 mM NaCl, pH 8.0.

Preparation of Monomeric Cytochrome c Oxidase: 80 μ M cytochrome oxidase was incubated in 5% Triton X-100, 320 mM Tris-Cl, pH 8.5, for 2 hr at 4 °C as described by Georgevich et al. (1983). The sample was then applied to a 1 x 12 cm DEAE agarose column and washed with 10 mM Tris-Cl, pH 8.5, 0.1% Triton X-100. The

monomeric cytochrome c oxidase was eluted with 200 mM NaCl, 10 mM Tris-Cl, 0.1% Triton X-100, pH 8.0.

Preparations of Cu_A-Modified Cytochrome c Oxidase: Two types of Cu_A-modified enzyme were prepared, one in which the Cu_A site had been converted to a type 1 copper (type 1 Cu_A-enzyme), and the other in which it been transformed to a type 2 copper center (type 2 Cu_A-enzyme). The type 1 Cu_A-enzyme was prepared as follows: native cytochrome c oxidase was diluted into 20 mL buffer of 50 mM potassium phosphate, 0.5% dodecyl-b-D-maltoside, pH 7.3 with a final enzyme concentration of 30 μ M; the sample was then heated at 40 °C for one hour and 45 minutes. The preparation of the type 2 Cu_A-enzyme was carried out as described by Nilsson et al. (1988a): 58 μ M cytochrome c oxidase was heated at 43 °C for one hour in buffer containing 15 mM sulfobetaine 12, 0.5 M Hepes and 0.15 M NaCl, pH 7.4; the resulting turbid solution was then centrifuged for 60 minutes at 27,000 g to remove any aggregated enzyme.

Metal Affinity Test of Cytochrome c Oxidase: 20 μ M native enzyme was incubated with either 80 μ M CuCl₂ or 80 μ M ZnCl₂ in 100 mM Tris buffer, pH 8.0 at room temperature for four hours; the sample was then dialyzed extensively against 40 mM EDTA. Control samples were treated identically, except for omission of the metal chloride from the incubation buffer.

Optical Spectroscopy and Electron Transfer Activity Assay: Optical spectra in the visible and near-IR region (350-900 nm) were collected on a Beckman DU-7 UV-visible Spectrophotometer interfaced to an IBM XT computer. The activity of cytochrome *c* oxidase was determined spectrophotometrically. Assays were performed by following the oxidation of 20 μ M ferrocycytochrome *c* at 550 nm in 50 mM sodium phosphate, 0.1% dedecyl-b-D-maltoside, pH 6.0. The concentration of cytochrome *c* oxidase was 5-20 nM. The turnover number of the untreated enzyme was typically about 500 s⁻¹.

EPR Spectroscopy: EPR spectra were recorded on a Varian E-line Century Series X-band Spectrometer equipped with a 12 bit analog-to-digital converter for the computer digitization of the signal. Sample temperature was maintained at 4 K by a liquid helium cryostat (Oxford instruments). Oxygen was removed from EPR samples by a single equilibration with argon gas immediately prior to freezing the sample for the measurements.

Metal Analysis: Metal contents of the enzyme preparations were determined by direct current plasma atomic emission spectrometry (DCP-AES) in the Laboratory of Dr. Stolper, Division of Geological and Planetary Sciences at Caltech. The instrument was calibrated by running standards of Cu/Fe/Zn/Mg (ranging from 0.1 to

10 ppm) in 0.1% nitric acid. Before the measurements were made on the protein samples, the enzyme preparations were first washed with double-distilled water to rid the solution of as much detergent as possible; nitric acid was then added to a final acid concentration of 0.1%. The concentration of cytochrome c oxidase was typically 5-10 μM in these analyses.

RESULTS:

Metal Content of Native Cytochrome c Oxidase: Three different native enzyme preparations were analyzed for their metal contents. Four measurements were carried out for each sample. The experimental error of an individual measurement is within $\pm 5\%$. The average metal atom ratio of the three native enzyme preparations are presented in Table 1. Although different batches of the enzyme were purified at different times and by different individuals, the observed atom ratios agreed well with each other. The average Cu/Fe ratio of 1.26 ± 0.05 indicates that about 20% of the total copper is Cu_x . The ratios of Zn/Fe and Mg/Fe show that one atom of zinc and one atom of magnesium is present per monomer. Taken together, these results suggest a stoichiometry of $5\text{Cu}/4\text{Fe}/2\text{Zn}/2\text{Mg}$ per dimer, which is consistent with the determination of Yoshikawa et al. (1988). The dialysis of native cytochrome c oxidase against 40 mM EDTA did not affect the metal contents; neither were metal atoms removed by passing the native enzyme through a DEAE column. The stoichiometry

Table 1: Metal Contents of Cytochrome c Oxidase Treated by Different Methods

Method of Treatment	Metal Atom ratios ^a				Assignment (per dimer)						
	Cu/Fe	Zn/Fe	Mg/Fe	Fe _a	Fe ₃	Cu _A	Cu _B	Cu _x	Zn	Mg	
Native Enzyme	1.26 ± 0.05	0.49 ± 0.03	0.50 ± 0.04	2	2	2	2	1	2	2	
+ Dialysis	1.25 ± 0.04	0.50 ± 0.05	0.51 ± 0.03	2	2	2	2	1	2	2	
+ DEAE Column	1.24 ± 0.05	0.49 ± 0.06	0.51 ± 0.04	2	2	2	2	1	2	2	
Monomerization	1.02 ± 0.06	0.32 ± 0.05	0.51 ± 0.05	2	2	2	2	0	2	2	
Subunit III depletion	0.98 ± 0.05	0.33 ± 0.06	0.49 ± 0.07	2	2	2	2	0	2	2	
Cu _A -Depletion	0.73 ± 0.07	0.32 ± 0.04	0.48 ± 0.05	2	2	0	2	1	2	2	
Cu _A -Modification (Type 1)	1.03 ± 0.04	0.34 ± 0.03	0.51 ± 0.05	2	2	2	2	0	2	2	
Cu _A -Modification (Type 2)	1.04 ± 0.06	0.30 ± 0.05	0.52 ± 0.04	2	2	2	2	0	2	2	
Cu _A -depletion (pHMB)											
Modified + Dialysis) ^b	0.70 ± 0.10	~0.1	~0.2	2	2	0	2	0	0	1	

^a Error reported as standard deviation of four analyses.

^b From the work of Yewey and Caughney (1988).

of 5Cu/4Fe/2Zn/2Mg is thus intrinsic to the cytochrome c oxidase dimer.

Metal Affinity of Cytochrome c Oxidase: The affinity of the enzyme for metal ions was tested by incubating the enzyme with high concentrations of CuCl₂ or ZnCl₂. As shown in Table 2, both zinc and copper ions bind to the enzyme with high affinity, but these bound metals can be removed by extensive dialysis against 40 mM EDTA.

Metal contents of the Cu_A-Depleted and Cu_A-Modified Enzymes: For the Cu_A-depleted sample, an atom ratio of Cu/Fe = 0.73 ± 0.07 was obtained. This result is consistent with the depletion of two Cu_A atoms from the dimer, as concluded previously, and in the present work, from EPR and near IR studies. These experiments showed the total abolition of 830 nm band as well as the unusual EPR signal near g = 2 normally assigned to Cu_A. In addition, the electron transfer activity of the Cu_A-depleted sample was more than 80% inhibited compared to that of an untreated control that showed a turnover of 500 s⁻¹ (Table 3), consistent with the depletion of Cu_A from the protein.

Loss of copper was also apparent in two different Cu_A-modified preparations, but to a lesser extent than in the case of the Cu_A-

Tabel 2: Metal Affinity Analysis of Cytochrome c Oxidase^a

Treatment	Cu/Fe	Zn/Fe	Enzyme Activity (%)
Control	1.30 ± 0.05	0.45 ± 0.06	100
Control/EDTA ^b	1.28 ± 0.05	0.44 ± 0.05	90
+ CuCl ₂	4.00 ± 0.02	0.49 ± 0.08	90
CuCl ₂ /EDTA ^c	1.38 ± 0.06	0.48 ± 0.07	95
+ ZnCl ₂	1.35 ± 0.07	3.58 ± 0.04	90
ZnCl ₂ /EDTA ^c	1.28 ± 0.07	0.55 ± 0.06	90

a Error reported as standard deviation of five analyses.

b Dialyzed against 40 mM EDTA.

c Dialyzed against 40 mM EDTA after exposure to metal.

Tabel 3: Effects of Different Treatments on the Topology and Electron Transfer Activity of Cytochrome c Oxidase

Treatment	Dimer or Monomer	Subunit III Removal	Activity (%)
Native Enzyme	Dimer	No	100
+ Dialysis	Dimer	No	90
+ DEAE Column	Dimer	No	90
Monomerization	Monomer	Yes	90
Subunit III Depletion	Monomer	Yes	85
Cu _A -Depletion	Dimer	No	20
Cu _A -Modification (Type 1)	Monomer	Yes	80
Cu _A -Modification (Type 2)	Monomer	Yes	25
Cu _A -Depletion (pHMB + Dialysis)	Monomer	Yes	20

depleted sample. As shown in Table 1, the Cu/Fe ratios of both the type 1 and type 2 Cu_A-modified enzymes are about 2/2 per functional unit. The EPR spectra of these preparations gave the expected type 1 Cu_A or type 2 Cu_A signal, and the intensities of these signals were the same as that of the native enzyme at the same concentration. These results clearly indicate that Cu_A was not removed in these preparations and suggest that the copper depleted in the two Cu_A-modified samples is Cu_x. This conclusion is consistent with the electron transfer activities observed for the two Cu_A-modified samples (Table 3). The type 1 Cu_A-enzyme retained the same activity as native enzyme, while the type 2 Cu_A-enzyme displayed a significant decrease in activity as reported previously (Nilsson et al., 1988b; Li et al., 1988).

Zinc was also found to be partially removed in the Cu_A-depleted and Cu_A-modified preparations. However, the magnesium content in these samples remained unchanged.

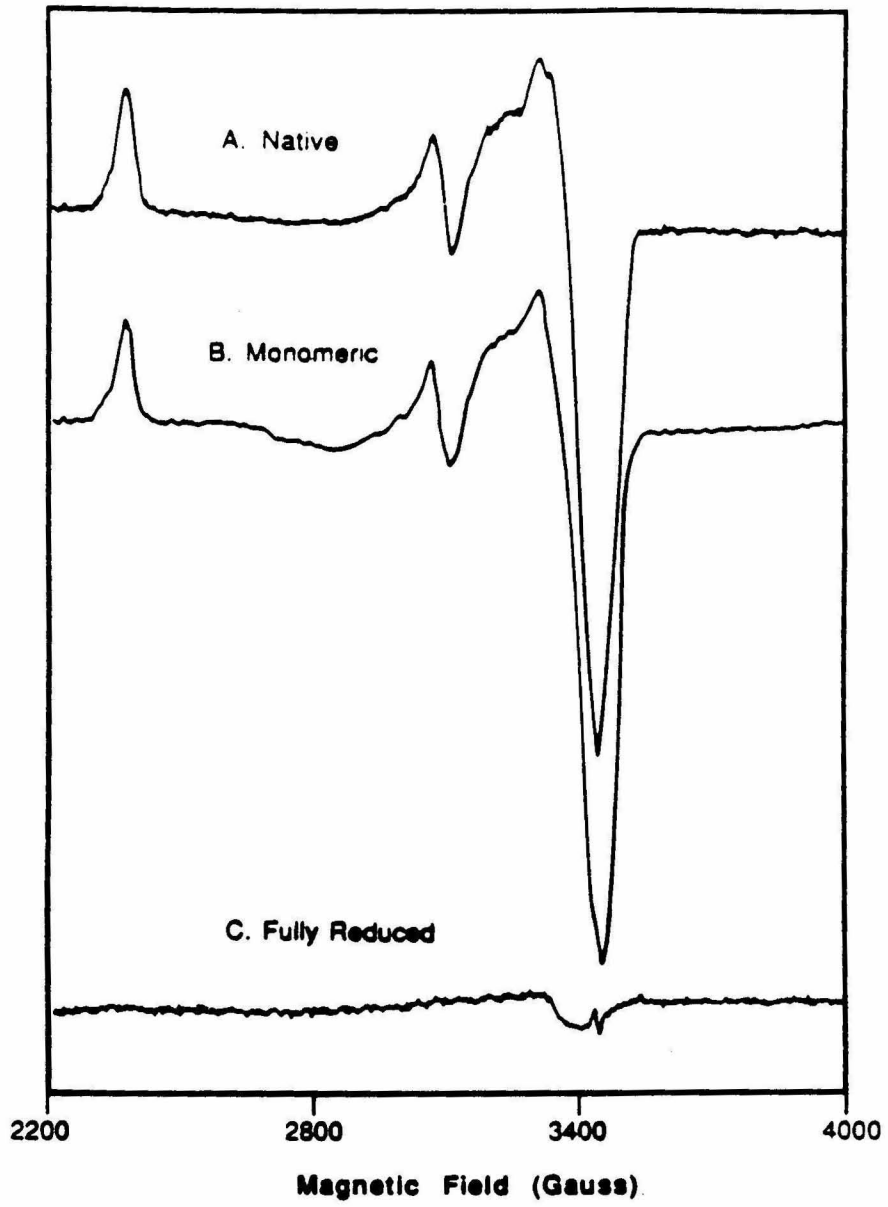
Metal Contents of Monomeric and Subunit III-Depleted Cytochrome cOxidase: Upon monomerization of the enzyme, the Cu/Fe ratio decreased from 1.25 to 1.02. Subunit 3 depletion also caused the same copper loss, decreasing the Cu/Fe ratio to 0.98 ± 0.05 . Low temperature EPR and near IR absorption measurements of both samples revealed that Cu_A was unaffected following these

treatments. The results are consistent with the removal of Cu_x upon subunit 3-depletion and monomerization of the protein.

As with Cu_A -depletion and Cu_A -modification, the protein monomerization and subunit 3-depletion also led to a 30% decrease in the zinc content. In contrast, the magnesium content was very stable toward these treatments. The same Mg/Fe ratios were obtained as in the case of the native enzyme.

Attempts to Observe the EPR Spectrum of Cu_x : It should be possible to observe the EPR spectrum of Cu_x , particularly if it exists as an isolated d^9 ion. The EPR spectrum at 4 K of the oxidized enzyme gave no indication of such a copper center. In fact, a comparison of the EPR spectrum of native oxidized oxidase with that of the monomeric enzyme, where Cu_x is supposedly absent according to the elemental analysis (Figure 1), revealed no evidence of perturbation of the EPR signal normally assigned to Cu_A . However, a weak EPR signal near $g = 1.96$, accounting for no more than 10% of 1 copper ion, was detected in the fully reduced enzyme. This signal was not observed when subunit III was depleted or when the enzyme was monomerized. Taken together, these results suggest that Cu_x is heterogeneous, largely reduced, and that the residual EPR-detected Cu_x seen in the EPR spectrum of the "fully" reduced enzyme is relatively inert toward reduction by reducing equivalents.

Fig 1. EPR Spectra of Cu_A for (A) Native, (B) Monomeric, (C) Fully reduced cytochrome c oxidase. The fully reduced enzyme was prepared by reducing the enzyme with dithionite anaerobically. Sample temperature, 4 K; microwave frequency 9.16 GHz; microwave power, 5mW; modulation amplitude, 10 G.



DISCUSSION:

The results of our metal analysis of bovine heart cytochrome *c* oxidase confirm the stoichiometry of 5Cu/4Fe/2Zn/2Mg per dimer previously reported by Einarsdottir and Caughey (1985) and Yoshikawa et al. (1988). As pointed out by Yewey and Caughey (1988), the precision of the metal analysis is critically important if a Cu/Fe ratio of 1.25 is to be distinguished from a ratio of 1.50. While the precision of the earlier determinations has been limited to no better than $\pm 20\%$, our present analyses are significantly more accurate. In the present determinations, the precision of an individual measurement is within $\pm 5\%$. Accordingly, the stoichiometry of the metal atoms can be ascertained with a high degree of confidence. The high precision was achieved by using an appropriate matrix in both the standard solutions and the samples. In addition, it was essential to rid the protein samples of as much detergent as possible and to go to higher protein concentrations.

The results of the present study confirm that Cu_x , Zn and Mg ions are intrinsic components of the enzyme. Although the enzyme exhibits high affinity for exogenous Cu and Zn ions as well, these can be readily removed from the enzyme by dialyzing against 40 mM EDTA. The stoichiometry of 5Cu/4Fe/2Zn/2Mg per dimer remains invariant after this dialysis, even following subsequent DEAE agarose column chromatography to remove possible bound metal ions that may not be removed by dialysis.

It is also noteworthy that Cu_x can be removed without perturbation of the other copper atoms. In four different enzyme preparations (monomeric, subunit 3-depleted, type 1 Cu_A -enzyme and type 2 Cu_A -enzyme), it is clear that Cu_x is absent and that the loss of this copper ion from the dimeric protein results in no detectable perturbation of the spectroscopic or functional properties of the enzyme. Since the enzyme exists as a monomer and subunit III is removed according to SDS-polyacrylamide gel electrophoresis in all four of these preparations, we are led to the logical conclusion that Cu_x is associated with subunit III and the dimeric structure of the protein. In support of this, when Cu_A is selectively removed without loss of subunit III as disruption of the dimeric structure, Cu_x is retained. However, when Cu_A is removed by dialysis of oxidase that has previously been rendered monomeric by p-hydroxymercuribenzoate treatment against EDTA, metal analysis indicates the loss of one additional copper ion per dimer (presumably Cu_x) in addition to the two Cu_A atoms (Yewey and Caughey, 1988).

Although the role of subunit III in the structure and function of cytochrome oxidase is still not fully understood, it has generally been noted that treatments employed to remove subunit III also tend to monomerize the enzyme (Finel and Wikstrom, 1986). Accordingly, it has been suggested that subunit III is involved in the oligomerization of the protein (Finel and Wikstrom, 1988). In light of the results

Although the role of subunit III in the structure and function of cytochrome oxidase is still not fully understood, it has generally been noted that treatments employed to remove subunit III also tend to monomerize the enzyme (Finel and Wikstrom, 1986). Accordingly, it has been suggested that subunit III is involved in the oligomerization of the protein (Finel and Wikstrom, 1988). In light of the results obtained here, we propose that Cu_x plays a structural role in the dimerization of the enzyme, and that a simple copper ion serves as a bridge between the two subunit III polypeptides within the dimer. Our attempts to observe the EPR spectrum of Cu_x gave no indication of its existence in the oxidized protein. However, in the fully reduced enzyme, an unusual signal near $g = 1.96$ was observed, although though this EPR signal accounted for no more than 10% of one copper ion. The implication is that Cu_x is already reduced in the oxidized enzyme as isolated, and that its structural environment is heterogeneous.

Acknowledgments: We thank Dr. Sally Newman in Dr. Stolper's group for many useful discussions and excellent assistance during the metal analyses.

REFERENCES:

- Bombelka, E.; Richter, F.-W.; Stroh, A. & Kadenbach, B., (1986) *Biochem. Biophys. Res. Commun.*, **140**, 1007-1014.
- Einarsdottir, O. & Caughey, W. S., (1984) *Biochem. Biophys. Res. Commun.*, **124**, 836-842.
- Einarsdottir, O. & Caughey, W. S., (1985) *Biochem. Biophys. Res. Commun.*, **129**, 840-847.
- Finel, M. & Wikstrom, M., (1986) *Biochim. Biophys. Acta*, **851**, 99-108.
- Finel, M., and Wikstrom, M., (1988) *Eur. J. Biochem.*, **176**, 125-129.
- Georgevich, G.; Darley-Usmar, V. M.; Malatesta, F. & Capaldi, R. A., (1983) *Biochemistry* **22**, 1317-1322.
- Hall, J.; Moubarak, A.; O'Brien, P.; Pan, L. P.; Cho, I. & Millett, F., (1988) *J. Biol. Chem.*, **263**, 8142-8149.
- Hartzell, C.R. & Beinert, H., (1974) *Biochim. Biophys. Acta*, **368**, 318-338.
- Kadenbach, B.; Jaransch, J.; Hartman, R. & Merle, P., (1983) *Analyt. Biochem.*, **129**, 517-521.
- Li, P. M.; Morgan, J. E.; Nilsson, T., Ma, M. & Chan, S. I., (1988) *Biochemistry* **27**, 7538-7546.
- Ludwig, B., (1980) *Biochim. Biophys. Acta* , **594**, 177-189

Martin, C. T.; Scholes, C. P. & Chan, S. I., (1988) *J. Biol. Chem.*, **263**, 8420-8429.

Naqui, A.; Powers, L.; Lundeen, M.; Comstantinescu, A. & Chance, B.(1988) *J. Biol. Chem.*, **263**, 12342-12345.

Nilsson, T.; Copeland, R. A.; Smith, P. A. & Chan, S. I., (1988a) *Biochemistry*, **27**, 8254-8260.

Nilsson, T.; Gelles, J.; Li, P. M. & Chan, S. I., (1988b) *Biochemistry*, **27**, 296-301.

Steffens, G. C. M.; Biewald, R. & Buse, G., (1987) *Eur. J. Biochem.*, **164**, 295-300.

Wikstrom, M.; Krab, K. & Saraste, M., (1981) *Cytochrome Oxidase, A Synthesis*, New York: Academic 2-13.

Winter, D. B.; Bruyninckx, W. J.; Foulke, F. G.; Grinich, N. P. & Mason, H. S., (1980) *J. Biol. Chem.*, **255**, 11408-11414.

Yewey, G. L. & Caughey, W. S., (1987) *Biochem. Biophys. Res. Commun.*, **148**, 1520-1526.

Yewey G. L. & Caughey, W. S., (1988) *Annals of the New York Academy of Sciences* **550**, 23-32.

Yoshikawa, S.; Tera, T.; Takahashi, Y.; Tsukihara, T. & Caughey, W. S., (1988) *Proc. Natl. Acad. Sci. USA*, **85**, 1354-1358.

CHAPTER III:
THE EFFECTS OF *p*HMB-MODIFICATION AND HEAT-
TREATMENT ON THE CU_A REDUCTION POTENTIAL OF
CYTOCHROME C OXIDASE

INTRODUCTION:

Cytochrome c oxidase catalyzes the terminal electron transfer in the mitochondrial respiratory chain from ferrocytochrome c to molecular oxygen. In addition, it is an electrogenic proton pump capable of translocating vectorially up to four protons from the matrix of the inner mitochondrial membrane to the cytosol for every dioxygen molecule reduced (Wikström, et al. 1981). To achieve this proton pumping, the electron transfer and proton translocation functions of the enzyme must be linked (Babcock and Callahan, 1983; Chan et al., 1988; Chan & Li, 1990). The question is not whether this linkage occurs, but rather about mechanism of this coupling and the site of redox linkage.

It is generally assumed that the largest free energy change during enzymatic reduction of dioxygen is associated with electron transfer from the primary acceptors (Cu_A and Fe_a) to the dioxygen intermediates anchored at the dioxygen reduction site. Accordingly, these "low-potential" centers have been considered to be the most plausible candidates for the site of redox linkage. Experiments by Wikström and Casey (1985) on intact mitochondria do seem to implicate one of these sites as the site of redox linkage. More importantly, Wikström (1989) has recently shown that only two of the four electrons transferred are linked to proton pumping. These latter

results clearly emphasize the role of the dioxygen chemistry in the proton pumping activity of the enzyme. Chan and Li (1989) have argued that protons can only be pumped during the second half of the turnover cycle, when the dioxygen reduction site of the enzyme has been activated to either the peroxy- or oxyferryl intermediate. Only electron transfers to these high redox potential dioxygen intermediates possess the required exergonicity to drive the proton pumping reaction(s).

Recently, several experiments from this laboratory seemed to implicate Cu_A as the site of redox linkage. First, when cytochrome oxidase is chemically modified by pHMB, a protein species containing a structurally altered type 2 Cu_A is obtained. This modified enzyme exhibits oxidase activity, albeit with activity that is only 20% that of the native enzyme (Gelles and Chan, 1985). Apparently, the redox potential of the type 2 Cu_A is also significantly lower than that of the native Cu_A , so that the modified copper site is no longer reducible by ferrocyanide. However, the modified copper site is reducible by reductants with lower redox potentials. Thus electron transfer from Cu_A to the dioxygen reduction site is effectively bypassed in the pHMB-modified enzyme when ferrocyanide is employed as the substrate. In addition, when the modified enzyme is reconstituted into membrane vesicles and assayed for proton pumping activity, rapid extravesicular alkalinization is observed (Nilsson et al., 1988). This

result has led to the suggestion that *p*HMB treatment of the enzyme creates a transmembrane channel that is highly permeable toward protons.

In a second series of experiments, Li et al. (1988) showed that heating cytochrome *c* oxidase under mild conditions also results in structural modification of the Cu_A site. In these experiments, subunit III is depleted; however, this subunit III depletion can be accomplished without Cu_A modification. The subunit III-depleted Cu_A-unmodified enzyme displayed proton pumping activity, albeit with a 50% lower H⁺/e⁻ stoichiometry. On the other hand, the heat-treated Cu_A-modified enzyme is heterogeneous, containing a mixture of native, type 2 and type 1 Cu_A sites, and depending on the distribution of the preparation among these various Cu_A species, the enzyme displays proton pumping activity to varying extents. The heat-treated type 1 Cu_A enzyme is of particular interest as it does not pump protons. Yet this copper site is electron transfer competent when ferrocycytochrome *c* is used as the substrate and the modified enzyme shows full oxidase activity. In contrast, the modified type 2 Cu_A enzyme obtained by heat treatment exhibits reduced oxidase activity, and when reconstituted into lipid vesicles, these vesicles exhibit the same proton permeability as the *p*HMB-modified enzyme in proton pumping assay experiments.

In this paper, we will look more closely into the question of how the protein modifications alluded to above affect the dioxygen reduction activity and the proton pumping behavior of the enzyme. It is possible that these treatments of the enzyme do disrupt the global structure of the protein sufficiently to modify significantly the intramolecular electron transfer pathways and rates, not to mention the proton-electron coupling in the redox linkage. The latter is particularly relevant if subunit III plays a role in the proton pumping function of the enzyme, since this subunit is typically dissociated from the enzyme or lost from the preparation following these treatments. However, in a recent resonance Raman study (Larsen et al., 1989) comparing the heme environments between these modified proteins and the native enzyme, we noted only minor perturbations of the protein in these regions of the structure. On the other hand, it is quite apparent from our earlier observations that heat treatment and *p*HMB-modification disrupt the tertiary folding of subunit II, particularly in the region of the Cu_A, to modify the redox potential of the Cu_A site. The purpose of the present study is to confirm this result and to place the matter on a more quantitative footing.

MATERIALS AND METHODS:

Materials : Dodecyl maltoside was obtained from Cal-Biochem; *p*-(hydroxymercuri) benzoic acid (*p*HMB), β-Nicotinamide adenine

dinucleotide (NADH) and horse heart cytochrome c (type VI) were purchased from Sigma. All other chemicals were of analytical grade.

Enzyme isolation and purification: Cytochrome c oxidase was isolated and purified from beef heart mitochondria as described by Hartzell and Beinert (1974) and stored at -80 °C before use. Enzyme concentrations were determined from $\Delta A_{\text{red-ox}}$ at 605-630 nm using an extinction coefficient of 27 mM⁻¹cm⁻¹.

Modification of cytochrome c oxidase with pHMB: 5 ml of 93 μ M cytochrome c oxidase was solubilized with 0.10 g dodecyl maltoside in 15 ml of 50 mM Tris-HCl, 50 mM NaCl, pH =7.7. The solution was then saturated with pHMB by addition of 38 mg of this sulfhydryl reagent with periodic stirring at 20 °C. The reaction time was 24 hours unless otherwise specified. At the end of the incubation the mixture was cooled to 4 °C and centrifuged at 20,000 rpm in a Sorvall SS-34 rotor for 40 minutes to remove undissolved pHMB. To remove unreacted pHMB from the solution, the supernatant was transferred to a stirred pressure ultrafiltration apparatus (Amicon 8010 cell with a XM 300 membrane) at 4 °C and subjected to four cycles of dilution to 10 ml and concentration to 1 ml under 10 psig of N₂ gas with fresh 50 mM K₂HPO₄, pH=6.63 buffer solution containing 0.5% Tween-20. K₂HPO₄ was used to buffer the solutions

since the pH of K_2HPO_4 is relatively insensitive to temperature. After the final concentration step, the enzyme solution was stored at $-80\text{ }^\circ\text{C}$ for future use. The typical EPR spectra of the pHMB-modified oxidase is showed in Fig. 1B.

Reduction of the pHMB-modified cytochrome c oxidase by ascorbate/cytochrome c: Enzyme samples were made anaerobic by repeated cycles of vacuum/Ar in an anaerobic optical cell. Addition of ascorbate/cytochrome c was accomplished using an anaerobic syringe. Following addition of one equivalent of ascorbate and 0.05 equivalent of cytochrome c, the samples were kept at $4\text{ }^\circ\text{C}$ overnight in order to fully reduce Fe_a . The percentage of Fe_a reduced was determined by the increases in absorbance at 443 nm and 605 nm (Fig. 2); approximately 95% of Fe_a was reduced by ascorbate/cytochrome c under these conditions, while Fe_{a3} , Cu_B and the modified Cu_A remained oxidized consistent with previous experiments (Gelles & Chan, 1985). This pHMB-modified ascorbate/cytochrome c pre-reduced enzyme is henceforth referred to as Fe_a pre-reduced pHMB-modified oxidase.

Reduction of the pHMB-modified enzyme by Carbon Monoxide : Enzyme samples placed in anaerobic optical cells were thoroughly de-

Fig.1 EPR signal from the Cu_A site in cytochrome c oxidase. (A) Native resting oxidase. (B) *p*HMB-modified oxidase. (C) Heat-treated oxidase. Spectrometer conditions: microwave Frequency 9.128 GHz; microwave power 5 mV; modulation frequency 100 KHz; modulation amplitude 10.0 G, sample temperature 77 K.

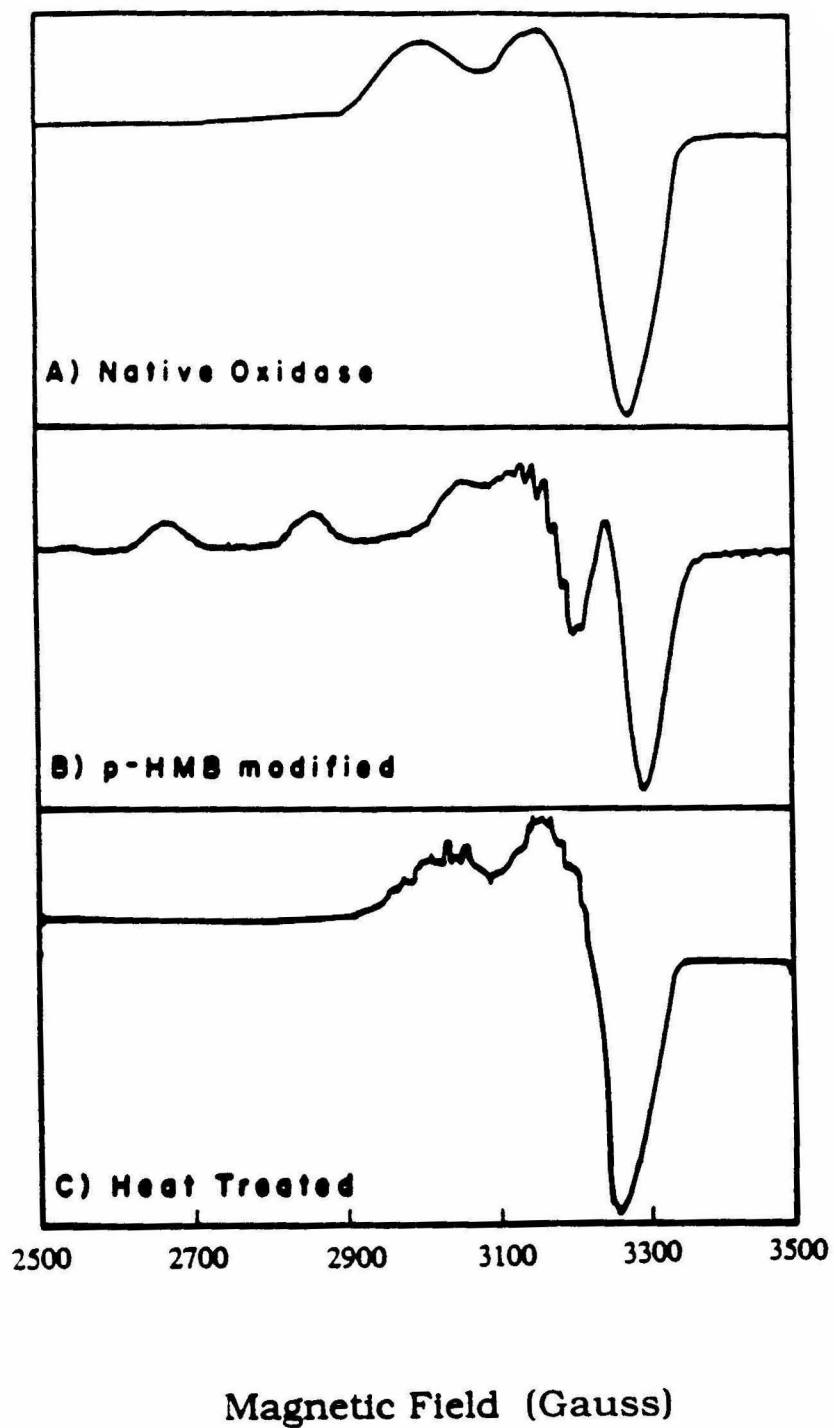
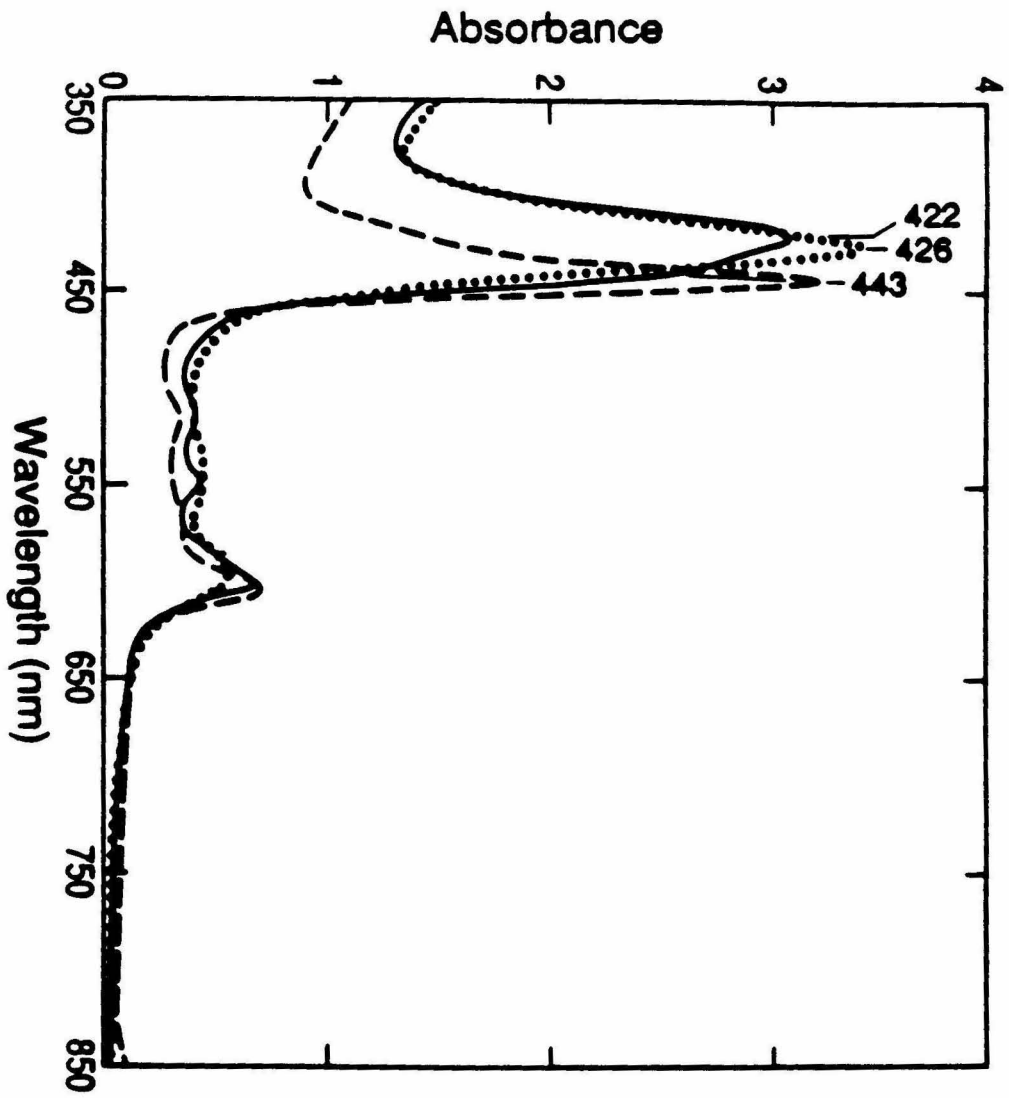


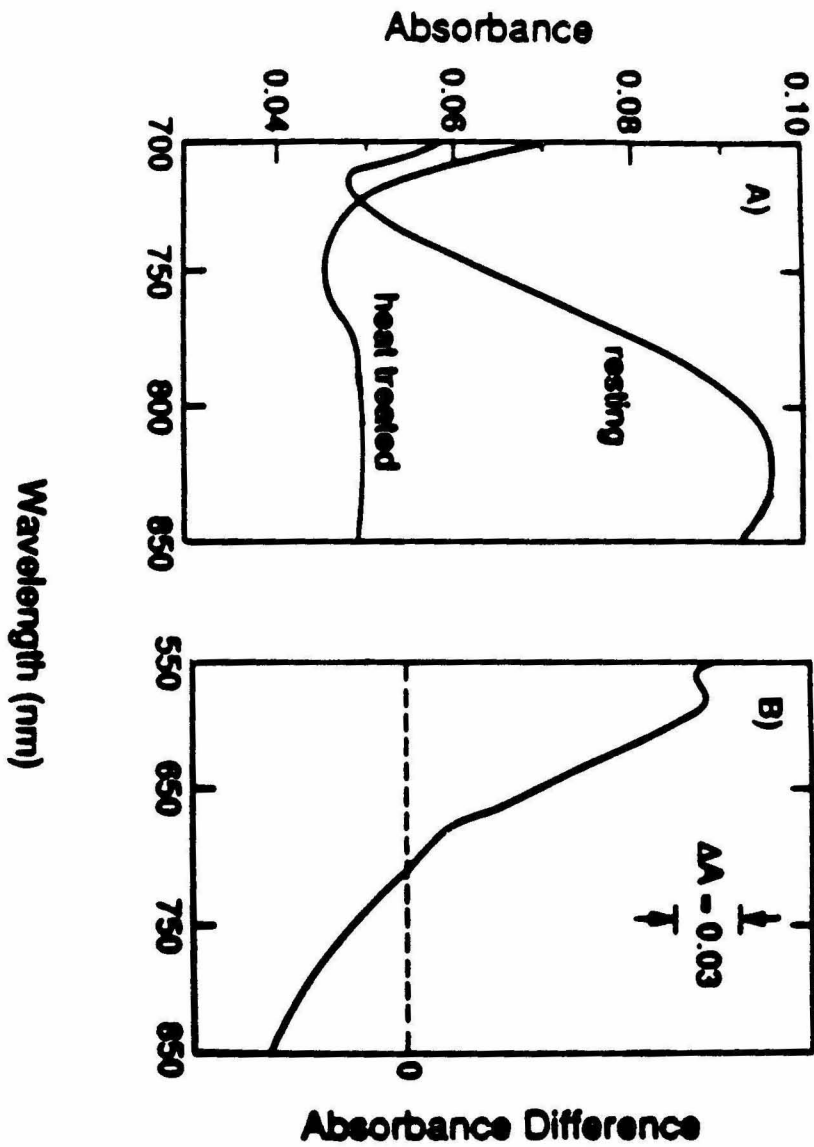
Fig. 2 Visible spectra of Cu_A -modified cytochrome c oxidase, sample temperature 4 °C. (—): Heat-treated oxidase (concentration 14 μM) fully reduced by NADH; (---): Ascorbate/cytochrome c reduced pHMB-modified oxidase (concentration 22 μM); (.....): CO reduced pHMB-modified oxidase (concentration 18 μM).



gassed and subsequently exposed to one atm of CO (99.99%, Matheson) at 4 °C for 22 hours. The degree of reduction of Fe_{a3} and Cu_B was determined from the absorbance at 590 nm using an extinction coefficient of 26 mM⁻¹cm⁻¹ (Fig. 2). Approximately 90% of Fe_{a3} and Cu_B were reduced by carbon monoxide according to the procedure, while Cu_A and Fe_a remained oxidized as previously shown (Gelles & Chan, 1985). This pHMB-modified CO pre-reduced enzyme is henceforth referred to as Fe_{a3}/Cu_B pre-reduced pHMB-modified oxidase.

Heat Treatment of Cytochrome c oxidase: Fully oxidized cytochrome c oxidase samples were diluted to a concentration of 42 μM in 50 mM K₂HPO₄; 0.5% dodecyl β-D maltoside (pH=7.3 at 20°C) in a 2 mm pathlength cell and incubated at 40°C for 75 min in a constant-temperature water bath. The heat-treated enzyme samples were then equilibrated to ice temperature before further treatment or characterization. EPR and UV-Visible spectra were used to ascertain the percentage of Cu_A that had been converted to a type 1 or type 2 copper center (Fig. 1C and Fig. 3). Typically, 90% of the Cu_A is converted to a type 1 blue copper according to this procedure (Li et al., 1988), and the heat-treated oxidase retained nearly 100% dioxygen reduction activity relative to the native oxidase.

Fig. 3 (A) Near-IR absorption spectra of native resting oxidase and heat-treated oxidase. (B) Absorption difference spectra: heat-treated minus native oxidase. Conditions: see experimental section.



Determination of the Cu_A reduction potential in pHMB-modified and heat-treated cytochrome c oxidase : Redox titrations were carried out under an atmosphere of argon at room temperature. AgCl/Ag was used as a reference electrode and was calibrated before each experiment by poisoning the reference electrode at 2 V vs. saturated calomel electrode (SCE) in a 4 N HCl solution for 15 minutes. The midpoint potential of this reference electrode was -43 mV vs. SCE at the buffer solution, which is 180 mV vs. standard hydrogen electrode (NHE). Platinum was used as a working electrode. The platinum electrodes were calibrated before each use with 10 mM 1:1 potassium ferricyanide/ferrocyanide in 0.1 M potassium phosphate, pH 7.0.

The Fe_a pre-reduced oxidase and Fe_{a3}/Cu_B pre-reduced oxidase were titrated with microliter quantities of sodium dithionite solution (0.2 M) in the presence of 0.5 equivalent of each of the redox mediators (see Table 1). The redox mediators used in these experiments were selected on the basis of their negligible optical absorbance in the UV-Visible region. They also have reduction potentials that allow the solution potential to be poised from -200 mV to 300 mV vs. NHE. These mediators are well known as artificial electron donors in studies of biological systems since they do not interact strongly with redox enzymes (Dawson, R. M. C. et al., 1986).

TABLE 1: Redox Mediators

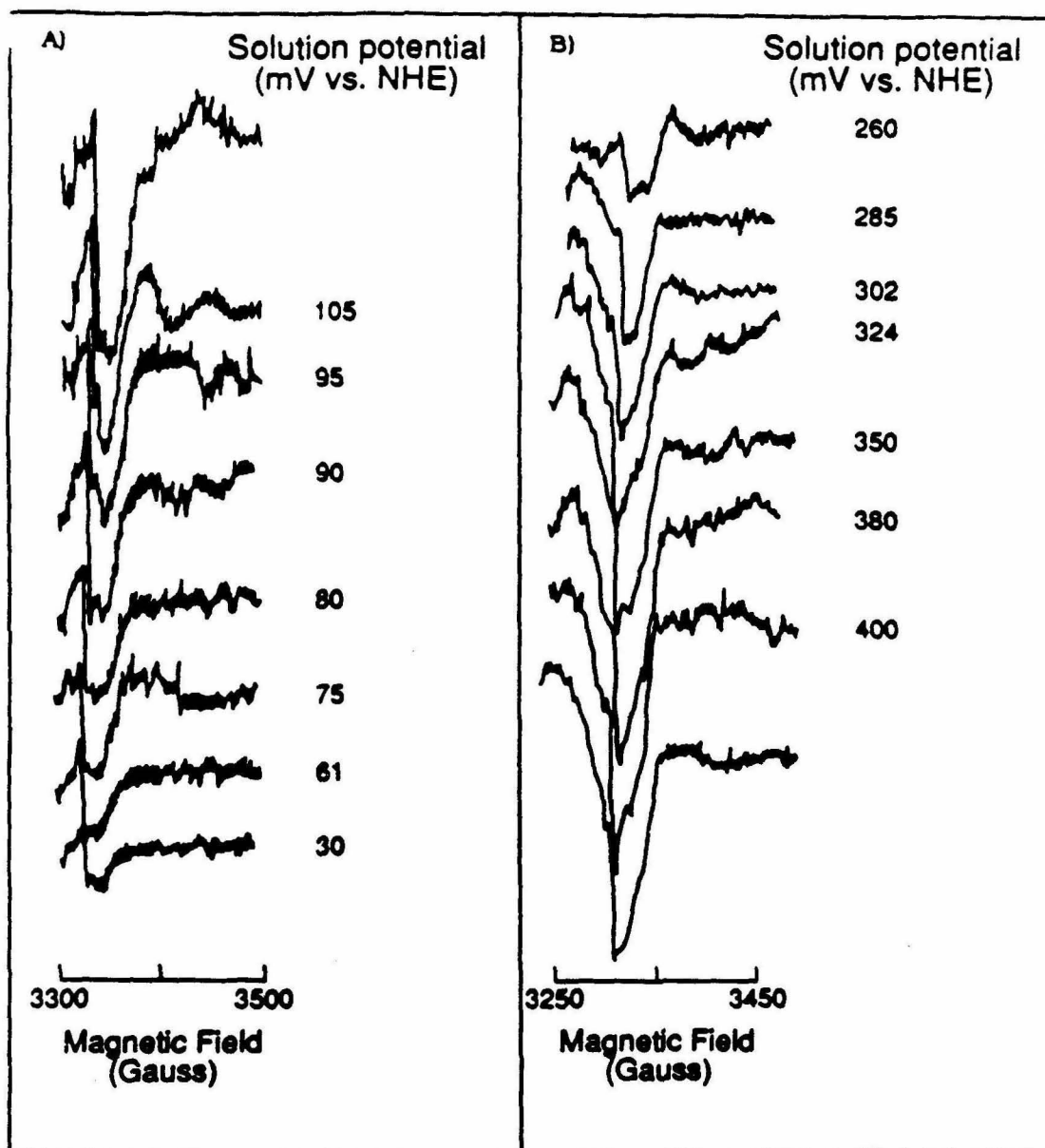
<u>Compounds</u>	<u>Reduction potential</u>
1,4-Benzoquinone	+270 mV
1,2-Naphthoquinone	+157 mV
2-methyl-1,4-Naphthoquinone	0 mV
2-hydroxy-1,4-Naphthoquinone	-139 mV

The reduction potentials of the solutions were measured by a digital multimeter (8000A FLUKE) after 0.5 hour of incubation. Following the experiment, samples were transferred anaerobically to 4 mm O.D. quartz EPR tubes and rapidly frozen in liquid nitrogen (Fig. 4A).

Determination of the Cu_A reduction potential of the heat-treated oxidase was conducted in a similar way, except that the enzyme was fully reduced first by the addition of 1.1 equivalent NADH, then titrated with microliter quantities of 0.1 M $\text{K}_3\text{Fe}(\text{CN})_6$ in the presence of redox mediators (Fig. 4B).

Apparatus: UV-Visible absorption spectra were recorded on a Beckman DU-7 spectrophotometer, interfaced to an IBM AT computer. EPR experiments were run on an E-line Century series EPR spectrometer at liquid nitrogen temperature. Samples for the optical experiments were loaded into anaerobic precision 10mm quartz cuvettes. EPR samples were contained in anaerobic 4 mm o. d. quartz EPR tubes. Redox titrations were carried out in a VAC glove box.

Fig. 4 Redox titration of the Cu_A site in two Cu_A -modified cytochrome c oxidase monitored by the Cu_A EPR spectra at liquid N_2 temperature. (A) One atm. CO pre-reduced pHMB-modified enzyme at $\text{pH}=6.63$. Redox titration was performed anaerobically with $0.2 \text{ M Na}_2\text{S}_2\text{O}_4$ in the presence of redox mediators, sample concentration $18 \mu\text{M}$. (B) Heat-treated enzyme at $\text{pH}=7.30$. Enzyme was prereduced by NADH, and redox titration was performed anaerobically with $0.1 \text{ M K}_3\text{Fe}(\text{CN})_6$ in the presence of redox mediators, sample concentration $40 \mu\text{M}$. Spectrometer conditions same as Fig. 1.



Nernst plots: The equilibrium concentration ratios of the oxidized to reduced forms (ox/red) of an isolated redox couple in solution can be related to the appearance midpoint reduction potential (E°) of the redox couple according to the Nernst equation:

$$E = E^\circ_1 + \frac{2.303RT}{n^*F} \log\left(\frac{\text{ox}}{\text{red}}\right)_1 \quad (1)$$

Here E is the applied potential, the subscript 1 refers to the redox couple under consideration and n^* is the appearance number of electrons involved in the redox reaction. However, in a metalloprotein with interacting multi-redox centers, such as cytochrome c oxidase, n^* , is non-integer, and the observed midpoint potential (E^0) is not a meaningful measure of the intrinsic thermodynamic properties of the site. Instead, E°_1 depends critically upon the interactions of the site under observation with the other redox centers; the manifestation of this redox interaction in the redox titration depends on the potentials of the interacting partners as well (Blair et al., 1986; Wang et al., 1986; Ellis et al., 1986).

In the simplest interaction model, it is assumed that only one interaction dominates the titration behavior of a given site, or equivalently, that all of the operative interactions may be combined into a single effective interaction for purposes of estimating the intrinsic reduction potentials of the redox centers when all the sites

are oxidized. Within this approximation, the equation which describes the simplest interaction system is:

$$\log\left(\frac{\text{OX}}{\text{Red}}\right)_1 = \frac{F(E-E^{\circ}_1)}{2.303RT} + \log\left\{1 + \exp\left[\frac{F}{RT}(E^{\circ}_2 - E)\right]\right\} - \log\left\{1 + \exp\left[\frac{F}{RT}(E^{\circ}_2 - E + \Delta E)\right]\right\} \quad (2)$$

where E°_1 and E°_2 denote, respectively, the intrinsic reduction potential of the site under observation and that of the interacting site. ΔE is the interaction potential between the two sites. When ΔE is positive, the interaction is cooperative; when ΔE is negative, it is anticooperative.

In a redox titration of such a system, two asymptotic potentials may be defined as corresponding, whether the site is being titrated from the fully oxidized system (i. e., both redox centers oxidized), or from the fully reduced states (i. e., both redox centers reduced). When the redox interaction is anticooperative, the upper asymptotic potential of the site under observation, E_1^{upper} , corresponds to E°_1 ; and the lower asymptotic potential E_1^{lower} , is $E^{\circ}_1 + \Delta E$. For a cooperative interaction, $E_1^{\text{lower}} = E^{\circ}$, and $E_1^{\text{upper}} = E^{\circ}_1 + \Delta E$ (Fig. 5).

Fig. 5 The relationship between intrinsic, midpoint, upper asymptotic, lower asymptotic potentials in the redox titration of a system with interacting redox centers.

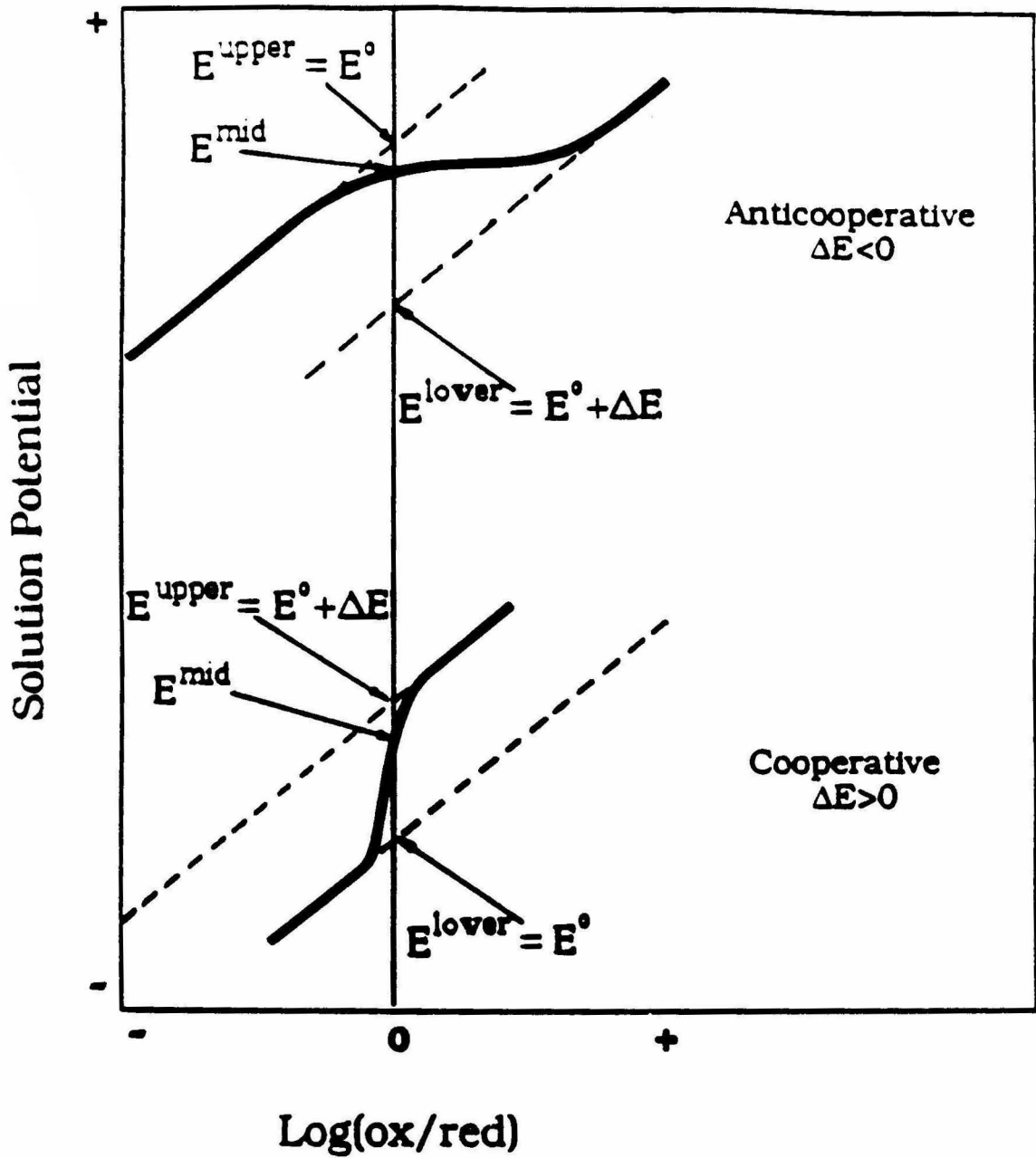


Fig. 6 Simulated Nernst plots for redox titration of a redox center (observed site) in redox interaction with a redox partner (interactant). (A) The intrinsic reduction potential of the interactant (E^0_2) interacting with the observed site is held at 150 mV, and that of observed site (E^0_1) is varied in 50 mV increments between -150 and 350 mV. The redox interaction (ΔE) is maintained at +50 mV (cooperative). (B) The intrinsic reduction potentials of both the observed site (E^0_1) and the interactant (E^0_2) are held at 150 mV while the interaction potential (ΔE) is varied in 10 mV increments between -10 and -90 mV (anticooperative).

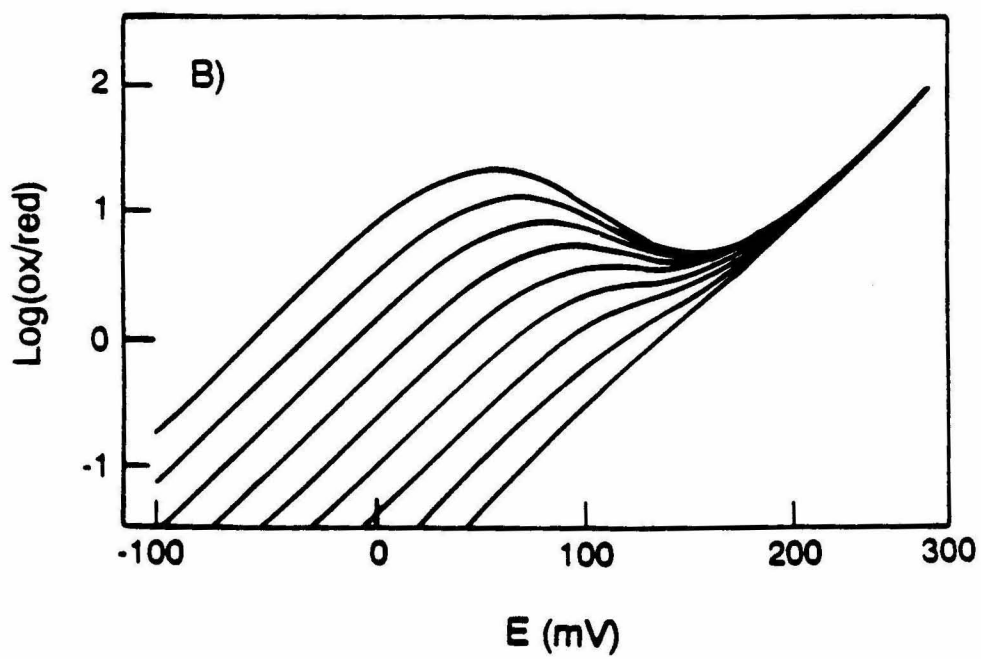
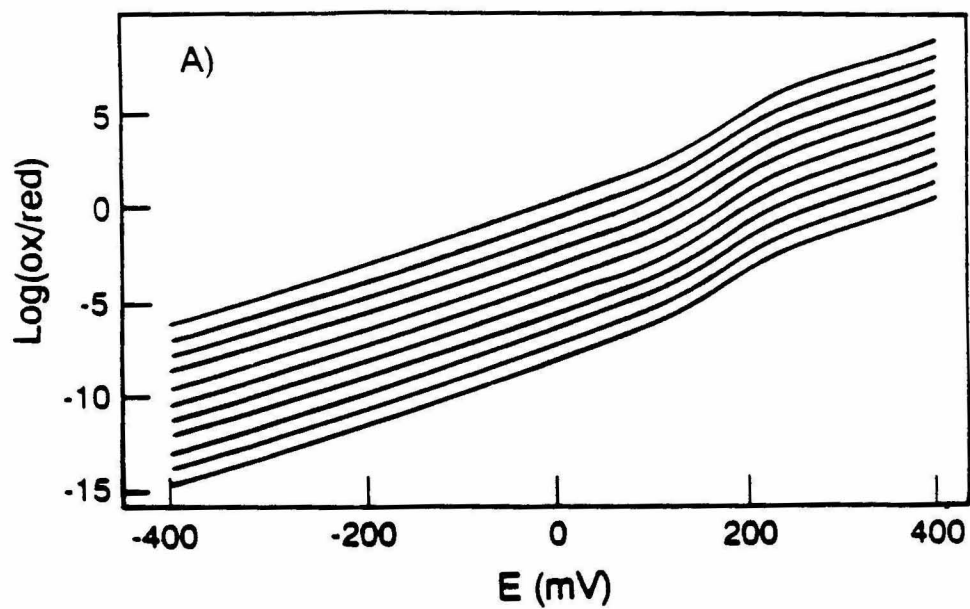
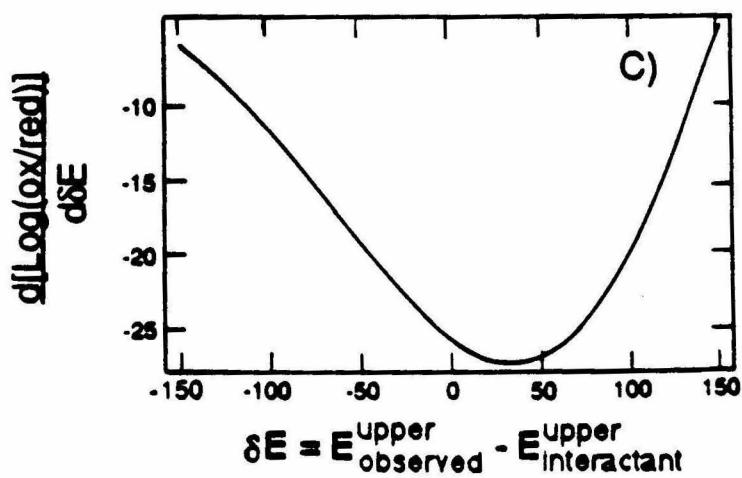
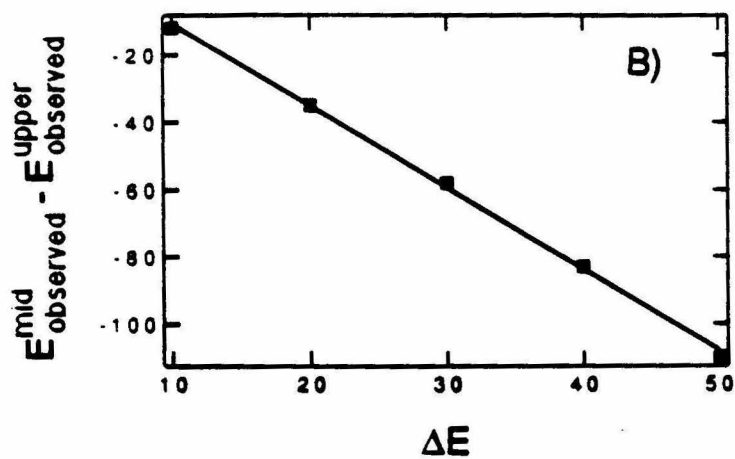
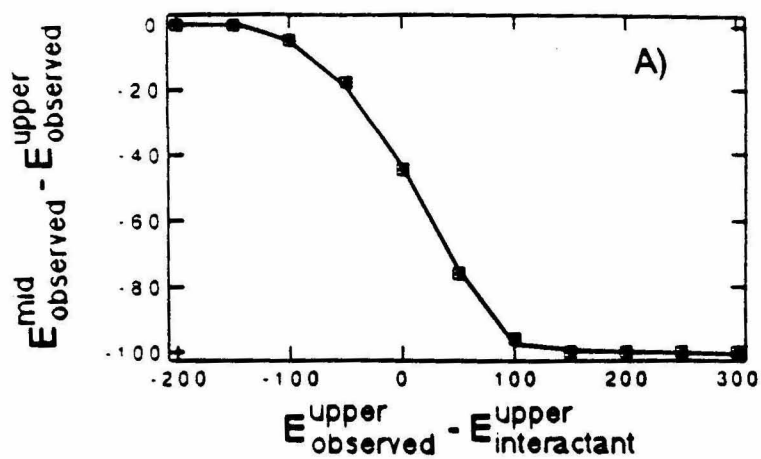


Fig. 6 (A) and (B) depict computer simulations of Nernst plots for redox titration of a redox center undergoing redox interactions with one other site. In (A), the intrinsic reduction potential of the interactant (E°_2) interacting with the observed site is held at 150 mV, and that of observed site (E°_1) is varied in 50 mV increments between -150 and 350 mV. The redox interaction (ΔE) is maintained at +50 mV (cooperative). In (B), the intrinsic reduction potentials of both the observed site (E°_1) and the interactant (E°_2) are held at 150 mV while the interaction potential (ΔE) is varied in 10 mV increments between -10 and -90 mV (anticooperative). From these Nernst plots, it is clear that the *observed* midpoint potential of the site under observation depends critically on the intrinsic reduction potential of the interactant (Fig. 7(A)), as well as the magnitude of the interaction potential between the two sites (Fig. 7(B)). Specifically, the closer the potentials of the two sites are matched, the stronger is the interaction between the sites manifested in the redox titration (see Fig. 7(C), the derivative of Fig. 7(A)).

The above analysis can be readily extended to m interacting sites. For this more general situation, the equilibrium (ox/red) value of site 1 can be expressed as:

Fig. 7 (A) A plot of the difference between the calculated midpoint and upper asymptotic potentials of a redox center (observed site) as a function of the difference in the upper asymptotic potentials between the observed and the interactant sites for case A in Fig 6. (B) A plot of the difference between the calculated midpoint and upper asymptotic potentials of the observed site as a function of the interaction potential between the observed and interacting sites for case B in Fig. 6 (C) The derivative of (A).



$$\begin{aligned}
\log\left(\frac{\text{ox}}{\text{red}}\right)_1 = & \\
& \frac{F(E-E^0_1)}{2.303RT} + \log\left\{1 + \sum_{k=2}^m \exp\left[\frac{F}{RT}(E^0_k - E)\right] + \sum_{k \geq 2}^m \sum_{j > k}^m \exp\left[\frac{F}{RT}(E^0_k + E^0_j - 2E + \Delta E_{kj})\right] \right. \\
& + \sum_{k \geq 2}^m \sum_{j > k}^m \sum_{l > j}^m \exp\left[\frac{F}{RT}(E^0_k + E^0_j + E^0_l - 3E + \Delta E_{kj} + \Delta E_{jl} + \Delta E_{kl})\right] + \dots \left. \right\} \\
& - \log\left\{1 + \sum_{k \geq 2}^m \exp\left[\frac{F}{RT}(E^0_k - E + \Delta E_{1k})\right] \right. \\
& + \sum_{k \geq 2}^m \sum_{j > k}^m \exp\left[\frac{F}{RT}(E^0_k + E^0_j - 2E + \Delta E_{1k} + \Delta E_{1j} + \Delta E_{jk})\right] \\
& \left. \sum_{k \geq 2}^p \sum_{j > k}^p \sum_{l > j}^p \exp\left[\frac{F}{RT}(E^0_k + E^0_j + E^0_l + \sum_{p}^{1jk} \sum_{n > p}^{jk} \Delta E_{pn} + \dots)\right]\right\} \quad (3)
\end{aligned}$$

In cytochrome c oxidase, *m* is four. Thus,

$$\begin{aligned}
\log\left(\frac{\text{ox}}{\text{red}}\right)_1 = & \\
& \frac{F(E-E^0_1)}{2.303RT} + \log\left\{1 + \exp\left[\frac{F}{RT}(E^0_2 - E)\right] + \exp\left[\frac{F}{RT}(E^0_3 - E)\right] + \exp\left[\frac{F}{RT}(E^0_4 - E)\right] \right. \\
& + \exp\left[\frac{F}{RT}(E^0_2 + E^0_4 - 2E + \Delta E_{24})\right] + \exp\left[\frac{F}{RT}(E^0_3 + E^0_4 - 2E + \Delta E_{34})\right] + \exp\left[\frac{F}{RT}(E^0_2 + E^0_3 - 2E + \Delta E_{23})\right] \\
& + \exp\left[\frac{F}{RT}(E^0_2 + E^0_3 + E^0_4 + \Delta E_{23} + \Delta E_{34} + \Delta E_{34})\right] \left. \right\} - \log\left\{1 + \exp\left[\frac{F}{RT}(E^0_2 - E + \Delta E_{12})\right] + \exp\left[\frac{F}{RT}(E^0_3 - \right. \right. \\
& \left. \left. E + \Delta E_{13})\right] + \exp\left[\frac{F}{RT}(E^0_4 - E + \Delta E_{14})\right] + \exp\left[\frac{F}{RT}(E^0_2 + E^0_3 - 2E + \Delta E_{12} + \Delta E_{13} + \Delta E_{23})\right] + \right. \\
& \exp\left[\frac{F}{RT}(E^0_2 + E^0_4 - 2E + \Delta E_{12} + \Delta E_{14} + \Delta E_{24})\right] + \exp\left[\frac{F}{RT}(E^0_3 + E^0_4 - 2E + \Delta E_{13} + \Delta E_{14} + \Delta E_{34})\right] \\
& \left. + \exp\left[\frac{F}{RT}(E^0_2 + E^0_3 + E^0_4 - 3E + \Delta E_{12} + \Delta E_{13} + \Delta E_{14} + \Delta E_{23} + \Delta E_{24} + \Delta E_{34})\right]\right\} \quad (4)
\end{aligned}$$

E°_1 , E°_2 , E°_3 and E°_4 are the intrinsic reduction potentials of the four metal sites when their respective interaction partners are oxidized and ΔE_{in} is the interaction potential that changes the reduction potential of site i when site n is reduced.

In the present study, some of the redox titrations were carried out with one of the redox centers of cytochrome c oxidase held in the reduced state (e. g., Fe_a in pHMB-modified oxidase). In this case, m becomes three and the intrinsic reduction potentials of sites 1, 2 and 3 are modified and replaced by their respective upper or lower asymptotic potentials when site 4 is reduced, depending on whether the interaction of site 4 with a specific site is cooperative or anticooperative. Equation (4) then becomes:

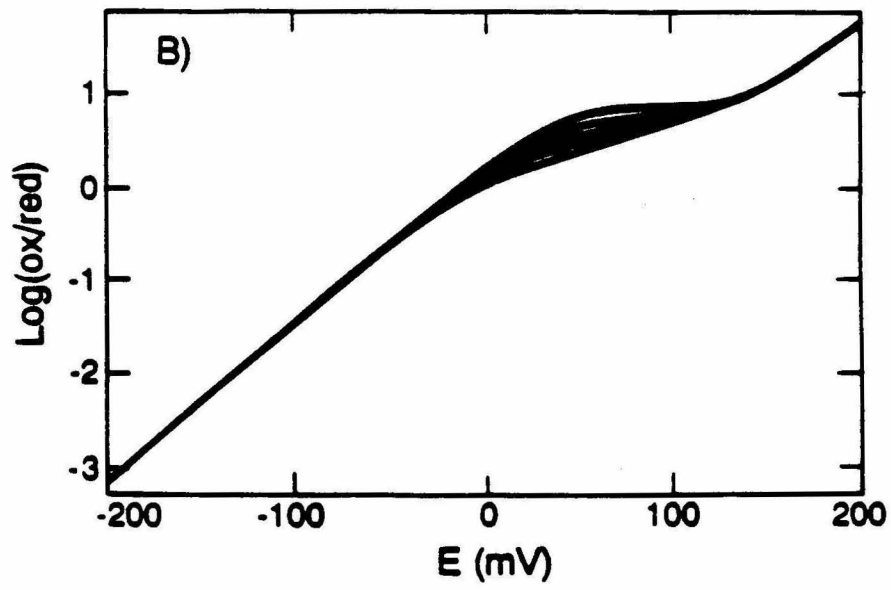
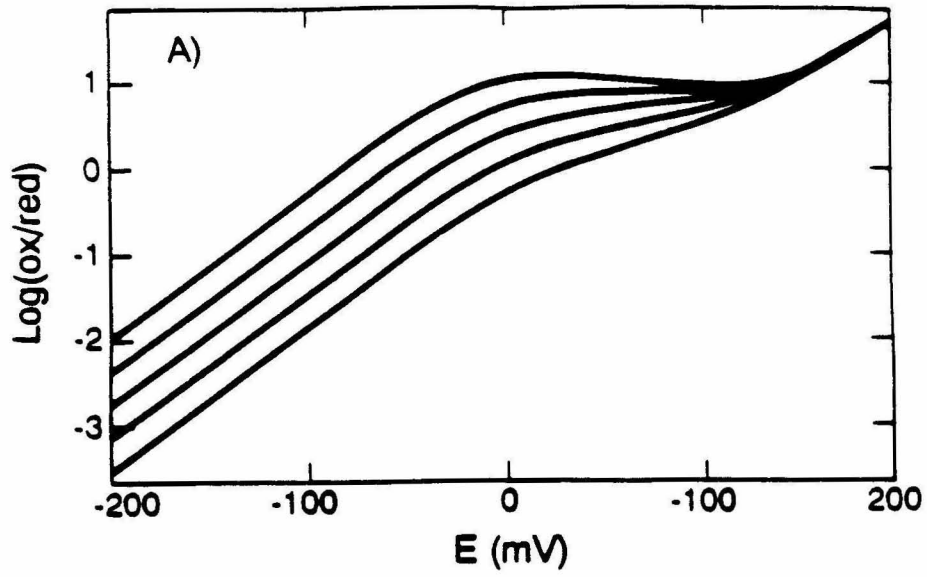
$$\begin{aligned} \log\left(\frac{ox}{red}\right)^1 &= \frac{F(E-E'_1)}{2.303RT} + \log\left\{1 + \exp\left[\frac{F}{RT}(E'_2-E)\right] \right. \\ &+ \exp\left[\frac{F}{RT}(E'_3-E) + \exp\left[\frac{F}{RT}(E'_2+E'_3-2E+\Delta E_{23})\right]\right\} \\ &- \log\left\{1 + \exp\left[\frac{F}{RT}(E'_2-E+\Delta E_{12})\right] + \exp\left[\frac{F}{RT}(E'_3-E+\Delta E_{13})\right] \right. \\ &\left. + \exp\left[\frac{F}{RT}(E'_2+E'_3-2E+\Delta E_{12}+\Delta E_{13}+\Delta E_{23})\right]\right\} \end{aligned} \quad (5)$$

where $E'_1 = E^\circ_1 + \Delta E_{14}$, $E'_2 = E^\circ_2 + \Delta E_{24}$ and $E'_3 = E^\circ_3 + \Delta E_{34}$, that is the "intrinsic" reduction potentials of sites 1, 2 and 3, respectively, when site 4 is reduced. Equation (5) simplifies further to (6) when the two interacting partners have the same redox potentials ($E_2 = E_3$), and they interact with the reduced site with the same interaction potential ($\Delta E'_{24} = \Delta E'_{34}$), so that $E'_2 = E_2 + \Delta E'_{24} = E'_3 = E_3 + \Delta E'_{34} = E'_{23}$.

$$\begin{aligned} \log\left(\frac{\text{ox}}{\text{red}}\right)_1 &= \frac{F(E-E'_1)}{2.303RT} + \log\left\{1 + 2\exp\left[\frac{F}{RT}(E'_{23}-E)\right]\right. \\ &+ \left.\exp\left[\frac{F}{RT}(2E'_{23}-2E+\Delta E_{23})\right]\right\} - \log\left\{1 + \exp\left[\frac{F}{RT}(E'_{23}-E+\Delta E_{12})\right]\right. \\ &+ \left.\exp\left[\frac{F}{RT}(E'_{23}-E+\Delta E_{13})\right] + \exp\left[\frac{F}{RT}(2E'_{23}+\Delta E_{12}+\Delta E_{13}+\Delta E_{23})\right]\right\} \end{aligned} \quad (6)$$

Fig. 8 (A) and (B) give computer simulations of eq. (6) under various conditions: (A) The modified "intrinsic" reduction potential of the observed site ($E^\circ_1 + \Delta E'_{14}$) is fixed at 100 mV; the corresponding potentials of the two interactants ($E'_{2,3}$) are fixed at 110 mV; the redox interaction between site 1 and site 3 (ΔE_{13}) is fixed at -30 mV; the redox interaction between sites 2 and 3 (ΔE_{23}) is fixed at -40 mV; and the magnitude of the interaction between site 1 and site 2 (ΔE_{12}) is varied in 10 mV increments between -10 and -50 mV. (B) The corresponding potential of the observed site ($E^\circ_1 + \Delta E'_{14}$) is held at 100 mV; the modified "intrinsic" reduction potentials of the two interactants ($E'_{2,3}$) are fixed at 110 mV; the interaction between sites

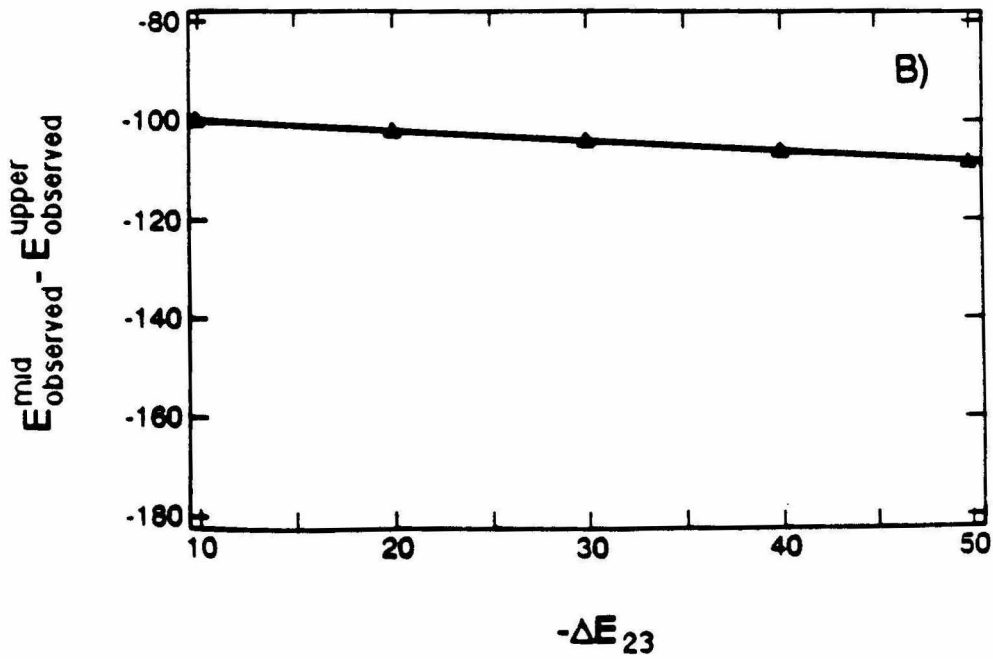
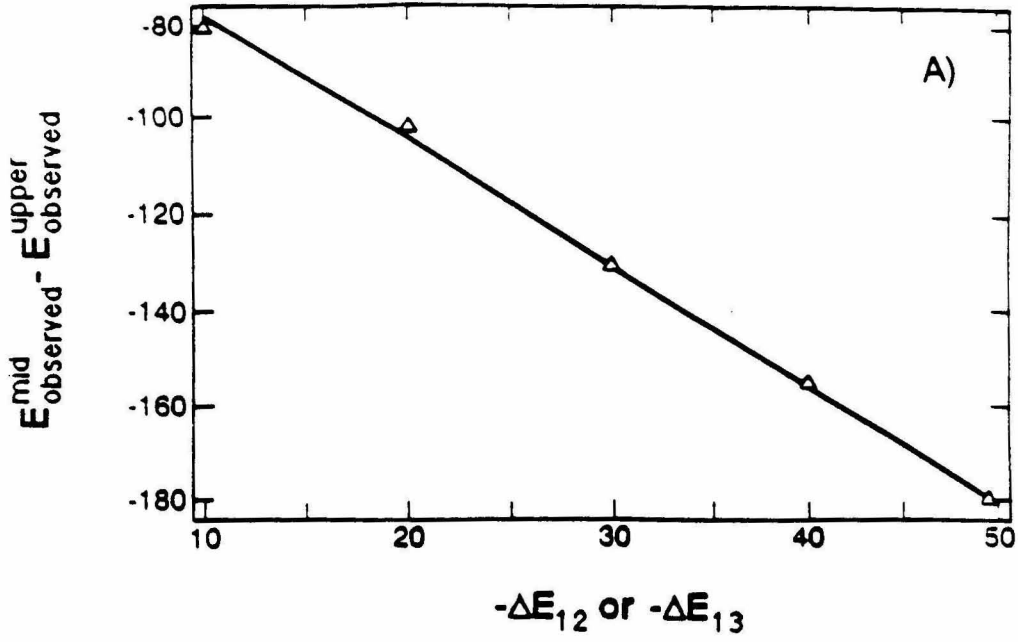
Fig. 8 Simulated Nernst plots for redox titration of a redox center (observed site) in redox interaction with multiple redox partners (interactants) in cytochrome c oxidase. Site 1: observed site; sites 2 and 3: interacting redox partners; site 4: reduced. (A) The modified "intrinsic" reduction potential of the observed site ($E^{\circ}_1 + \Delta E'_{14}$) is fixed at 100 mV; the corresponding potentials of the two interactants ($E'_{2,3}$) are fixed at 110 mV; the redox interaction between sites 1 and 3 (E_{13}) is fixed at -30 mV; the redox interaction between sites 2 and 3 (ΔE_{23}) is fixed at -40 mV; and the interaction potential between sites 1 and 2 (ΔE_{12}) is varied in 10 mV increments between -10 and -50 mV. (B) The corresponding potential of the observed site ($E^{\circ}_1 + \Delta E'_{14}$) is held at 100 mV; the modified "intrinsic" reduction potentials of the two interactants ($E'_{2,3}$) are fixed at 110 mV; the interaction potential between sites 1 and 2 (ΔE_{12}) is fixed at -20 mV; the redox interaction between site 1 and 3 (ΔE_{13}) is fixed at -20 mV; the redox interaction between site 1 and 3 (ΔE_{13}) is fixed at -30 mV; and the redox interaction between sites 2 and 3 (ΔE_{23}) is varied in 10 mV increments between -10 and -50 mV.



1 and 2 (ΔE_{12}) is fixed at -20 mV; the redox interaction between sites 1 and 3 (ΔE_{13}) is fixed at -30 mV; while the redox interaction between sites 2 and 3 (ΔE_{23}) is varied in 10 mV increments between -10 and -50 mV. Since the Nernst plots in Fig. 8 (A) and (B) are very similar to Fig. 6 (B), it is evident that it is impossible to distinguish between a simple interacting system with only 2 redox centers and a more complex situation involving more than 1 redox interactions. Nevertheless, these simulations do indicate that ΔE_{12} and ΔE_{13} together account for the departure of the Nernst plots from linearity (Fig 9 (A) and (B)). Moreover, to a good approximation, the Nernst plots can be simulated quite well by the simple interaction model with an overall effective $\Delta E = \Delta E_{12} + \Delta E_{13}$, provided that the reduction potentials of the interactants are sufficiently similar.

Similar relationships may be derived for redox titrations in which additional redox centers are held in the reduced state. However, in preparations of the mixed valence cytochrome c oxidase, where both metal centers of the binuclear clusters are reduced and inhibited by CO, the problem merely reduces to the simple two-site case. Here again, for proper comparison, the intrinsic reduction potentials of the redox active centers must be modified to account for redox interactions with the reduced sites.

Fig. 9 (A) A plot of the difference between the calculated midpoint and upper asymptotic potentials of the observed site as a function of interaction potential between the observed site (site 1) and one of the interacting sites for case A of Fig. 8. (B) A plot of the difference between the midpoint and upper asymptotic potentials of the observed site as a function of interaction potential between the two interacting sites (site 2 and site 3) for case B of Fig. 8.



Data analysis: (1) In the titration experiments on the pHMB-modified oxidase, the solution redox potentials were recorded after 0.5 hour of temperature equilibrium at room temperature and equilibrium (ox/red) values of the modified Cu_A site were determined from the amplitude changes of the type 2 Cu_A EPR spectra at $g=2.05$ recorded at liquid N_2 temperature. While electron redistribution can occur during the sample cooling, several lines of evidence based on redox titration of native oxidase at room-temperature by optical absorbance spectroscopy and low temperature EPR measurements suggest that such electron redistribution is minimal (Goodman, 1984). When the redox titrations were carried out on the Fe_a pre-reduced oxidase, computer fitting of the Nernst plots to equation (6) gave the intrinsic reduction potential (upper asymptotic potential) of the modified Cu_A site when Fe_a is reduced, the corresponding potential of Cu_B and/or Fe_{a3} , as well as the overall effective interaction potential between the modified Cu_A site and Cu_B , Fe_{a3} . When the redox titrations were done on the CO-inhibited pHMB-modified enzyme, we obtained the intrinsic reduction potentials of both Fe_a and the modified Cu_A center when the binuclear site is reduced, together with the interaction potential between the two redox active centers. From these results, the total interaction potential between the modified Cu_A site and the three other redox centers in the enzyme can be estimated.

(2) In redox titrations of the Cu_A site in the heat-treated type 1- Cu_A oxidase, the equilibrium (ox/red) values were determined from amplitudes of the EPR spectra of the modified- Cu_A site at $g=1.98$ after 0.5 hour of incubations of the fully reduced enzyme with varying equivalents of $\text{K}_3\text{Fe}(\text{CN})_6$. The same procedure was used to analyze the Cu_A redox titration data for the heat-treated oxidase.

RESULTS :

The EPR spectra of cytochrome c oxidase at liquid N_2 temperature (Fig. 1 and Fig. 4) contain contributions primarily from the Cu_A center. In all our experiments, the Nernst plots for the titrations of the modified Cu_A site exhibited a redox behavior distinct from that expected for an isolated one-electron acceptor [eq. (1)]. Values of n^* and the observed Cu_A appearance midpoint potentials are summarized in Table 2. The larger the deviation of n^* from unity, the stronger are the interactions between the Cu_A site and the other redox centers. The average slope of the Cu_A Nernst plot for the Fe_a pre-reduced *p*HMB-modified enzyme corresponds to $n^*=0.9$, and for $\text{Fe}_{a3}/\text{Cu}_B$ pre-reduced *p*HMB-modified oxidase, $n^*=1.2$. For the heat-treated type 1- Cu_A enzyme, $n^*=0.6$.

TABLE 2

Reduction Potentials and Interaction Parameters Estimated From Potentiometric Titrations of the pHMB-modified and the Heat-treated Cytochrome *c* Oxidase^a

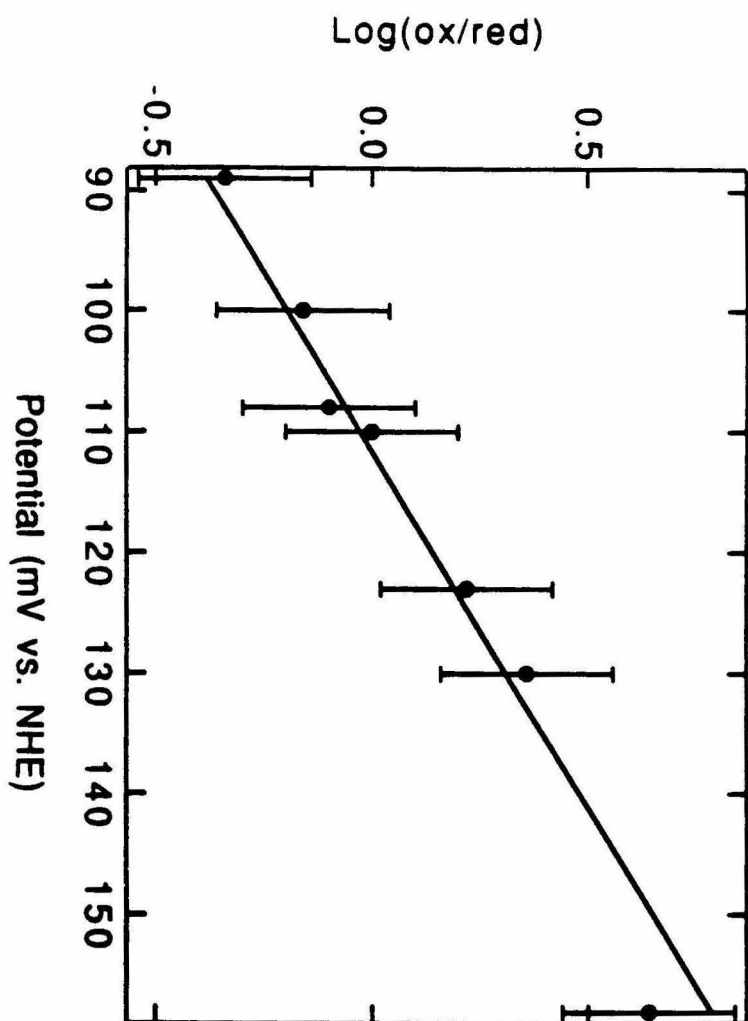
Enzyme species	Fe _a pre-reduced pHMB-modified	Fe _a /Cu _b pre-reduced pHMB-modified	Heat-treated	Fe _a /Cu _b pre-reduced native oxidase
n [*]	0.9	1.2	0.6	0.8
Cu _a appearance midpoint potential (mV)	110	89	300	275
Cu _a lower asymptotic potential (mV)	111	86	288	240
Cu _a upper asymptotic potential (mV)	128	100	358	280
interactant asymptotic potential (mV)	356	290	393	280
interaction potential (mV)	-17	-14	-70	-40
Cu _a intrinsic potential (mV)	128	100	358	280

a: All the potentials are referred to NHE.

In the titration of the Fe_a pre-reduced pHMB-modified oxidase, in which Fe_a is held in its reduced state, the redox equilibrium involves several additional protein species in which one or more of the other redox centers are reduced. Fitting the Cu_A Nernst plot to the simple interaction model with $n=1$ yielded an intrinsic reduction potential ($E'_{\text{Cu}_A} = E^{\circ}_{\text{Cu}_A} + \Delta E_{\text{Cu}_A-\text{Fe}_a}$) of 128 mV vs. NHE for the modified Cu_A site, a total redox interaction ($\Delta E_{\text{Cu}_A-\text{Fe}_a} + \Delta E_{\text{Cu}_A-\text{Cu}_B}$) of about -17 mV, and asymptotic potentials of 356 mV vs. NHE for the interacting sites Cu_B and/or Fe_{a3} ($E'_{\text{Fe}_{a3}} = E^{\circ}_{\text{Fe}_{a3}} + \Delta E_{\text{Fe}_{a3}-\text{Fe}_a}$, and /or $E'_{\text{Cu}_B} = E_{\text{Cu}_B} + \Delta E_{\text{Cu}_B-\text{Fe}_a}$) (Fig. 10).

In the $\text{Fe}_{a3}/\text{Cu}_B$ pre-reduced pHMB-modified oxidase, in which both Fe_{a3} and Cu_B are stabilized in their reduced states, only Fe_a and Cu_A are part of the redox equilibrium. From analysis of the Nernst plots, the intrinsic reduction potential of the modified Cu_A site ($E'_{\text{Cu}_A} = E^{\circ}_{\text{Cu}_A} + \Delta E_{\text{Cu}_A-\text{Cu}_B} + \Delta E_{\text{Cu}_A-\text{Fe}_{a3}}$) was deduced to be 100 mV vs. NHE, the redox interaction between the modified Cu_A and Fe_a ($\Delta E_{\text{Cu}_A-\text{Fe}_a}$) is -14 mV, the asymptotic potential of the interactant Fe_a ($E'_{\text{Fe}_a} = E^{\circ}_{\text{Fe}_a} + \Delta E_{\text{Fe}_a-\text{Cu}_B} + \Delta E_{\text{Fe}_a-\text{Fe}_{a3}}$) is 290 mV vs. NHE (Fig. 11). In the case of heat-treated type 1 Cu_A oxidase (Fig. 12), all metal centers are participating in the redox equilibrium. When the Nernst plots were fitted to the simple interaction model with $n=1$, the Cu_A (intrinsic reduction potential (E'_{Cu_A}) is 358 mV vs. NHE, the total interaction potential ($\Delta E_{\text{Cu}_A-\text{Fe}_a} + \Delta E_{\text{Cu}_A-\text{Cu}_B} + \Delta E_{\text{Cu}_A-\text{Cu}_B}$) is -70 mV, and

Fig.10 Nernst plots for the modified Cu_A -site of Fe_a pre-reduced pHMB-modified oxidase. The line is the computer-generated best fit to the simple two-site interaction model: $E_1=128$, $E_2=356$, $\Delta E=-17$ mV.



the asymptotic potential of the interactant(s) Fe_a , Cu_B , Fe_{a3} ($E^\circ_{\text{Fe}_a}$, $E^\circ_{\text{Cu}_B}$, $E^\circ_{\text{Fe}_{a3}}$) is 393 mV vs. NHE.

Thus, from these potentiometric titrations, we find that the intrinsic reduction potential of the type 2 Cu_A site in the pHMB-modified oxidase is about 150 mV more negative than that of the Cu_A site in native oxidase and that for the type 1 Cu_A in the heat-treated oxidase is almost 100 mV more positive.

DISCUSSION:

The reduction potential of the Cu_A site of native cytochrome oxidase has been measured under a variety of conditions including varying pH values, differing detergents (Gelder et al., 1977), varying temperatures (Wang et al., 1986) and in the presence of various inhibitors. It is generally agreed that the Cu_A site has a midpoint potential of 240 ± 10 mV versus NHE. In addition, it is now known that the Cu_A site participates in anticooperative redox interaction of -40 mV with Fe_a (Goodman, 1984). Blair et al. (1982) have suggested that there may be a similar redox interaction between the Cu_A site and Fe_{a3} and/or Cu_B .

Fig. 11 Nernst plots for the modified Cu_A -site of $\text{Fe}_{23}/\text{Cu}_B$ pre-reduced pHMB-modified oxidase. The line is the computer-generated best fit to the simple two-site interaction model: $E_1=100$, $E_2=290$, $\Delta E=-14$ mV.

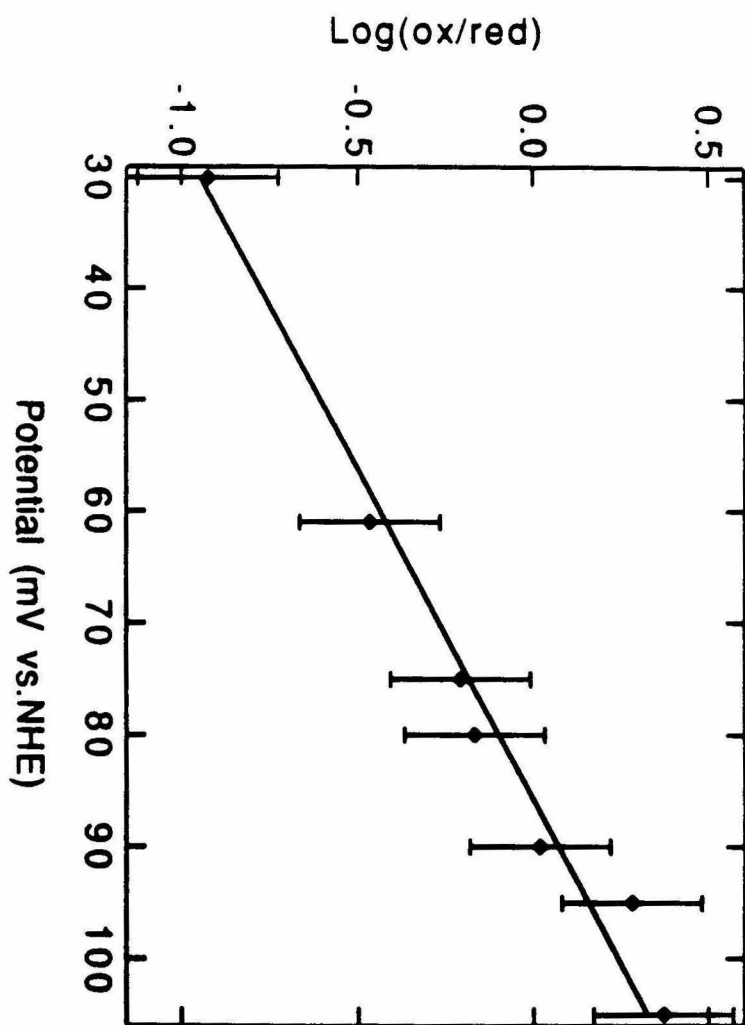
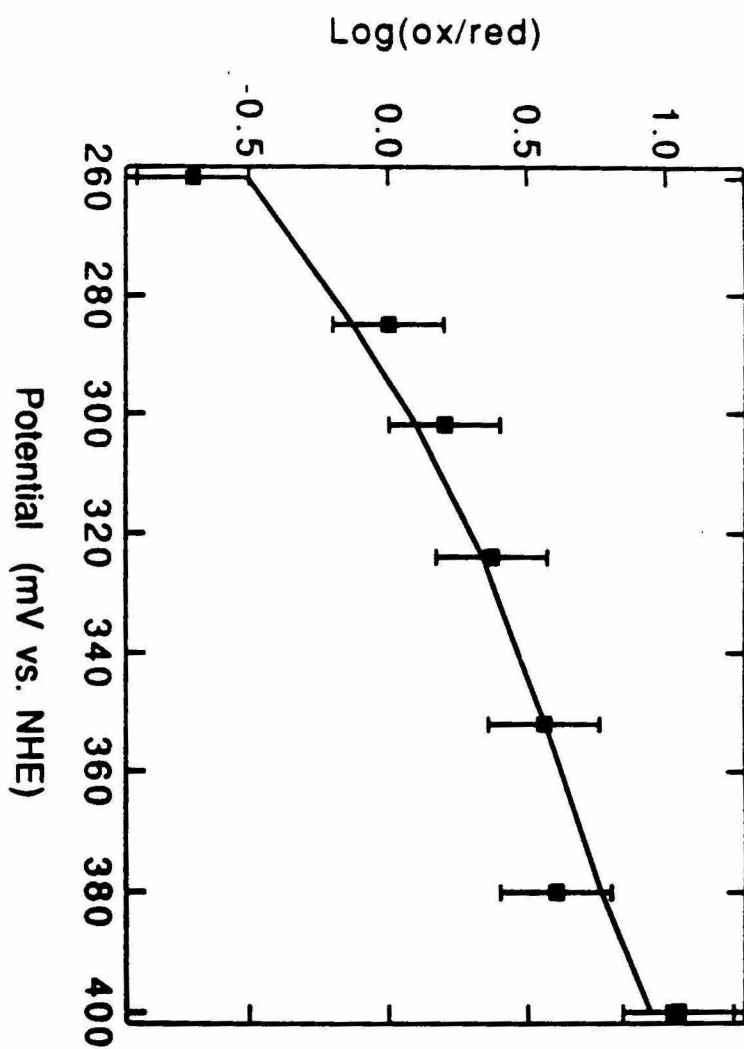


Fig.12 Nernst plots for the modified Cu_A -site of heat treated oxidase. The line is computer-generated best fit to the simple two-site interaction model: $E_1=358$, $E_2=393$, $E'=-70$ mV.



Titration of the Cu_A site in the $\text{Fe}_{a3}/\text{Cu}_B$ pre-reduced pHMB-modified oxidase shows that the conversion of the Cu_A center to a type 2 copper site has lowered the redox potential of the center by as much as 150 mV. As expected, the anticooperative redox interaction between the modified Cu_A and the Fe_a has decreased (from -40 to -14 mV), while the redox potential of the interactant, namely Fe_a , remains essentially the same as that of the Fe_a in the CO-inhibited mixed-valent enzyme. The significantly lower redox potential of the type 2 Cu_A site is confirmed by the results of a similar redox titration of the Fe_a pre-reduced pHMB modified oxidase. Again, the redox potentials of the interactant(s), namely $\text{Fe}_{a3}/\text{Cu}_B$, do not depart significantly from the corresponding potentials for these sites in the native oxidase. A small anticooperative redox interaction of -17 mV is noted between the modified Cu_A site and the binuclear center.

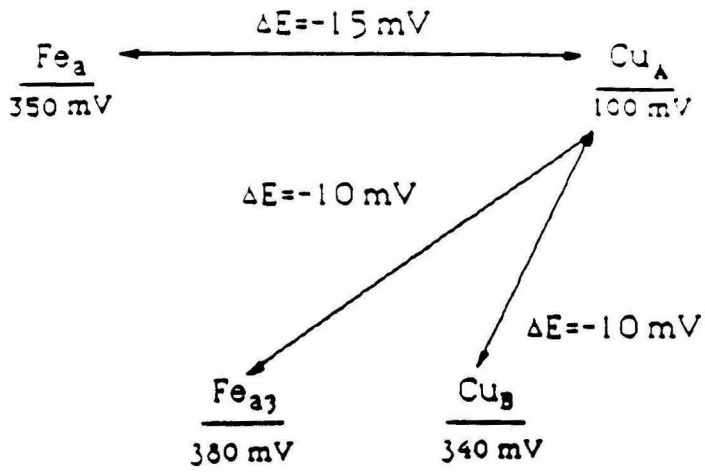
In contrast, the redox potential of the type 1 blue Cu_A in the heat-treated oxidase is more positive than that of the Cu_A in the native enzyme by ~100 mV. More interestingly, this center exhibits anticooperative redox interaction with the other metal centers of ~-70 mV, similar to the redox interaction previously noted for Cu_A and the binuclear center in the native enzyme.

Fig. 13 summarizes the redox interactions among the various redox centers for both modified oxidases. The assignment of the interaction potentials is based on the experimental data derived here as well as the expected manifestation of the redox interaction on the redox potential differences between the interacting sites. The interactions among the metal centers are best explained by a mechanism in which these sites communicate via the protein scaffolding (Wang et al. 1986). From these results, we surmise that the Cu_A site is in a "tense" state in the native enzyme, and it has adopted a more relaxed configuration in the modified type 1 or type 2 form. In a later paper, we shall provide evidence for conformational linkage between subunits II and III. Since subunit III has been depleted in both the type 1 Cu_A and type 2 Cu_A oxidases studied, it may be that subunit III plays a role in stabilizing the "tense" configuration of the native Cu_A site.

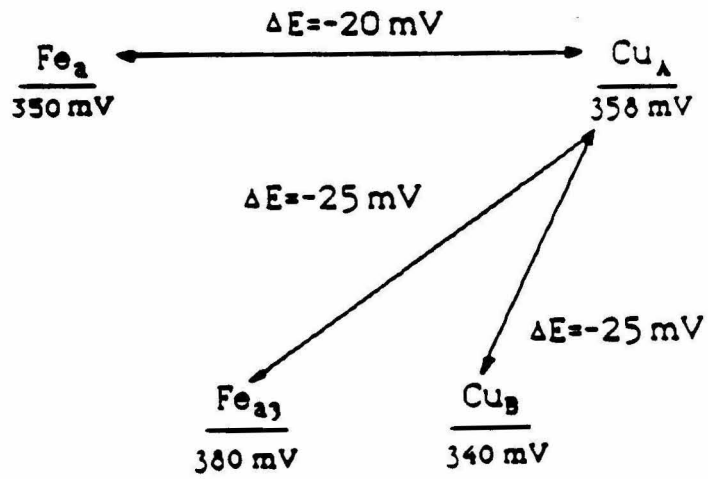
Cu_A-modification influences the dioxygen reduction activity: In native oxidase, the reduction potential of Cu_A is somewhat higher than cytochrome c , and electron transfer from ferrocytochrome c to Cu_A is thermodynamically allowed. In fact, the electron transfer is kinetically facile. This situation maintains for the heat-treated cytochrome oxidase as well, since the Cu_A reduction potential of the type 1 Cu_A site is significantly higher than that in the native enzyme. The almost identical dioxygen reduction activity between the native and heat-

Fig.13 Proposed interaction schemes for the two modified oxidases examined in this study.

pHMB-Modified Oxidase



Heat-Treated Oxidase



treated oxidase most certainly reflects this electron transfer competence of the modified Cu_A site, i.e., facile electron transfer into or out of the site. On the other hand, the redox potential of the type 2 Cu_A site is 150 mV lower than that of the native Cu_A site. Direct electron transfer from ferrocytochrome \underline{c} to cytochrome a seems more likely to be the electron input pathway, and the significantly lower dioxygen activity (~20 %) either reflects the slower electron input from ferrocytochrome \underline{c} to cytochrome a compared to the ferrocytochrome \underline{c} to Cu_A electron transfer, or a more sluggish downhill electron transfer to the binuclear center from cytochrome a compared to Cu_A .

Cu_A modification affects the proton pumping activity: Based on the model of redox-linkage proposed by this laboratory, neither the pHMB-modified nor the heat-treated oxidase is expected to sustain proton pumping activity. In the case of the pHMB-modified oxidase, electron transfer from ferrocytochrome \underline{c} through Cu_A is bypassed. In the case of the heat-treated enzyme, the Cu_A site has lost the ability to undergo a ligand exchange or structural arrangement upon electron reduction. Experimentally, neither modified forms of the enzyme supports proton pumping. The situation with the pHMB-modified is ambiguous, because the enzyme modification has led to a proton or aqueous channel that is highly permeable toward protons. Hence, reconstituted membrane vesicles containing the modified enzyme

cannot sustain a protonmotive force, even if one is created by proton pumping. However, the vesicles containing the heat-treated enzyme do show respiratory control. Therefore, we would like to suggest that the heat-treated enzyme plays a role in the cytochrome oxidase proton pumping paradigm.

Acknowledgment: We thank Dr. Walther Ellis for helpful discussion on the data analysis.

REFERENCES:

- Babcock, G. T. & Callahan, P. M., (1983) *Biochemistry*, **22**, 2314.
- Blair, D. F., Bocian, D. F., Babcock, G. T. & Chan, S. I., (1982) *Biochemistry*, **21**, 6928.
- Blair, D. F.; Ellis, W. R.; Wang, H.; Gray, H. B. & Chan, S. I., (1986) *J. Bio. Chem.*, **261**, 11524.
- Chan, S. I.; Li, P. M.; Nilsson, T.; Gelles, J.; Blair, D. F. & Martin, C. T., (1988) *Oxidases and Related Redox Systems*, pages 731-747.
- Chan, S. I. & Li, P. M., (1990) *Biochemistry*, **29**, 1-12.
- Dawson, R. M. C.; Elliott, D. C.; Elliott, W. & Jones, K., (1986) *Data for Biochemical Research*, third edition, Clarendon press, Oxford.
- Ellis, W. R.; Wang, H.; Blair, D. F.; Gray, H. B. & Chan S. I., (1986) *Biochemistry*, **25**, 161.
- Fine, M. & Wikström, M., (1988) *Eur. J. Biochem.*, **176**, 125.
- Gelles, J. & Chan, S. I., (1985) *Biochemistry*, **24**, 3963.
- Gelles, J.; Blair, D. F. & Chan, S. I., (1986) *Biochim. Biophys. Acta*, **853**, 205.
- Goodman, G., (1984) *J. Bio. Chem.*, **259**, 15094.
- Hartzell, C. R. & Beinert, H., (1974) *Biochim. Biophys. Acta*, **368**, 318-338.
- Krab, K. & Wikström, M., (1987) *Biochim. Biophys. Acta*, **895**, 25-39.

Larsen, R. W.; Ondrias, M. R.; Copeland, R. A.; Li, P. M. & Chan, S. I., (1989) *Biochemistry*, **28**, 6418.

Li, P. M.; Morgan, J. E.; Nilsson, T.; Ma, M. & Chan, S. I., (1988) *Biochemistry*, **27**, 7538.

Nilsson, T.; Gelles, J.; Li, P. M. & Chan, S. I., (1988) *Biochemistry*, **27**, 296.

Sone, N. & Nicholls, P., (1984) *Biochemistry*, **23**, 6550.

Tsudzuki, T. & Wilson, D. F., (1971) *Arch. Biochem. Biophys.* **145**, 149-154.

Wang, H.; Blair, D. F.; Ellis, W. R.; Gray, H. B. & Chan, S. I., (1986) *Biochemistry*, **25**, 167.

Wikström, M.; Krab, K. & Saraste, M., (1981) *Cytochrome Oxidase: A Synthesis*, Academic press, London.

Wikström, M. & Casey, R. P., (1985) *J. Inorg. Biochem.* **23**, 327-334.

Wikström, M., (1989) *Nature*, **338**, 776-778.

CHAPTER IV:

THE EFFECTS OF DCCD-MODIFICATION AND SUBUNIT III-
DEPLETION ON THE PROPERTIES OF CU_A IN BOVINE
CYTOCHROME C OXIDASE

INTRODUCTION:

Cytochrome c oxidase is an integral membrane protein complex that couples the downhill transfer of electrons from ferrocytochrome c to molecular oxygen to the vectorial translocation of protons against the electrochemical gradient across the inner membrane of the mitochondrion (Wikström et al., 1981). The enzyme is a redox-linked proton pump. There have been numerous attempts recently to understand the principles of redox linkage and to elucidate the molecular mechanism of the linkage (see Chan and Li (1990) for a review). Two different types of redox linkage have been proposed: one *indirect*, based on conformational coupling of the proton translocating elements of the proton pumping machinery with the redox center participating in the linkage (Malmström, 1985); and the other *direct*, where the redox center serving as the site of linkage is also a proton translocator (Gelles, et al., 1986; Babcock et al., 1983). Direct experimental evidence in support of one or both type(s) of redox linkage has remained elusive.

Recently, however, several experiments from this laboratory seem to implicate the Cu_A center as the site of redox linkage. A number of protocols have recently been developed that disrupt the structure of the Cu_A site, all of which have been shown to affect the proton pumping activity of the enzyme (Nilsson, et al., 1988; Li, et al. 1988). Of particular interest has been a form of the enzyme that has been derived from mild heat treatment, wherein Cu_A has been transformed into a type 1 blue copper center. This copper site is

electron transfer competent when ferrocycytochrome *c* is used as the substrate and the modified enzyme exhibits full oxidase activity. However, reconstitution of the modified enzyme revealed no proton pumping activity, even though the proteoliposomes are coupled with reasonable respiratory control (Sone, et al., 1984; Li, et al., 1988).

Over the years there has also been much speculation about the possible role of subunit III in the proton pumping function of cytochrome *c* oxidase. The primary consideration is that subunit III is a membrane-spanning polypeptide, thus satisfying one of the requirements for a putative proton-translocating domain of the enzyme. However, a number of experiments have suggested some role for subunit III in proton pumping. The most direct implication has come from covalent modification of the enzyme by dicyclohexylcarbodiimide (DCCD). DCCD modifies Glu 90 of subunit III (Prochaska, et al., 1981); when the modified enzyme was incorporated into phospholipid vesicles and assayed for proton pumping activity, the H^+/e^- stoichiometry was observed to decrease by 50% (Brunori, et al., 1987; Prochaska, & Fink, 1987). In contrast, the electron transfer activity of the enzyme was essentially unchanged. In support of these observations, similar results were obtained when the subunit III-depleted enzyme was reconstituted and assayed for proton pumping, provided that the structure of the Cu_A site was not disrupted during the subunit III-depletion (Li, et al., 1988). Reconstitution of the two-subunit cytochrome *c* oxidase from *paracoccus denitrificans* into phospholipid vesicles also resulted in coupled proteoliposomes that sustained proton pumping with a H^+/e^- stoichiometry of 0.5. In light

of these results, a number of groups have suggested that subunit III plays some role in the proton pumping function of cytochrome c oxidase, even if only a regulatory one (Prochaska & Fink, 1987 and references there). Since both DCCD modification and subunit III-depletion consistently decrease the H^+/e^- stoichiometry by 50% without affecting the electron transfer activity, it has been suggested that subunit III is involved, either directly or indirectly, with a proton translocating channel that is conformationally coupled to the site of redox linkage (Chan & Li, 1991).

While the above evidences implicating Cu_A and subunit III in the proton pumping function of cytochrome c oxidase may border on being circumstantial, they cannot be totally dismissed. Since it has been suggested that Cu_A is a primary electron acceptor (Hill, 1991; Pan et al., 1991) as well as the site of redox linkage (Gelles, et al., 1986), it is reasonable to expect some kind of interaction between subunit III and Cu_A if subunit III plays a role in the proton pumping function of the enzyme. It would be of considerable interest if the conformational coupling between the site of linkage and the proton translocating element(s) of the proton pumping were regulated by subunit III. Towards drawing a link among these otherwise unconnected observations, we have examined here the effects of DCCD-chemical modification and subunit III-depletion on the properties of the Cu_A site. We report here the results of these treatments on the structure of the Cu_A site as manifested by its spectroscopic and redox properties.

MATERIALS AND METHODS:

Materials: Dodecyl maltoside and DCCD were obtained from Sigma. All other chemicals were of analytical grade.

Enzyme isolation and purification: Cytochrome *c* oxidase was isolated and purified from beef heart mitochondria as described by Hartzell and Beinert (1974) and stored at -80 °C before use. Enzyme concentrations were determined from $\Delta A_{\text{red-ox}}$ at 605-630 nm using an extinction coefficient of 27 mM⁻¹cm⁻¹.

Subunit III-depletion of cytochrome c oxidase: 1 ml of 390 ml cytochrome *c* oxidase was solubilized in 200 ml of 20 mM Tris, 0.1 M NaCl, 1 mM EDTA and 5 mg/ml dodecyl maltoside, pH=7.7. The solution was then incubated for 24 hours at room temperature. At the end of the incubation the mixture was cooled to 4 °C and was concentrated by centrifuging at 5,000 rpm in a concentrating tube (centriprep 30, Amicon) (Finel, et al., 1986). To remove the dissociated subunit III from solution, the solution was passed through a Bio Rad 0.5 A column. Depletion of subunit III was confirmed as described (Pan et. al., 1991).

Inhibition of cytochrome c oxidase with DCCD: Following Casey et. al. (1980), 500 ml of 308 mM oxidase was solubilized in 9 ml of 0.5 % Tween-20, 5 mM MES, pH 6.8, and 150 ml of 82 mM DCCD in ethanol was added to this enzyme solution. The mixture was then incubated at 13 °C for three hours. At the end of the incubation, the solution was

removed by passing the concentrated solution through a DEAE column.

Determination of the Cu_A reduction potential of subunit III-depleted and DCCD-inhibited oxidase: All the titrations were undertaken immediately after the enzyme modification. Enzyme samples were placed in anaerobic optical electrochemical cells with saturated calomel electrode as reference and platinum as the working electrode. The platinum electrode were calibrated before each use with 10 mM 1:1 potassium ferricyanide/ferrocyanide in 0.1 M potassium phosphate, pH 7.0. The reference electrode (SCE) was connected to the optical cell via a salt bridge.

Enzyme samples were first pre-reduced by 1 atm of carbon monoxide (99.99%, Matheson) in the presence of the redox mediator Ru(NH₃)₅PyClO₄ (Li et al., 1991); this incubation took 1 hour at room temperature. The degree of reduction of heme a₃ and Cu_B was determined from the absorbance at 590 nm using an extinction coefficient of 27 mM⁻¹cm⁻¹. The enzymes were further fully reduced by the addition of 2.2 equivalent NADH, and then titrated with microliter quantities of 0.25 M K₃Fe(CN)₆. The reduction potentials of the solutions were measured by a digital multimeter (8000A FLUKE) after 20 mins of incubation, and UV-Vis absorbance spectra were recorded at each of the solution potentials measured.

The redox state of Cu_A in the DCCD-inhibited oxidase was monitored by the intensity of the absorption band centered at 823 nm.

The redox state of Cu_A in the DCCD-inhibited oxidase was monitored by the intensity of the absorption band centered at 823 nm, and that of Cu_A for subunit III-depleted oxidase was observed by the intensity of the absorption band centered at 836 nm. The absorbance was quantitated by measuring the area under the spectrum; a straight line connecting the data points at 740 and 900 nm was used as the baseline. This area was taken as a measure of the concentration of the oxidized Cu_A in the calculation of $\log(\text{ox/red})$ at each solution potential.

Nernst plots: As discussed in a recent paper from this laboratory (Li, et. al., 1991), Fe_{a3} and Cu_B are held in the reduced state in the carbon monoxide pre-reduced oxidase, and only Fe_a and Cu_A can participate in redox interactions. For redox titration of a system with two interacting redox centers, the equilibrium concentration ratios of the oxidized to reduced forms (ox/red) of the observed site (Fe_a or Cu_A) is given by:

$$\log\left(\frac{\text{ox}}{\text{red}}\right)_1 = \frac{F(E-E'_1)}{2.303RT} + \log\{1 + \exp\left[\frac{F}{RT}(E'_2 - E)\right]\} - \log\{1 + \exp\left[\frac{F}{RT}(E'_2 - E + \Delta E_{12})\right]\}$$

where $E'_1 = E^\circ_1 + \Delta E_{1-\text{heme } a3} + \Delta E_{1-\text{Cu}_B}$, $E'_2 = E^\circ_2 + \Delta E_{2-\text{heme } a3} + \Delta E_{2-\text{Cu}_B}$. E°_1 and E°_2 denote, respectively, the intrinsic reduction potential of the site under observation (Cu_A) and that of the interacting site (Fe_a), and ΔE_{12} is the interaction potential between the two sites (Blair, et al., 1986; Li, et al., 1991).

Apparatus: UV-Visible absorption spectra were recorded at room temperature on a Beckman DU-7 spectrophotometer, interfaced to an IBM AT computer. EPR experiments were run on an E-line Century series EPR spectrometer at liquid nitrogen temperature. Samples for the optical experiments were loaded into anaerobic 10 mm precision quartz cuvettes. EPR samples were contained in anaerobic 4 mm o. d. quartz EPR tubes.

RESULTS:

Available evidence indicates that the 830 nm absorbance band of native cytochrome c oxidase (Figures 1 and 2) is due almost entirely to Cu_A (Blair et al., 1982); the EPR spectrum of cytochrome c oxidase at liquid N₂ temperature (Figures 3 and 4) also contains contributions primarily from the Cu_A center.

Figures 1 and 2 show, respectively, the effects of DCCD-modification and subunit III-depletion on the near-IR absorbance band of the oxidized enzyme. DCCD-inhibition caused the Cu_A absorbance maximum at 830 nm to blue shift to 823 nm while depletion of subunit III red shifted the band to 836 nm. These treatments also produced effects on the Cu_A EPR. Small but reproducible effects were observed upon DCCD modification, including the onset of superhyperfine splittings in the perpendicular component of the EPR spectrum (Figure 3). Depletion of subunit III gradually changed Cu_A

Fig. 1 Effect of DCCD-incubation on the near IR absorption of bovine cytochrome c oxidase.

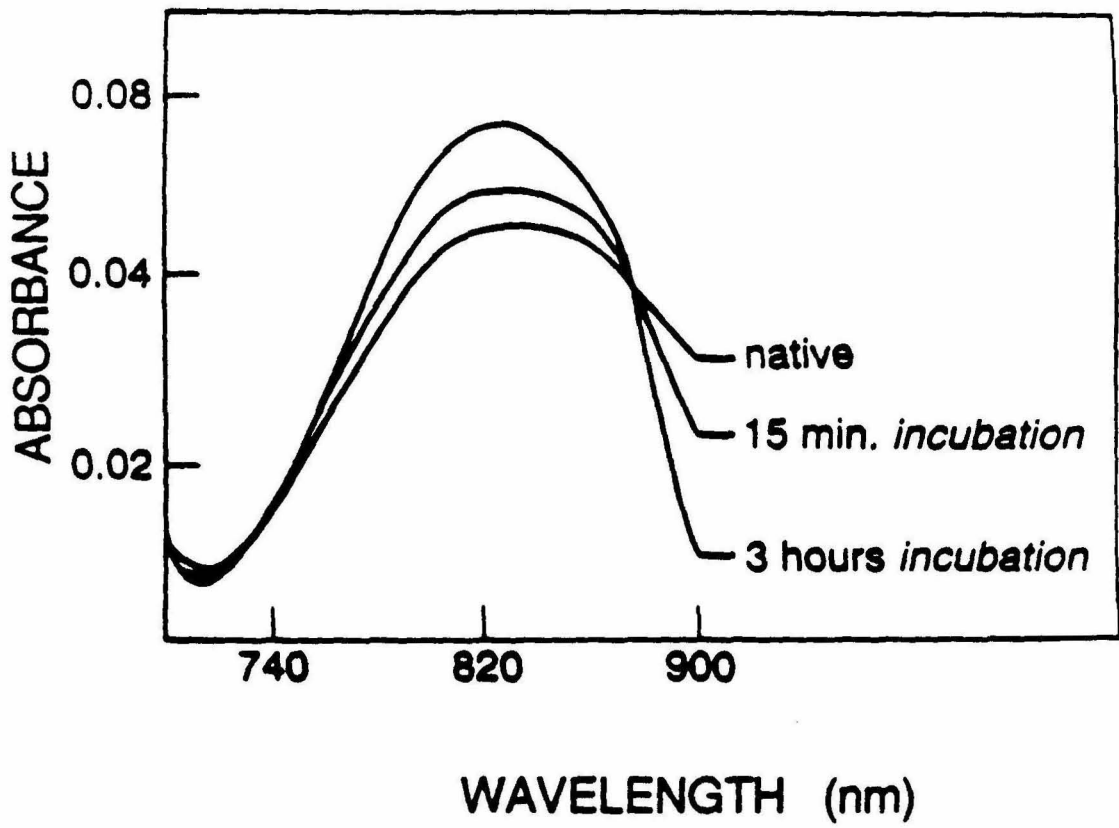


Fig. 2 Effect of subunit III depletion on the Near-IR absorption spectrum of bovine cytochrome c oxidase. Solid line: native oxidase. Dash line: subunit III-depleted oxidase (right after depletion). Solid dash line: subunit III- depleted oxidase (1 week after depletion).

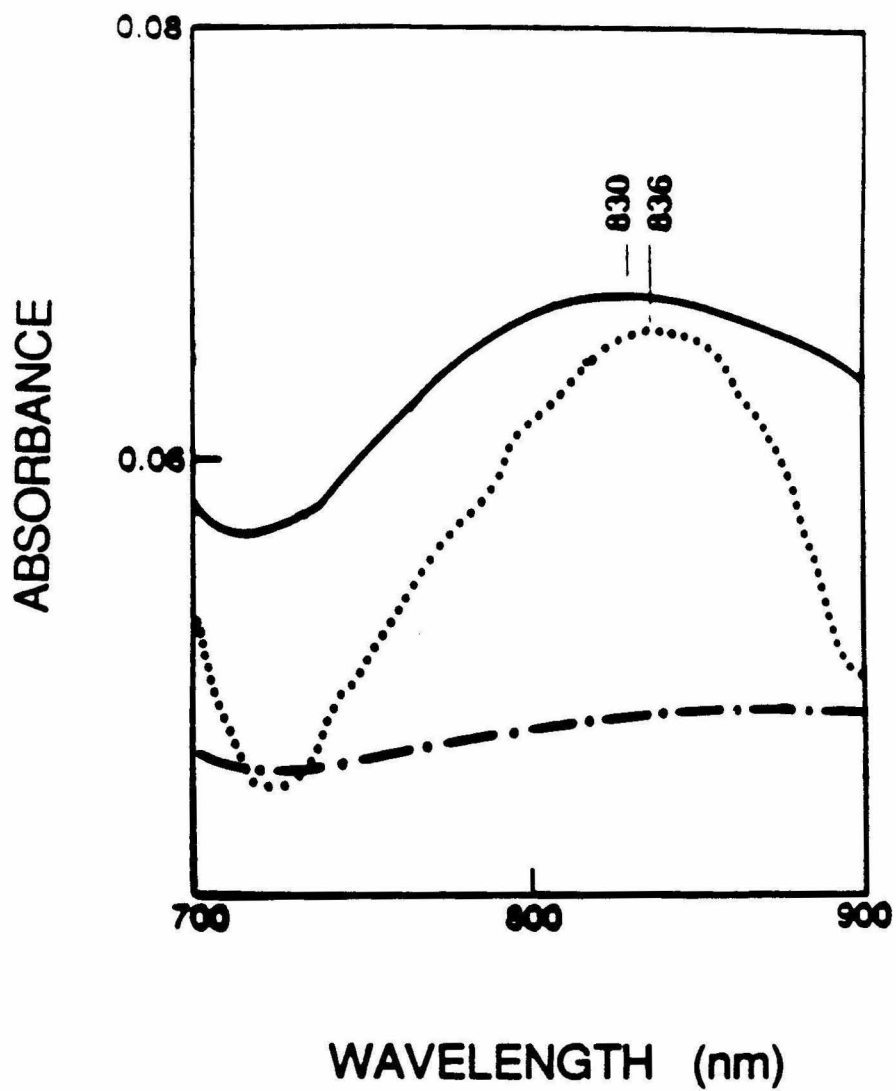


Fig. 3 EPR signal from the Cu_A site of native and DCCD-modified cytochrome c oxidase. Conditions: microwave frequency 9.128 GHz; microwave power 5mW; modulation amplitude 10.0 G; sample temperature 77 K.

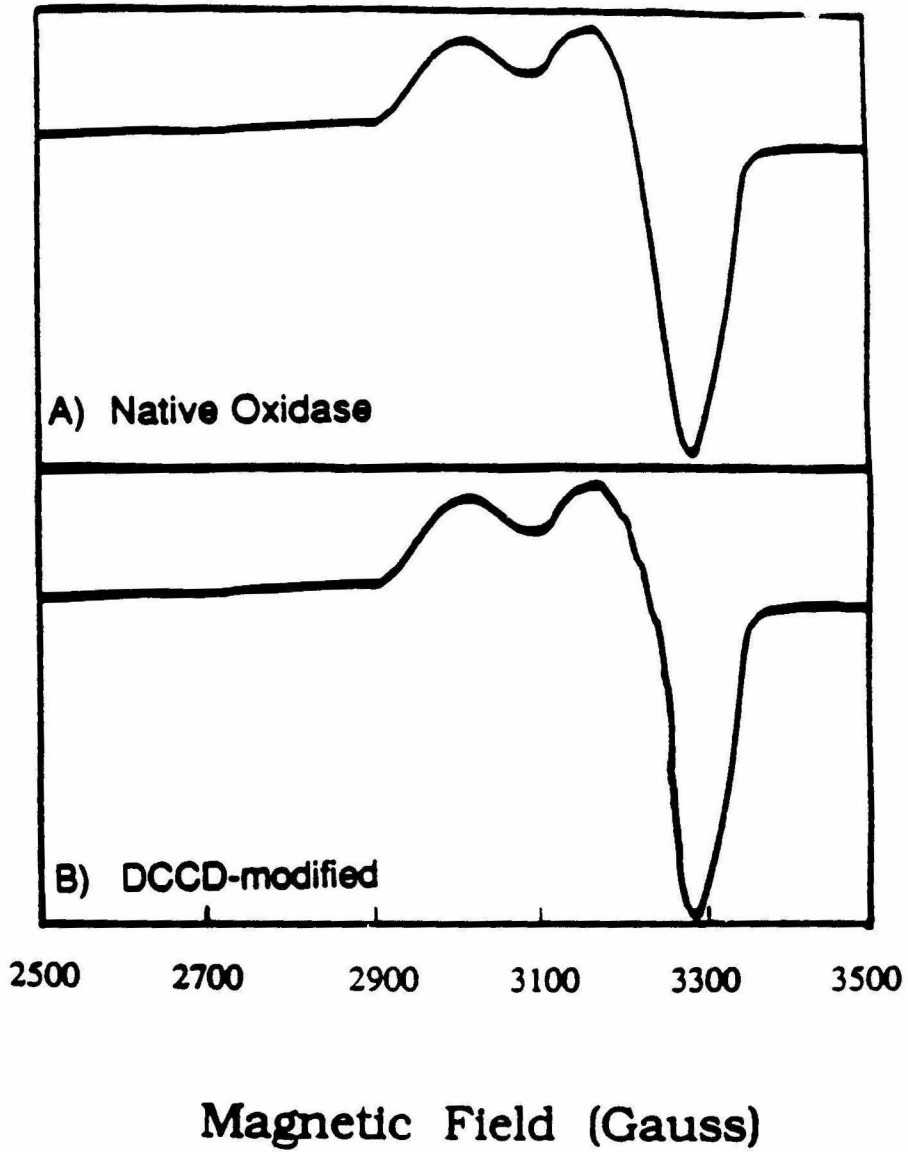
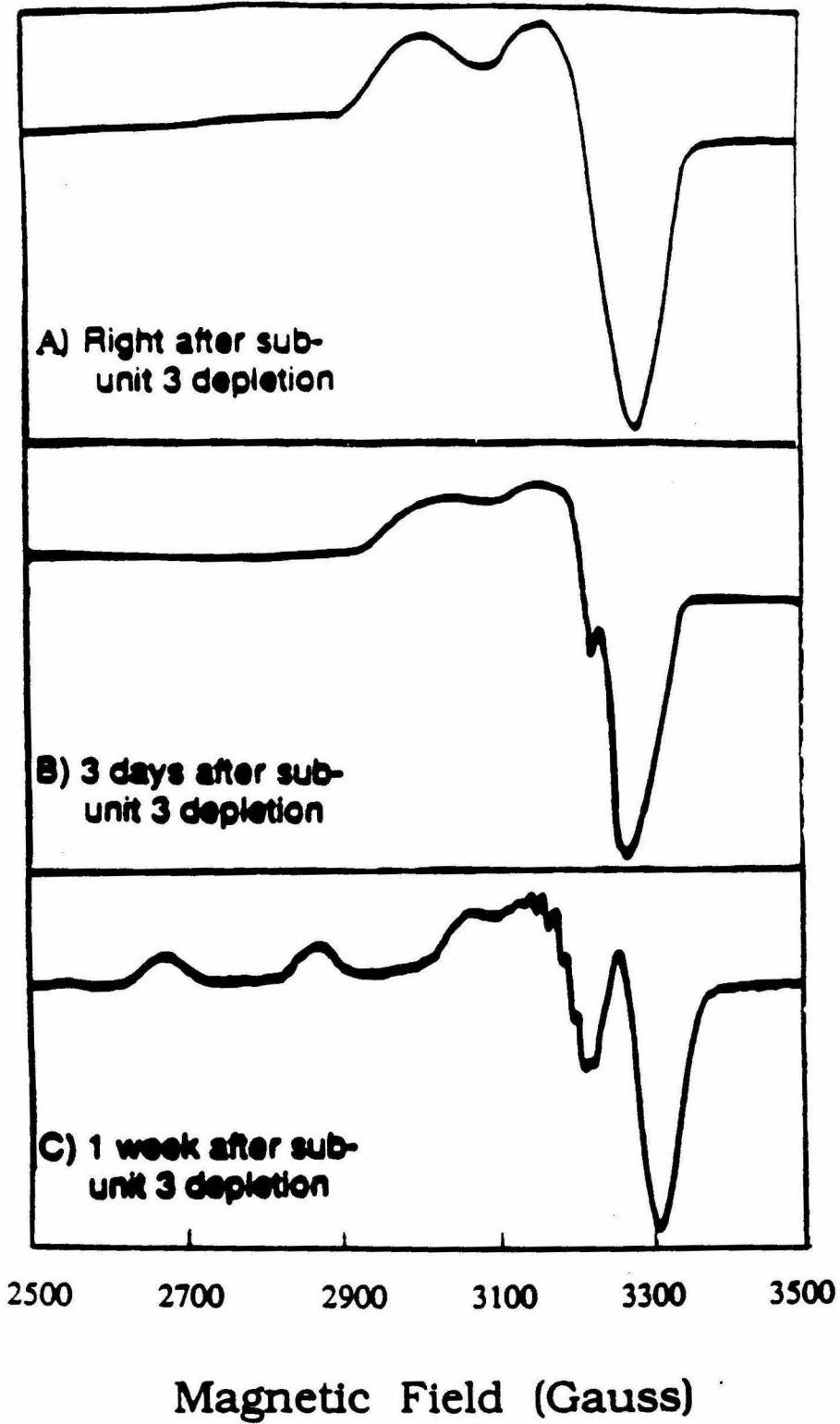


Fig. 4 Effect of subunit III-depletion on the Cu_A EPR signal of bovine cytochrome c oxidase. Condition: microwave frequency 9.128 GHz; microwave power 5 mW; modulation modulation amplitude 10.0 G; sample temperature 77 K.



into a type 2 Cu center (Figure 4), indicating that the ligation about the copper ion is unstable in the absence of subunit III. The optical and EPR evidence suggests that DCCD modification of Glu 90 (Prochaska, et al., 1981) in subunit III weakened one of the Cu-S (cysteine) linkages, while subunit III depletion led ultimately to displacement of one of the cysteine ligands from the site.

As expected, the Nernst plots for the redox titrations of the Cu_A site of DCCD-inhibited and subunit III-depleted oxidase exhibited redox behaviors distinct from that expected for an isolated one-electron acceptor (Blair, et al., 1986; Li, et al., 1991). The observed appearance midpoint potentials and the intrinsic reduction potentials of the modified Cu_A are compared with the corresponding values in the native oxidase in Table 1.

In the titration of Fe_{a3}/Cu_B pre-reduced DCCD-inhibited oxidase (Figure 5), Fe_{a3} and Cu_B are held in their reduced states. Fitting the Cu_A Nernst plot to the simple interaction model with n=1 yielded an intrinsic reduction potential ($E'_{CuA} = E^0_{CuA} + \Delta E_{CuA-Fea3} + \Delta E_{CuA-CuB}$) of 290 mV vs. NHE for the Cu_A site, a redox interaction ($\Delta E_{CuA-Fea}$) of about -100 mV, and an asymptotic potential of 273 mV vs. NHE for the interacting site, i. e. cytochrome a (Figure 6). Similarly, in the titration of Fe_{a3}/Cu_B pre-reduced subunit III-depleted oxidase, Fe_{a3} and Cu_B are held in their reduced states. Analyzing the Nernst plot for this species by the simple interaction model resulted in an intrinsic reduction potential ($E'_{CuA} = E^0_{CuA} + \Delta E_{CuA-Fea3} + \Delta E_{CuA-CuB}$) of 236 mV vs. NHE

TABLE 1

Redox Parameters Estimated From Potentiometric Titrations of the
DCCD-Modified and the Subunit III-Depleted Cytochrome *c* Oxidase^a

Enzyme species	Fe _{asy} /Cu _B pre-reduced DCCD inhibited	Fe _{asy} /Cu _B pre-reduced subunit III depleted	Fe _{asy} /Cu _B pre-reduced native oxidase
n^+	0.8	0.8	0.8
Cu _A appearance midpoint potential (mV)	273	220	275
Cu _A lower asymptotic potential (mV)	190	210	240
Cu _A upper asymptotic potential (mV)	290	236	280
interactant asymptotic potential (mV)	273	288	340
interaction potential (mV)	-100	-10	-40
Cu _A intrinsic potential (mV)	290	236	280

a: All redox potentials are referred to NHE.

Fig. 5 Near-IR absorbance difference spectra obtained during a potentiostatic titration of Fe_{a3}/Cu_B pre-reduced DCCD-modified cytochrome c oxidase at 20 °C. The indicated potentials are relative to SCE. All spectra are referenced to the spectrum of the fully reduced enzyme obtained at a potential of -200 mV. The enzyme concentration was approximately 40 μM.

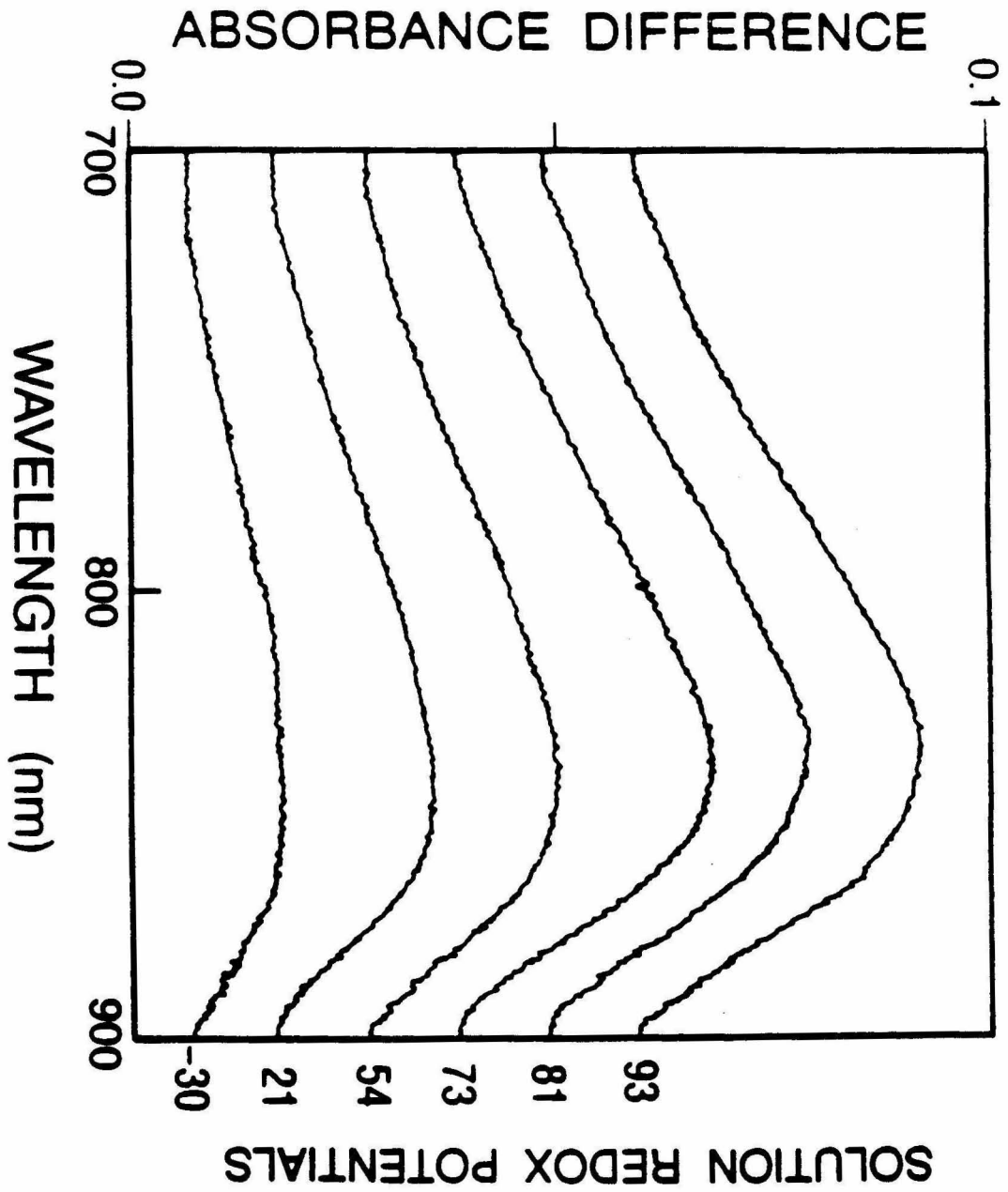
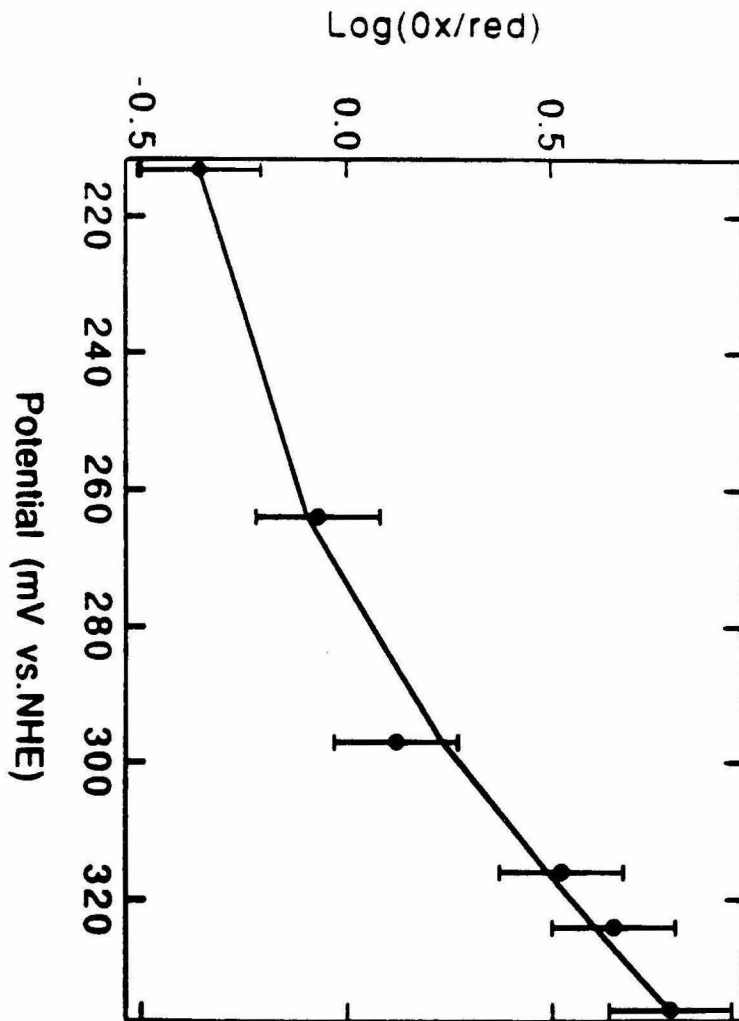


Fig. 6 Nernst plot for the Cu_A site of $\text{Fe}_{a3}/\text{Cu}_B$ pre-reduced DCCD-modified bovine cytochrome c oxidase. The line is the computer-generated best fit to the simple two-site interaction model: $E_1=290$ mV, $E_2=273$ mV, $\Delta E=-100$ mV.



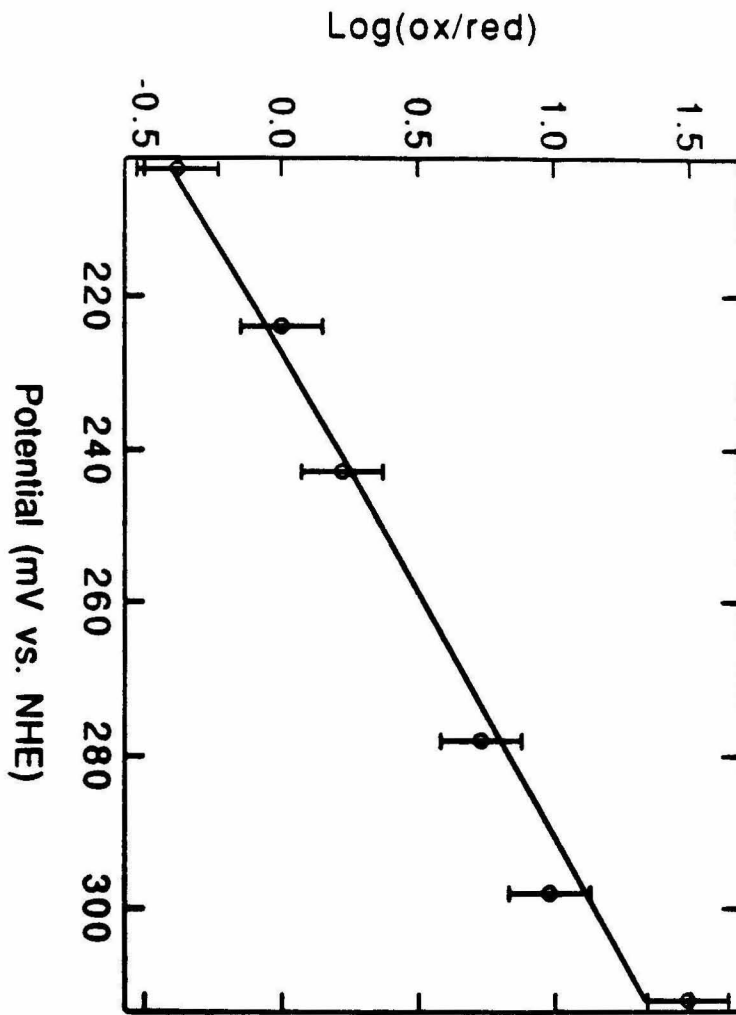
for the Cu_A site, a redox interaction ($\Delta E_{\text{Cu}_A\text{-Fea}}$) of about -10 mV, and an asymptotic potential of 288 mV vs. NHE for the interacting site, namely, cytochrome a (Figure 7).

It is clear from the above results that the structure of the Cu_A site is conformationally linked to subunit III. Two treatments that affect subunit III, DCCD modification and subunit III depletion, are shown to modify the spectroscopic signatures of Cu_A and even affect the stability of the site toward structural distortions and/or rearrangements. Although the intrinsic reduction potentials of Cu_A for both the DCCD-inhibited and subunit III-depleted oxidase are not altered appreciably, the redox interaction between Cu_A and cytochrome a is changed significantly in both incidences. In the absence of subunit III, the redox interaction between Cu_A and cytochrome a is essentially eliminated. On the other hand, when Glu 90 of subunit III is chemically modified by DCCD (Prochaska, et al., 1981), this redox interaction becomes highly anticooperative.

DISCUSSION:

Recent studies have clearly shown that the proton pumping activity of cytochrome c oxidase is linked to its dioxygen reduction activity. Wikström (1989) has shown that only two of the four electrons transferred to dioxygen are linked to proton pumping; Chan and Li (1990) have argued on energetic grounds that the protons vectorially translocated must be coupled to electron transfers from the site of linkage to the two high potential dioxygen intermediates that

Fig. 7 Nernst plot for the Cu_A site of $\text{Fe}_{a3}/\text{Cu}_B$ pre-reduced subunit III-depleted bovine cytochrome c oxidase. The line is the computer-generated best fit to the simple two-site interaction model: $E_1 = 236$ mV, $E_2 = 288$ mV, $\Delta E = -10$ mV.



are formed during turnover. Experiments by Wikström and Casey (1985) on intact mitochondria implicate one of the "low-potential" centers as the site of redox linkage. Two direct redox-linkage models based on these low potential centers have been proposed (Gelles, et al., 1986, Babcock et al., 1983). In both of these models a proton is vectorially translocated across the osmotic barrier for each electron transferred during redox linkage. However, since the mechanistic H^+/e^- stoichiometry is 2, there must be an additional proton pumping pathway that is conformationally coupled to the redox center participating in the linkage to translocate a second proton.

DCCD-modification and subunit III-depletion consistently diminish the observed H^+/e^- stoichiometry during proton pumping by 50% (Brunori, et al., 1987; Prochaska, & Fink, 1987; Li, et al., 1988). Accordingly, it has been suggested that subunit III plays a role in the proton pumping function of the enzyme. Two possibilities come to mind. First, subunit III could provide the proton translocation channel itself. Alternatively, the second proton translocated is associated with one or more of the other membrane-spanning subunits, e.g. I and II, but subunit III regulates the interaction between the site of linkage and the indirectly coupled proton translocation channel. Since DCCD is a large, hydrophobic molecule, it seems rather unlikely that it covalently modifies a glutamic acid residue that is part of a transmembrane proton channel in order to block proton translocation in its inhibitory effect on the proton pumping activity of the enzyme. A recent site-directed mutagenesis study confirms this glutamic acid is not involved in proton translocation (Haltia, et al.,

1991). However, these experiments do not rule out a role for this subunit in the proton pumping function of the enzyme. In any case, the second scenario seems more reasonable in light of the observations reported here.

The results of this study reinforce a recent proposal from this laboratory that the Cu_A structure is locally unstable and that subunit III stabilizes the tense ligand structure of the site (Li et al., 1991). If so, subunit III can regulate, through redox changes at the Cu_A site, the allosteric interaction between various parts of the protein structure, particularly subunits I and II, to accomplish free energy transduction. In this manner, the reduction and reoxidation of the Cu_A site may be linked to conformational transitions that culminate in vectorial proton transfer. Whether the proton pumping machinery entails one *direct* redox-linked proton pumping element at the Cu_A site, as has been conjectured, and a second indirect proton pumping site that is conformationally linked to the redox site, as is proposed here, remains an open question. Nevertheless, a picture is emerging that Cu_A is a component of the proton pumping machinery of cytochrome c oxidase, and that subunit III plays an important allosteric role in communicating the redox changes at the Cu_A site to the proton translocating elements of the enzyme.

REFERENCES:

- Babcock, G. T. & Callahan, P. M., (1983) *Biochemistry*, **22**, 2314.
- Blair, D. F.; Ellis, W. R.; Wang, H. H.; Gray, H. B. & Chan, S. I., (1986) *J. Biol. Chem.*, **261**, 11524.
- Blair, D. F.; Bocian, D. F.; Babcock, G.T. & Chan, S. I., (1982) *Biochemistry*, **21**, 6928.
- Brunori, M.; Antonini, G.; Malatesta, F. & Sarti, P., (1987) *Eur. J. Biochem.*, **169**, 1-8.
- Casey, R. P.; Thelen, M. & Azzi, A., (1979) *J. Biol. Chem.* , **255**, 3994-4000.
- Chan, S. I. & Li, P. M., (1990) *Biochemistry*, **29**, 1-11.
- Finel, M. & Wikström, M., (1986) *Biochim. Biophys. Acta*, **851**, 99-108.
- Gelles, L.; Blair, D. F. & Chan, S. I., (1986) *Biochim. Biophys. Acta*, **853**, 205.
- Haltia, T.; Saraste, M. & Wikström, M., (1991) *The EMBO Journal*, **10**, 2015-2021.
- Hartzell, C. R. & Beinert, H., (1974) *Biochim. Biophys. Acta*, **368**, 318-338.
- Hill, B., (1991) *J. Biol. Chem.*, **266**, 2219-2226.

- Li, P. M.; Morgan, J. E.; Nilsson, T.; Ma, M. & Chan, S. I., (1988) *Biochemistry*, **27**, 7538.
- Li, Z.; Larsen, R., Pan, L-P & Chan, S. I., *J. Biol. Chem.* (in press).
- Malmström, B. G., (1985) *Biochim. Biophys. Acta*, **811**, 1-12.
- Nilsson, T.; Gelles, J., Li, P. M. & Chan, S. I., (1988) *Biochemistry*, **27**, 296.
- Pan, L-P.; Li, Z.; Larsen, R. & Chan, S. I., (1991) *J. Biol. Chem.*, **266**, 1367-1370.
- Pan, L-P; Hazzard, J. T.; Lin, J.; Tollin, G. & Chan, S. I., (1991) *J. Am. Chem. Soc.*, **113**, 5908-5910.
- Prochaska, L. J.; Bisson, R.; Capaldi, R. A.; Steffens, G. C. M. & Buse, G., (1981) *Biochem. Biophys. Acta*, **637**, 360-373.
- Prochaska, L. J. & Fink, P. S., (1987) *J. Bioenergetics Biomembranes*, **19**, 143-166.
- Sone, N. & Nicholls, P., (1984) *Biochemistry*, **23**, 6550.
- Wikström, M.; Krab, K. & Saraste, M., (1981) *Cytochrome Oxidase: A Synthesis*, Academic Press, London.
- Wikström, M. & Casey, R. P., (1985) *J. Inorg. Biochem.* **23**, 327-334.
- Wikström, M., (1989) *Nature*, **338**, 776-778.

CHAPTER V:

CHLORIDE DEPLETION OF CYTOCHROME C OXIDASE

INTRODUCTION:

Cytochrome c oxidase is the terminal enzyme of the electron transport chain in mitochondria. Spanning the mitochondrial inner membrane, this enzyme catalyzes the reduction of dioxygen to water, using protons derived from the matrix side of the membrane to cytosol side. The functional form of the enzyme is known to contain two copper (Cu_A , Cu_B) and two iron (Fe_a , Fe_{a3}) atoms, the latter in the form of heme a . Each of the four metal centers of cytochrome c oxidase is known to function in a redox capacity as evidenced by optical and EPR measurements at various stages during enzymatic turnover. Fe_a and Cu_A catalyze the transfer of electrons from cytochrome c to Fe_{a3} and Cu_B . In addition, one of these metal centers also participates in proton pumping. Fe_{a3} and Cu_B are close (ca. 5 Å) to each other and form the site of dioxygen reduction (Wikström, et al., 1981). A number of experiments relating to the structure of the binuclear Cu_B - Fe_{a3} site have been reported. It is believed that the iron atom of Fe_{a3} and its associated Cu_B form a coupled binuclear center. The most dramatic feature of this interaction is the lack of EPR signals from the individual metals. This unusual situation arises from antiferromagnetic coupling between the high-spin ferric ion and the $Cu_B(II)$, forming an $S=2$, EPR-silent pair (Aasa, et al., 1976; Hartzell, et al., 1974; Brudrig, et al., 1986). The strong magnetic interaction between Fe_{a3} and Cu_B found to exist in the resting enzyme (as isolated) is thought to be mediated by a shared, bridging ligand. The

identity of this bridging ligand has been proposed to be an imidazole nitrogen from a histidine residue (Palmer, et al., 1976), cysteine sulphur (Powers, et al., 1981) or an oxygen atom. Whatever its identity it is agreed that this ligand must undergo some rearrangement to render the enzyme reactive to oxygen. Experimental evidence based upon cyanide binding kinetics indicates that the bridging ligand occupies the oxygen-binding site. Although EPR-silent, Fe_{a_3} has been shown to be high-spin in the oxidized state based upon magnetic susceptibility (Falk, et al., 1977) and MCD (Thomson, et al., 1977) results. By preferential reduction of one or the other of the metal centers, the coupling is disrupted and its partner metal may be induced to exhibit EPR signals (at $g=6$ for the Fe_{a_3} (Aasa, et al., 1976; Hartzell, et al., 1974) and at $g=2.053$, 2.109 and 2.278 for Cu_{B} (Stevens, et al., 1979)). Nitric oxide, which binds to the Cu_{B} site in the oxidized enzyme, also decouples the metals allowing the ferric heme a_3 high spin $g=6$ EPR signal to be seen (Stevens, et al., 1979). The exact nature and number of ligands around Cu_{B} are still uncertain. However, ENDOR studies of this site (Cline, et al., 1983) and comparison with type 3 Cu(II) sites, indicate that Cu_{B} may have three nitrogen (imidazole) ligands with H_2O or OH^- as a fourth ligand. In the case of Fe_{a_3} , Stevens and Chan (Stevens, et al., 1981), using ^{14}NO or ^{15}NO and ^{15}N -labeled histidine as well as resonance Raman data, have demonstrated that this heme has an imidazole nitrogen as its proximal ligands.

Understanding the $\text{Cu}_B\text{-Fe}_{a3}$ binuclear structure is the key to understanding the dioxygen reduction mechanism of this enzyme, and may provide relevant information concerning the coupling of this reaction to the proton translocating function of the enzyme (Blair, et al., 1983; Gelles, et al., 1986). Recent Fe extended X-ray absorption fine structure (EXAFS) experiments by Scott and Chan (1988) showed that if cytochrome c oxidase was isolated and purified in Cl^- -free buffer solution, the peak thought to be sulphur in EXAFS spectrum disappeared. This result suggests that Cl^- could be the bridging ligand. In this report we will attempt to deplete Cl^- from resting oxidase and demonstrate the difference between resting oxidase and the Cl^- depleted oxidase. Our results will show that Cl^- could be a bridging ligand between Fe_{a3} and Cu_B .

MATERIALS AND METHODS:

Enzyme isolation and purification: Cytochrome c oxidase was purified from beef heart mitochondria by the method of Hartzell and Beinert (1974), and stored at -80°C before use. Enzyme concentrations were determined spectrophotometrically using a reduced minus oxidized $\Delta\epsilon$ value of $27\text{ mM}^{-1}\text{cm}^{-1}$ at 604 nm. Typical enzyme concentration was $225\ \mu\text{M}$.

Materials: Horse heart cytochrome c (sigma type vi) was used without purification. All buffer solutions were prepared with NANO pure II distilled water. Typical buffer solution contains 50 mM MOPS (SIGMA) 0.5% Tween-20 (Pierce, specially purified under nitrogen), pH 7.00. MOPS and Tween-20 were selected because they are Cl^- free compounds. Resin (Sigma, Amberlite IRA-93, free base form, 1.2 meq/ml, weakly basic anionic exchange) was washed four times with distilled water and once with acetone. The resin was brought to the desired pH 6.85 by suspending it in 50 mM MOPS; the resin was then filtered, air dried and kept in a plastic bottle.

Apparatus: All UV-Visible absorption spectra were recorded on a Beckman DU-7 spectrophotometer, interfaced to an IBM AT computer. EPR experiments were done on an E-line Century series EPR spectrometer. An Oxford ESR-900 cryostat with a liquid helium transfer system was used for temperature control. A carbon-glass resistor was used to measure the temperature inside the cavity after each spectrum was recorded. All samples for the optical experiments were contained in precision 2 mm quartz cuvettes, while the EPR samples were contained in 5 mm o. d. quartz EPR tube. Enzyme transfer between spectra cell and dialysis tubing was carried out at a VAC glove box.

Reduction of cytochrome c oxidase: Enzyme samples were made anaerobic by repeated cycles of vacuum/Ar in an anaerobic optical cell. Addition of ascorbate/cytochrome c was accomplished using an anaerobic syringe. Following addition of 4.4 equivalent of ascorbate and 0.05 equivalent of cytochrome c, the sample were kept at 4 °C and were allowed to react for 20 minutes.

Dialysis: 200 µl of the reduced cytochrome c oxidase was transferred into a dialysis tubing in an oxygen-free glove box. The reduced enzyme was dialyzed against one liter of oxygen-free 50 mM MOPS (pH=7.00) buffer solution containing 0.5% tween-20 and 1 cm³ resin. Typical dialysis time was 90 minutes. The dialysis system was air-tight and was kept at 4 °C. After dialysis, the enzyme was exposed to air and reoxidized. This form of enzyme will be called "dialyzed oxygenated oxidase" in this paper.

Quantitative analysis: The resin obtained from the dialysis medium was filtered, washed by distilled water, then ion exchanged with 0.8 mM HNO₃ solution. The supernatant was treated with one drop of 0.1 M AgNO₃ to detect Cl⁻. The formation of a white precipitate that is insoluble in NH₄OH was used to indicate the presence of Cl⁻.

Cyanide binding kinetics: The kinetics of reaction of dialyzed oxygenated oxidase with KCN was followed optically at 432 nm. The reaction was initiated by the addition of 50 μ l of freshly prepared five mM KCN to 100 μ l dialyzed oxygenated oxidase. The reaction was performed at 20 °C.

UV-Visible spectra: Optical spectra of dialyzed oxygenated oxidase were recorded at various times, beginning from the initial formation of pulsed enzyme, to an incubation time of 30 hours. The influences of F^- , Cl^- and Br^- on the spectra were determined by addition of 100 μ l of 5 mM NaF, NaCl or NaBr into 100 μ l of dialyzed oxygenated oxidase.

EPR spectra: The influences of F^- , Cl^- and Br^- on cytochrome c oxidase EPR spectra were determined by addition of 100 μ l of 5mM NaF, NaCl or NaBr into 100 μ l of dialyzed oxygenated oxidase. Spectra were recorded at 4 K.

RESULTS AND DISCUSSION:

Cytochrome c oxidase exists in at least three distinct conformations differing in the structure of the binuclear cluster. When

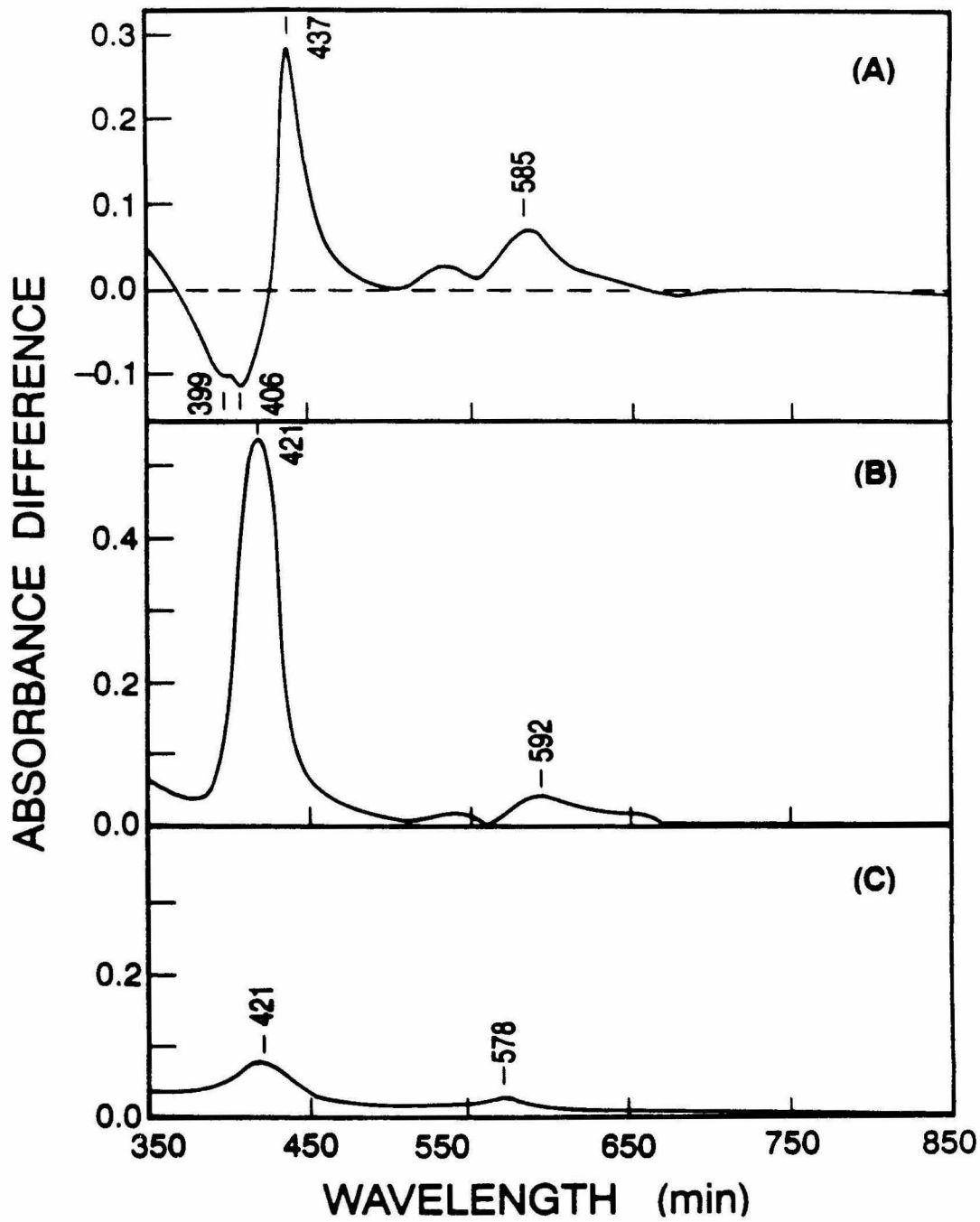
reduced cytochrome c oxidase is reoxidized, these conformations appear to form sequentially. Within five ms, the enzyme decays from a form that has a Soret maximum at 428 nm, and exhibits an EPR signal with resonances at $g=5$, 1.78 and 1.69 into an intermediate that no longer exhibits the EPR signal, but which still exhibits a Soret band maximum at 427 nm. It has been proposed that Fe_{a3} and Cu_B is weakly exchange-coupled with no dipolar coupling in the initial conformation, but the two metal ions of the binuclear cluster become more strongly exchange-coupled in the second intermediate. Ultimately, the second intermediate also decays into the so-called "resting state". This state is also EPR silent, but the Soret maximum has shifted from 428 nm to 417 nm. It thus appears that when cytochrome c oxidase decays from the pulsed to the resting enzyme, either the two metal ions of the binuclear cluster come closer together, or a bridging ligand enters the coordination sphere of both ions to couple the two ions electrostatically.

In accordance with this hypothesis, resting oxidase as isolated is conspicuously unreactive towards ligands, such as cyanide, azide or formate. In contrast, the same ligands bind rapidly to the pulsed enzyme, or during turnover conditions. These observations have led to the proposal that oxidized cytochrome c oxidase exists in open or closed conformations, and it is possible that the pulsed enzyme exists in the closed and open conformations as well.

The nature of the bridging ligand in resting oxidase has received considerable attention over the past decade. Magnetic susceptibility measurements suggest that the binuclear couple is an $S=2$ couple, resulting from antiferromagnetic coupling between a high spin Fe_{a3} with a d^9 Cu_B ion. Evidence for a high spin Fe_{a3} has come from MCD. For native oxidase, a peak in the Fe extended X-ray absorption fine structure (EXAFS) Fourier Transform (FT) at a phase-shifted distance (R') of ~ 2.1 Å can be ascribed to the presence of a S^- or Cl^- containing sixth ligand to the Fe_{a3} with an Fe-(S,Cl) distance of ~ 2.4 Å. Fe EXAFS results of oxidase sample prepared in the absence of chloride ion buffer give rise to a FT that does not exhibit this $R' \sim 2.1$ Å peak. These experiments implicate a sulfur or chloride ion as the possible bridging ligand.

Fig. 1A shows the optical difference spectra between dialyzed oxygenated oxidase and resting oxidase. The dialyzed oxygenated oxidase has been incubated for 60 min. (ensure that it has been oxidized completely). This spectrum is different from normal oxygenated oxidase or pulsed oxidase, but similar to spectra of Ferryl Fe_{a3} /cupric Cu_B enzyme (Power, et al., 1981; Witt, 1988) or CN-inhibited oxidase (Blumberg, et al. Blair, et al., 1982). It is well known that oxygenated oxidase will be converted to resting oxidase within

Fig. 1 Optical difference spectra between dialyzed/oxygenated enzyme and resting enzyme. (A) The reduced oxidase was dialyzed anaerobically for 90 min., and the difference spectrum was recorded 60 min. after the enzyme was reoxidized by O₂. (B) The reduced oxidase was dialyzed anaerobically for 90 min., and the difference spectrum was recorded recorded 30 hours after the enzyme was reoxidized by O₂. (C) The reduced oxidase was dialyzed anaerobically for 0.5 hour, and the difference spectrum was recorded 30 hours after the enzyme was reoxidized by O₂. Typical enzyme concentration: 110 μM (pH=7.00, 50 mM MOPS buffer solution containing 0.5% Tween-20); temperature 20 °C.



several hours (Lember, et al, 1967). In contrast, the optical spectra of dialyzed oxygenated oxidase did not return to the resting form even after it was incubated for 30 hours, as shown in Fig. 1B. Note that the difference spectra displays reduced absorbance when dialysis time was less than one hour (Fig. 1C). No new bands appear upon F^- , Cl^- , or Br^- addition to oxygenated dialyzed oxidase. However F^- , Cl^- and Br^- exhibit a notable influence on the position of Soret band maximum as shown in Table 1.

Fig. 2 displays the EPR spectra of cytochrome c oxidase under different conditions. The spectra of Cl^- substituted cytochrome c oxidase is similar to native oxidase. The difference in EPR spectra between native oxidase and Br^- substituted oxidase consist of a decrease in the $g=12$ resonance in the Br^- substituted enzyme. Both F^- substituted oxidase and dialyzed oxygenated oxidase have similar, unusual EPR signals appearing. The optical and EPR spectra differences between F^- , Cl^- , Br^- substituted oxidase and dialyzed oxygenated oxidase can be explained in terms of molecular orbital theory, and we will suppose OH^- group is the substitute ligand for dialyzed oxygenated oxidase.

Table 1: The UV-Visible Spectra Properties for Cytochrome c Oxidase

	Species					
	Resting	Reduced	+F ⁻	Dialyzed +Cl ⁻	Oxygenated +Br ⁻ incubated	
Soret band peak position (nm)	421.5	442	419	421	423	416
<u>Integral Soret band</u>						
Integral α band	7.7		6.2	7.0	11.3	

Fig. 2 EPR spectra of cytochrome c oxidase. (A) Native enzyme. (B) Cl^- substituted dialyzed/oxygenated oxidase in Cl^- containing media. (C) Br^- substituted dialyzed/oxygenated oxidase in Br^- containing media. (D) F^- substitute dialyzed oxygenated oxidase in F^- containing media. (E) Dialyzed/oxygenated oxidase incubated with O_2 for 10 hours. Conditions: enzyme concentration, $60 \mu\text{M}$ (pH=7.00 50 mM MOPS buffer solution containing 0.5% Tween-20); temperature, 4 K; microwave power 0.5 mW, modulation amplitude 16 G, microwave frequency 9.24 GHz.

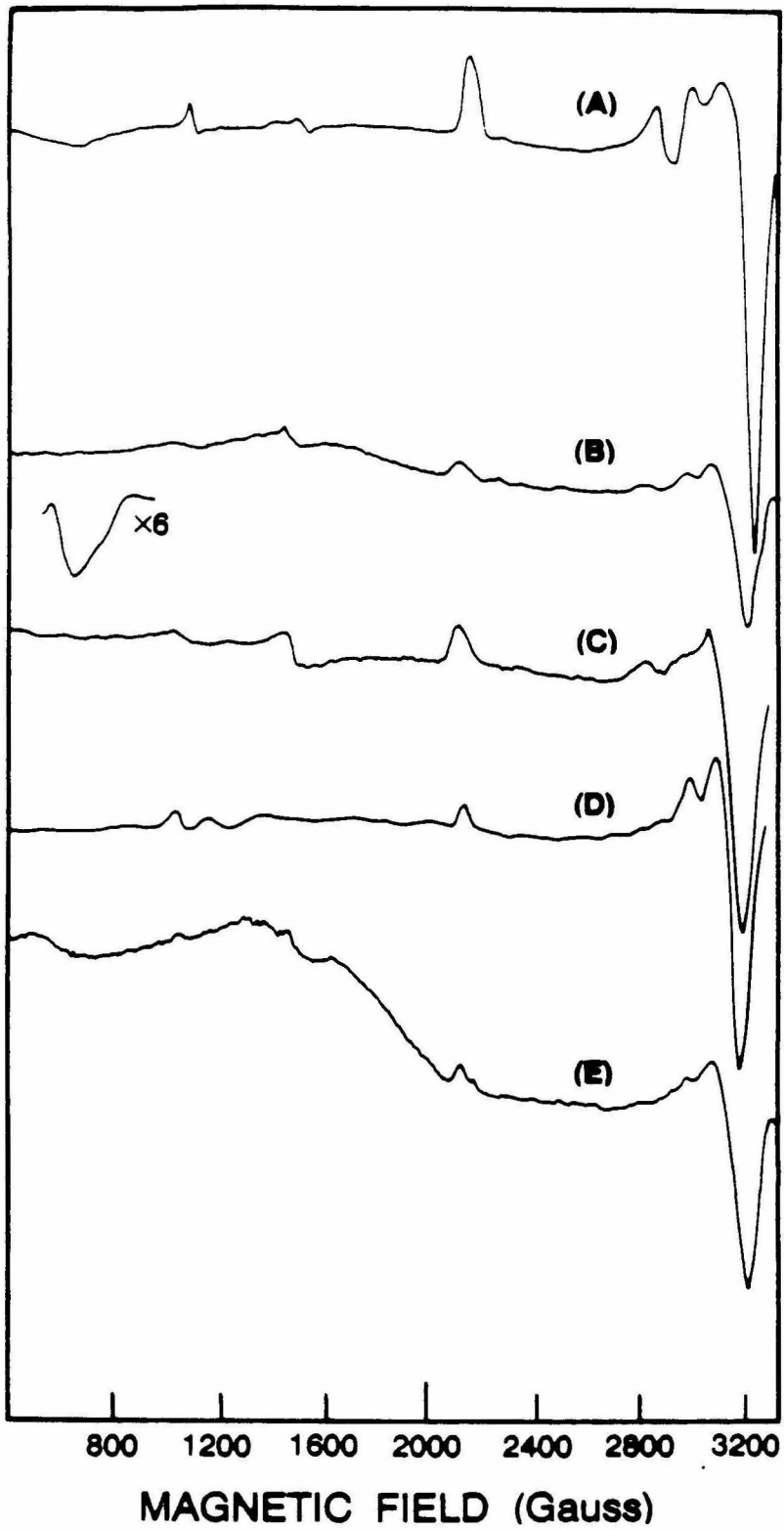
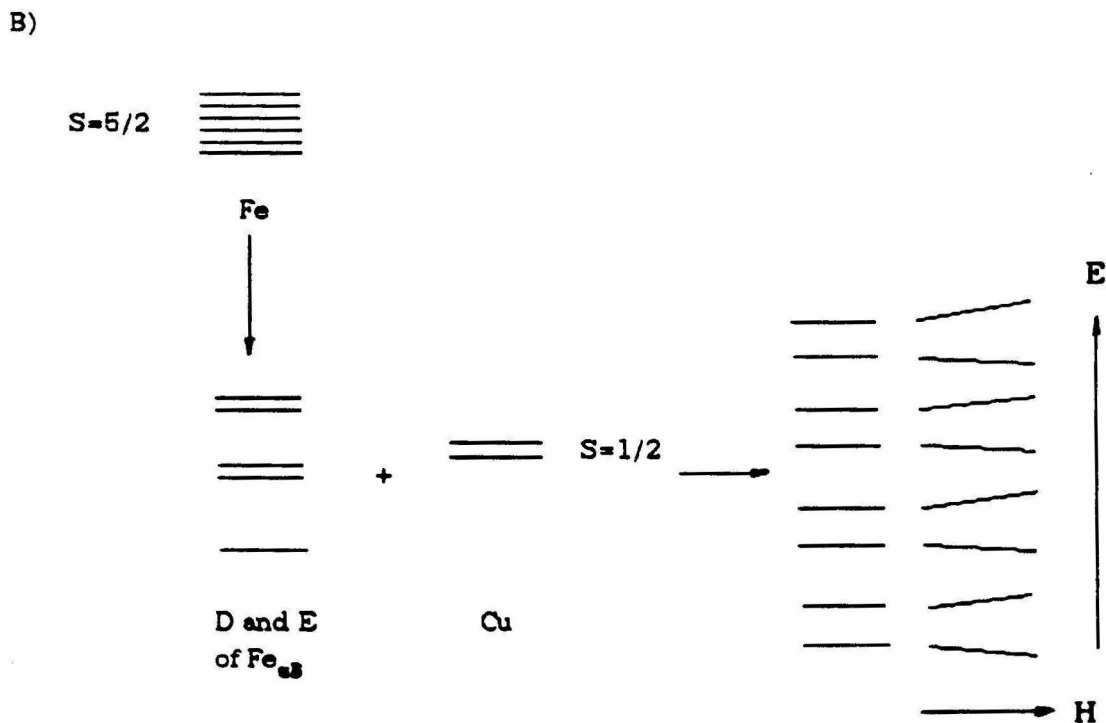
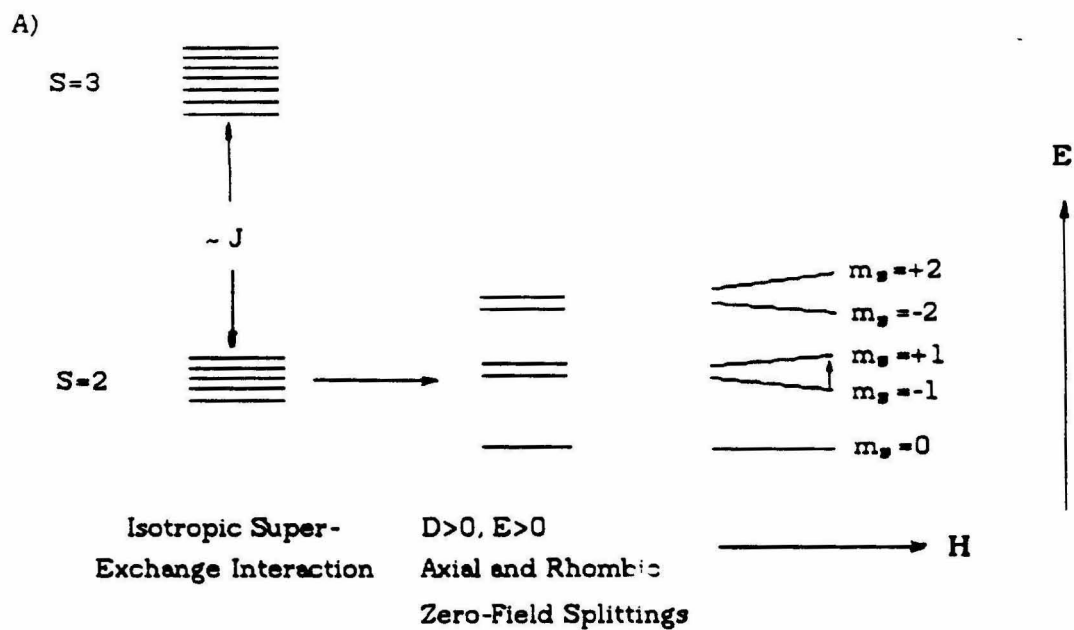


Fig. 3A displays, diagrammatically, the spin energy distribution for Cl^- -substituted dialyzed/oxygenated enzyme.

If Cl^- mediates a strong isotropic super exchange coupling between Fe_{a3} and Cu_{B} , then the J value is expected to be large relative to the zero field splitting. It would, then, be possible to observe a transition from an $S=2$ state only, thus giving rise to a $g=12$ signal which is due to an $m_s=-1$ to $m_s=+1$ transition. Br^- -substituted dialyzed/oxygenated enzyme may belong to this class. However, transition is not allowed for the regular EPR range. F^- (and OH^-) largely eliminates the exchange interaction between Cu_{B} and Fe_{a3} as shown in Fig. 3, and multiple EPR resonances are expected. No NO-induced EPR signal was observed for the dialyzed oxygenated oxidase (data not shown). D value is axial zero-field splitting. OH^- , F^- , Cl^- , and Br^- have different D values. The optical Soret band peak blue shifted as the substitute ion's D value increased, and the peak distribution is consistent with Fe_{a3} absorption maximum. Br^- has higher polarizability, so Soret band dipole strength D_{ab} (integrating area under an absorption band) of Br^- substituted oxidase is much bigger than other forms of oxidase.

Fig. 3 The energy level diagrams for the $\text{Fe}_{\text{A}3}\text{-Cu}_{\text{B}}$ center in (A) Cl^- or Br^- substituted dialyzed/oxygenated enzyme. (B) F^- or OH^- substituted dialyzed/oxygenated enzyme.



The results from optical and EPR spectra suggest that some functional groups were depleted during dialysis and that this group could be an ion such as Cl^- or Br^- . Qualitative analysis further suggests that this ion must be Cl^- . After dialyzed oxidase is reoxidized, another ligand L binds to $\text{Fe}_{\text{a}3}(\text{III})$. At the beginning of reoxidization, $\text{Fe}_{\text{a}3}\text{-L}$ is in a low-spin state, but it gradually becomes high-spin during incubation. This conclusion is supported by the absorption peak blue shift observed during incubation.

It is well known that reaction of resting oxidase with cyanide is a slow, heterogeneous process (Naaqui, et al., 1984). Table 2 shows rate constants for different conformations of cytochrome c oxidase reacting with cyanide. The dialyzed oxygenated oxidase behaved much like membranous oxidase in crystalline cytochrome c oxidase vesicles.

Fig. 4 shows the influence of Cl^- concentration on kinetics of cyanide binding to dialyzed/oxygenated oxidase. The reaction of fresh dialyzed/oxygenated oxidase with cyanide is fast and homogeneous. Incubation lowers the rate constant, although the reaction remains homogeneous. Addition of Cl^- to dialyzed/oxygenated oxidase before the addition of cyanide slows down the reaction, and the reaction becomes heterogeneous. Thus Cl^- has an important role in inhibition of cyanide binding; possibly, Cl^- is the ligand which is displaced by

Table 2: Rate Constants for Reaction of Cytochrome c Oxidase with Cyanide

Species	k^I ($M^{-1} s^{-1}$) ^d	k^{eff} (s^{-1}) ^e
Resting ^a (H. B.)		5.5×10^{-5b}
Oxygenated ^a (H. B.)	2.0	
Membranous ^{a,c}		2.3×10^{-3}
Membramous ^{a,c}	4.0	
Dialyzed oxygenated (1 hr. incubation)	5.0	
Dialyzed oxygenated (30 hr. incubation)	0.25	

a: Palmer, et al., 1976.

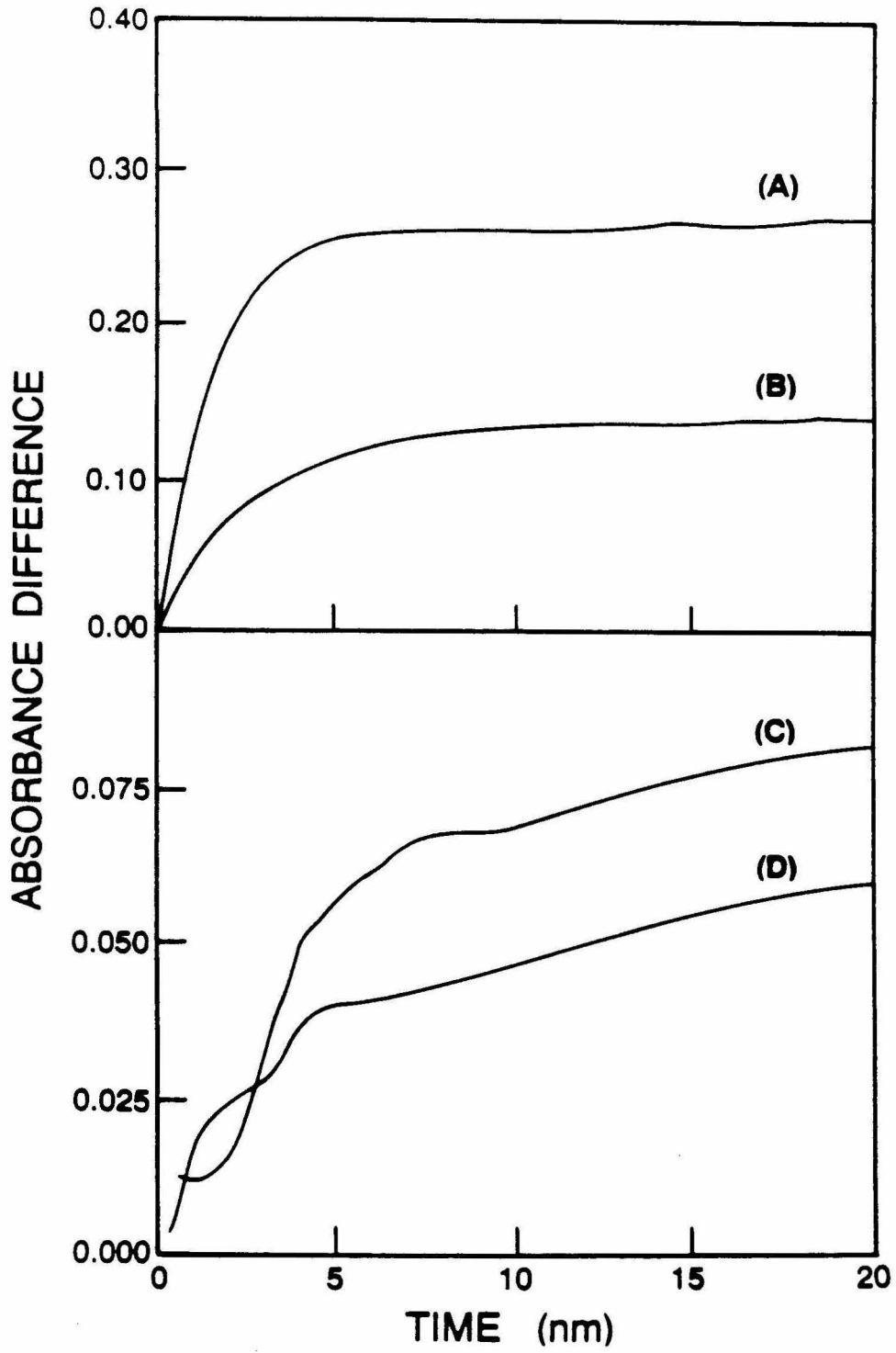
b: The dominant phase (75%)

c: Crystalline cytochrome c oxidase

d: Second-order rate constant

e: Effective first-order rate constant

Fig. 4 Influence of Cl^- concentration on the kinetics of cyanide binding to dialyzed/oxygenated oxidase. The reaction was initiated by addition of 50 μl freshly prepared 5 mM KCN to 100 μl dialyzed/oxygenated oxidase, and the binding of cyanide was monitored by following the absorption at 432 nm. Chloride concentrations: (A) 0 mM, (B) 0.04 mM, (C) 1 mM, (D) 2.5 mM. Conditions: enzyme concentration is 67 μM (pH=7.00, 50 mM MOPS buffer solution containing 0.5% Tween-20); temperature is 20 $^\circ\text{C}$.



in cyanide inhibition of resting oxidase.

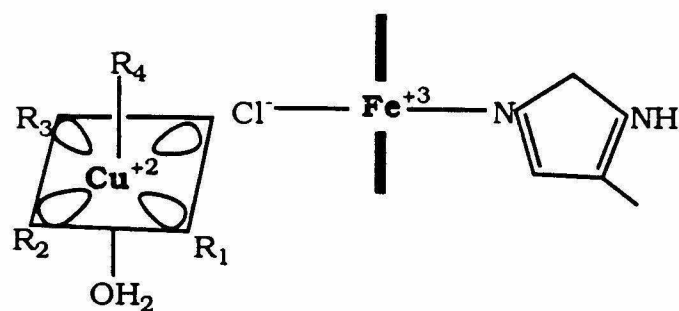
CONCLUSIONS:

The lack of EPR signals from the $\text{Fe}_{\text{a}3}\text{-Cu}_{\text{B}}$ site in the resting conformation is the result of a strong antiferromagnetic exchange interaction between the high-spin $\text{Fe}_{\text{a}3}(\text{S}=5/2)$ and $\text{Cu}_{\text{B}}(\text{S}=1/2)$, mediated by a bridging ligand. This bridging ligand in the resting form is Cl^- . Cl^- has been depleted by dialysis of reduced oxidase. After complete reduction of cytochrome \underline{c} oxidase and depletion of Cl^- , $\text{Fe}_{\text{a}3}(\text{II})$ could be only five-coordinate. Once oxidase is reoxidized, $\text{Fe}_{\text{a}3}(\text{III})$ is in a low-spin state and has six ligands. The 6th ligand could be OH^- , and can be substituted by F^- or Br^- . Low-spin $\text{Fe}_{\text{a}3}\text{-OH}$ will gradually relax to high-spin $\text{Fe}_{\text{a}3}\text{-OH}$. Changes in the optical spectrum reflect this electron spin relaxation. Cl^- is a weak-field ligand of Cu_{B} and weakly bound to $\text{Fe}_{\text{a}3}$, so NO can reorient Cu_{B} 's ligand field, decoupling Cu_{B} from $\text{Fe}_{\text{a}3}$. OH^- , however, is a strong-field ligand of $\text{Fe}_{\text{a}3}$ and, although NO can bind to Cu_{B} , it is not strong enough to reorient Cu_{B} 's ligand field and uncouple Cu_{B} from $\text{Fe}_{\text{a}3}$. Fig. 5 shows the proposed sequence of conformations.

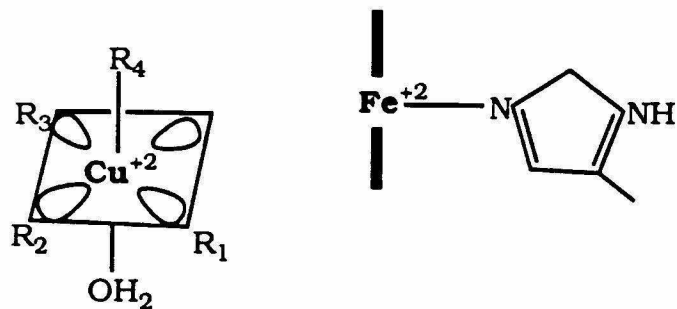
Fig. 5 Proposed sequence of conformations upon reduction, dialysis, reoxidation and incubation of oxidase.

Comformations

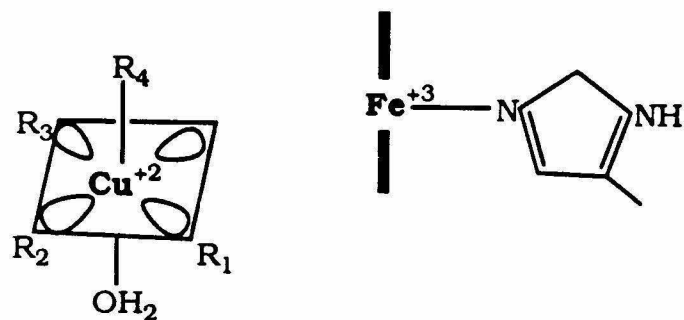
Enzyme



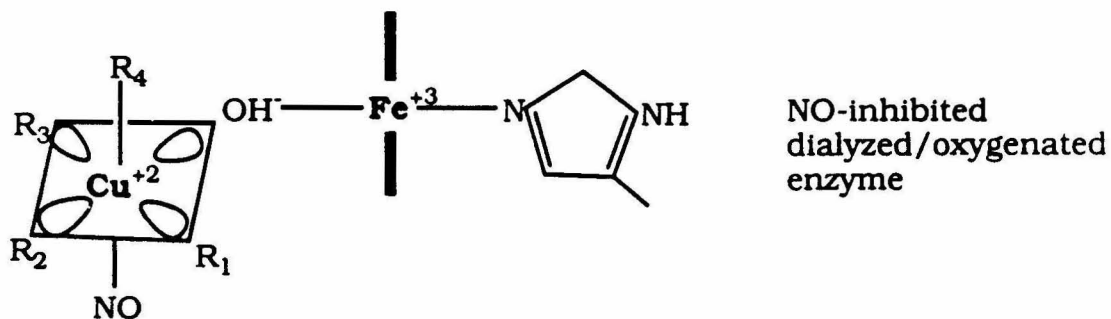
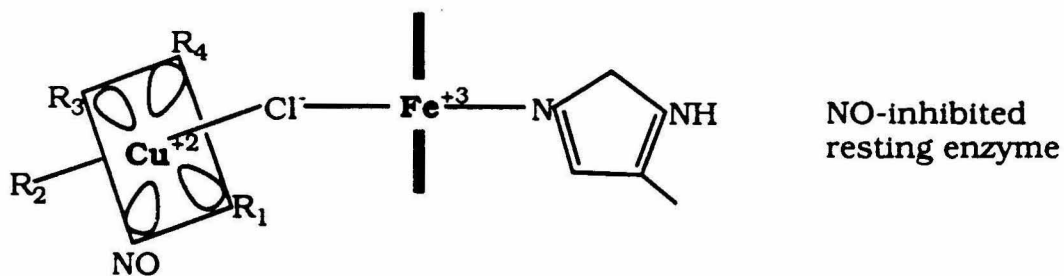
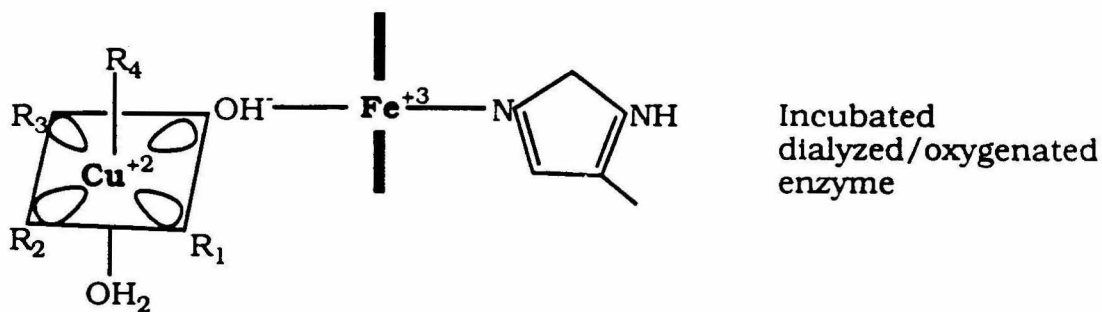
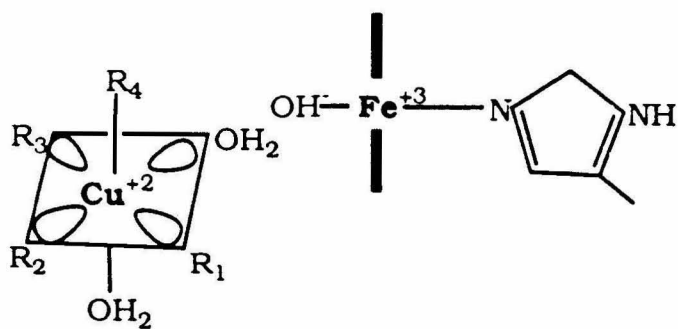
Resting



Reduced/dialyzed



Pulsed



REFERENCES:

- Aasa, R.; Albracht, S. P. J.; Falk, K. E.; Lanne, B. & Vanngard, T., (1976) *Biochim. Biophys. Acta*, **442**, 260.
- Blair, D. F.; Bocian, D. F.; Babcock, G. T. & Chan, S. I., (1982) *Biochemistry*, **21**, 6928.
- Blair, D. F.; Martin, C. T.; Gelles, J.; Wang, H.; Brudvig, G. W.; Stevens, T. H. & Chan, S. I., (1983) *Chemica scripta*, **21**, 43.
- Brudvig, G.; Morse, R. & Chan, S. I., (1986) *J. Magn. Reson.*, **67**, 198-201.
- Cline, J.; Reinhammar, B.; Jensen, P.; Venters, R. & Hoffman, B. M., (1983) *J. Biol. Chem.*, **258**, 5124.
- Falk, K. E.; Vanngard, T. & Angstrom, J., (1977) *FEBS Lett.*, **75**, 23.
- Frey, T.; Chan, S. H. P. & Schatz, G., (1978) *J. Bio. Chem.*, **253**, 4389.
- Gelles, J.; Blair, D. F. & Chan, S. I., (1986) *Biochim. Biophys. Acta*, **853**, 205.
- Hartzell, C. R. & Beinert, H., (1974) *Biochim. Biophys. Acta* , **368**, 318.
- Kent, T. A.; Young, L. J.; Palmer, G.; Fee, J. A. & Munck, E., (1983) *J. Biol. Chem.*, **258**, 8543.

- Lemberg, M. R. & Stanbury, J., (1967) *Biochim. Biophys. Acta* , **143**, 37.
- Naaqui, A.; Kumar, C.; Ching, Y.; Powers, L. & Chance, B., (1984) *Biochemistry* , **23**, 6222.
- Palmer, G.; Babcock, G. T. & Vickery, L. E., (1976) *Proc. Natl. Acad. Sci. USA*, **73**, 2206.
- Powers, L.; Chance, B.; Ching, Y. & Angiolillo, P., (1981) *Biophys. J.* **34**, 465.
- Scott, R. A.; Li, P. M. & Chan, S. I., (1988) *Cytochrome Oxidase Structure, Function, and Physiopathology*, Annals of the New York Academy of Science, **550**, 53-58.
- Stevens, T. H.; Brudvig, G. W.; Bocian, D. F. & Chan, S. I., (1979) *Proc. Natl. Acad. USA* , **76**, 3320.
- Stevens, T. H. & Chan, S. I., (1981) *J. Biol. Chem.*, **256**, 1069.
- Thomson, A. J.; Brittain, T.; Greenwood, C. & Springill, J. P., (1977) *Biochem. J.*, **165**, 327.
- Wikstrom, M.; Krab, K. & Saraste, M., (1981) *Cytochrome Oxidase: A Synthesis* , Academic Press.
- Witt, S. N., Ph D. Thesis, Caltech, (1988).

CHAPTER VI:
CONCLUSIONS

The primary focus of this study has centered on the examination of the structural and thermodynamic properties of the Cu_A site of mammalian cytochrome c oxidase.

The accurate analysis of the Cu, Fe, Zn and Mg contents in cytochrome c oxidase confirms that Cu_A is only a single copper center, which supports the Chan model of redox linkage based on Cu_A structure. Instead of the previous hypothesis that Cu_A and Cu_X form a binuclear copper center, we found that Cu_X plays a structural role in the dimerization of the enzyme: it serves as a bridge between the two subunit III polypeptides within the dimer.

*p*HMB-modification of cytochrome c oxidase and heat-treatment of the oxidase have been shown to alter the dioxygen reduction and proton pumping activities of cytochrome c oxidase. The intrinsic reduction potentials and the midpoint reduction potential of the Cu_A site in these modified forms of cytochrome c oxidases have been measured under various conditions. The results show that the intrinsic reduction potential decreases by almost 150 mV upon *p*HMB modification, whereas an increase of 100 mV is observed upon heat treatment. In addition, the redox interaction between Cu_A and the remaining metal centers are perturbed upon Cu_A modification.

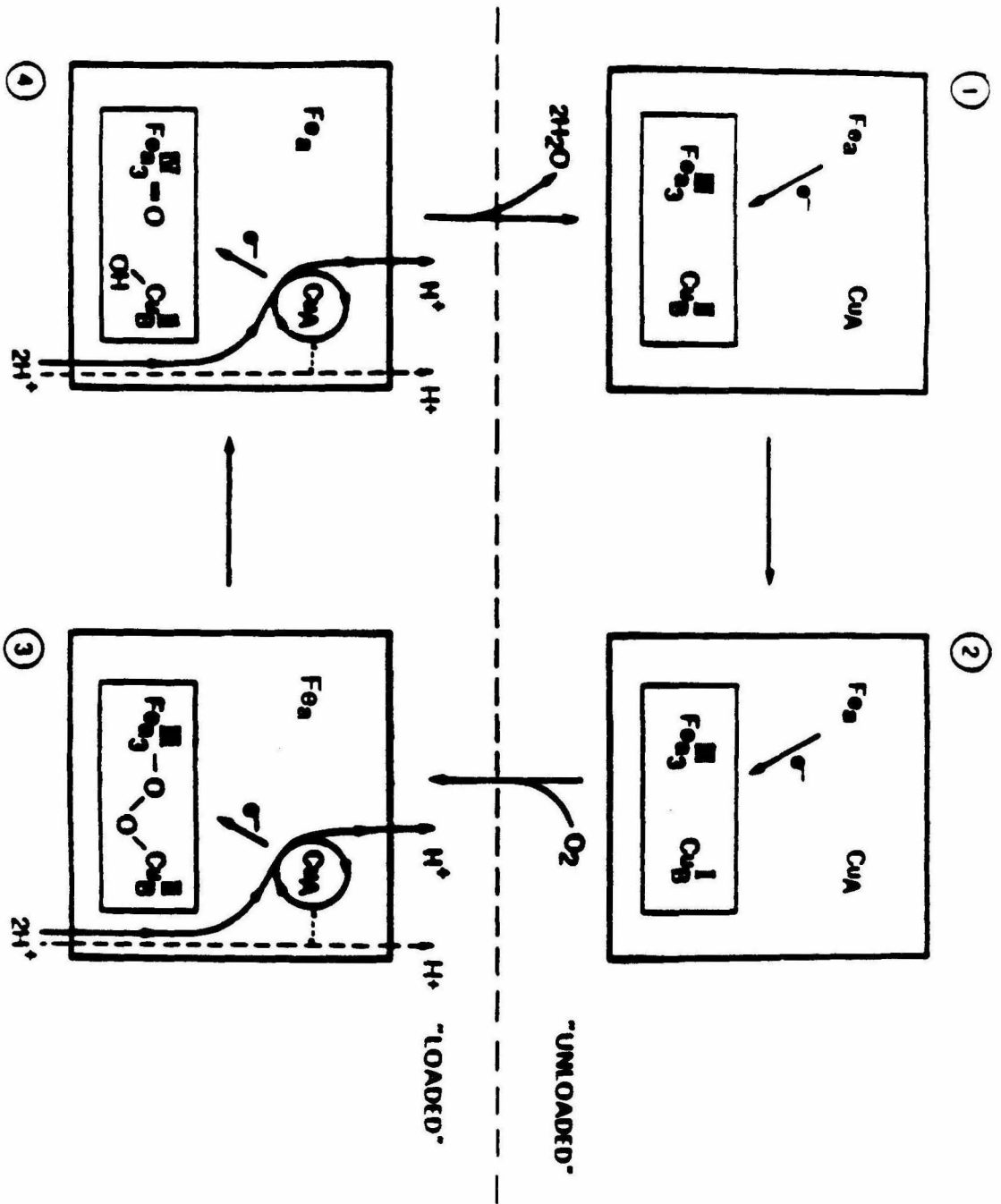
In native oxidase, the reduction potential of Cu_A is somewhat higher than that of cytochrome \underline{c}_1 and electron transfer from ferrocycytochrome \underline{c} to Cu_A is thermodynamically allowed and kinetically facile. This situation obtains from the heat-treated cytochrome oxidase as well, since the Cu_A reduction potential of the type 1 Cu_A site is significantly higher than that in the native enzyme. The almost identical dioxygen reduction activity between the native and heat-treated oxidase most certainly reflects this electron transfer competence of the modified Cu_A site. On the other hand, the redox potential of the type 2 Cu_A site is 150 mV lower than that of the native Cu_A site, direct electron transfer from ferrocycytochrome \underline{c} to cytochrome \underline{a} seems more likely to be the electron input pathway. The significantly lower dioxygen activity either reflects the slower electron input from ferrocycytochrome \underline{c} to cytochrome \underline{a} compared to ferrocycytochrome \underline{c} to Cu_A electron transfer, or a more sluggish downhill electron transfer to the binuclear center from cytochrome \underline{a} compared to Cu_A .

Based on the model of redox-linkage proposed by this laboratory, neither the pHMB-modified nor the heat-treated oxidase is expected to sustain proton pumping activity. In the case of the pHMB-modified oxidase, electron transfer from ferrocycytochrome \underline{c} through Cu_A is bypassed. In the case of the heat-treated enzyme, the Cu_A site has lost the ability to undergo a ligand exchange or structural arrangement upon electron reduction.

DCCD-modification and subunit III-depletion of cytochrome c oxidase decrease the observed H⁺/e⁻ stoichiometry in proton pumping to 0.5 during enzyme turnover under coupled conditions. DCCD-modification distorts the Cu_A ligand structure, while subunit III-depletion destabilizes the Cu_A structure leading ultimately to the displacement of one of the cysteine ligands. The intrinsic reduction potential of Cu_A is not significantly altered in the two modified oxidases. However, the redox interaction between Cu_A and cytochrome a becomes dramatically different. These results reinforce the proposal that Cu_A structure is locally unstable and that subunit III stabilized the tense ligand structure of the site. Subunit III regulates, through redox changes at the Cu_A site, the allosteric interaction between various parts of the protein structure, particularly subunits I and II, to accomplish free energy transduction. Subunit III plays an important allosteric role in communicating redox changes at the Cu_A site to the proton translocating elements of the enzyme.

Figure 1 illustrates a completed turnover cycle of cytochrome c oxidase, which involved the intramolecular electron transfer, dioxygen reduction, direct redox-linked proton pumping and indirect redox-linked proton pumping events. Electron transfer from heme a to the dioxygen unloaded binuclear site is slow, dioxygen binding to the binuclear center, and the subsequent reduction dramatically increasing the driving force for electron transfer and also causing a

Fig. 1 A proposal of a completed turnover cycle of cytochrome c oxidase.



protein conformational change. The conformational change switches electron transfer now to pass through the Cu_A center; reduction of Cu_A center results in one proton being pumped from the matrix site. At the same time, part of the energy released by reduction of Cu_A was used to trigger the opening of the other proton translocation element(s). The communication between Cu_A and the other proton pumping element(s) was regulated by subunit III.

APPENDIX

DERIVATION OF MULTI INTERACTION MODEL

A) If there are only three interaction sites:

E: applied potential,

E_1 : upper asymptotic potential of site 1 (under observation)

E_2 : upper asymptotic potential of site 2

E_3 : upper asymptotic potential of site 3

ΔE_{12} : interaction potential between site 1 and site 2

ΔE_{13} : interaction potential between site 1 and site 2

ΔE_{23} : interaction potential between site 2 and site 3

Nernst equation: $E = E_i^0 + \left(\frac{RT}{nF}\right) \cdot \ln\left(\frac{O_i}{R_i}\right)$ Let $c = nF/RT$

so $\frac{O_i}{R_i} = \exp[c \cdot (E - E_i^0)]$

There are in total 8 redox states:

$P_1 = O_1O_2O_3$

$P_2 = R_1O_2O_3$

$P_3 = O_1R_2O_3$

$P_4 = O_1O_2R_3$

$P_5 = R_1R_2O_3$

$P_6 = O_1R_2R_3$

$P_7 = R_1O_2R_3$

$P_8 = R_1R_2R_3$

$P_1/P_2 = \exp[c \cdot (E - E_1)]$

$P_1/P_3 = \exp[c \cdot (E - E_2)]$

$P_1/P_4 = \exp[c \cdot (E - E_3)]$

$P_1/P_5 = (P_1/P_2) \cdot (P_2/P_5) = \exp[c \cdot (E - E_1)] \cdot \exp[c \cdot (E - E_2 + \Delta E_{12})]$

$P_1/P_6 = (P_1/P_3) \cdot (P_3/P_6) = \exp[c \cdot (E - E_2)] \cdot \exp[c \cdot (E - E_3 + \Delta E_{23})]$

$$P_1/P_7 = (P_1/P_4) \cdot (P_4/P_7) = \exp[c^*(E-E_3)] \cdot \exp[c^*(E-E_1+\Delta E_{13})]$$

$$\begin{aligned} P_1/P_8 &= (P_1/P_4) \cdot (P_4/P_7) \cdot (P_7/P_8) \\ &= \exp[c^*(E-E_3)] \cdot \exp[c^*(E-E_1+\Delta E_{13})] \cdot \exp[c^*(E-E_2+\Delta E_{12}+\Delta E_{23})] \end{aligned}$$

$$P_1 = P_1$$

$$P_2 = P_1 \cdot \exp[c^*(E_1-E)]$$

$$P_3 = P_1 \cdot \exp[c^*(E_2-E)]$$

$$P_4 = P_1 \cdot \exp[c^*(E_3-E)]$$

$$P_5 = P_1 \cdot \exp[c^*(E_1+E_2-2E-\Delta E_{12})]$$

$$P_6 = P_1 \cdot \exp[c^*(E_2+E_3-2E-\Delta E_{23})]$$

$$P_7 = P_1 \cdot \exp[c^*(E_3+E_1-2E-\Delta E_{13})]$$

$$P_8 = P_1 \cdot \exp[c^*(E_1+E_2+E_3-3E-\Delta E_{12}-\Delta E_{13}-\Delta E_{23})]$$

$$\sum_{n=1}^8 P_n = P_1 \{ 1 + \exp[c^*(E_1-E)] + \exp[c^*(E_2-E)] + \exp[c^*(E_3-E)]$$

$$+ \exp[c^*(E_1+E_2-2E-\Delta E_{12})] + \exp[c^*(E_2+E_3-2E-\Delta E_{23})]$$

$$+ \exp[c^*(E_1+E_3-2E-\Delta E_{13})] + \exp[c^*(E_1+E_2+E_3-3E-\Delta E_{12}-\Delta E_{13}-\Delta E_{23})] \}$$

$$\text{site 1 oxidized: } (P_1+P_3+P_4+P_6)/\sum P_n$$

$$\text{site 1 reduced: } (P_2+P_5+P_7+P_8)/\sum P_n$$

$$\text{site 1 ox/red} = (P_1+P_3+P_4+P_6)/(P_2+P_5+P_7+P_8)$$

$$= \{ 1 + \exp[c^*(E_2-E)] + \exp[c^*(E_3-E)] + \exp[c^*(E_2+E_3-2E-\Delta E_{23})] \} /$$

$$\{ \exp[c^*(E_1-E)] + \exp[c^*(E_1+E_2-2E-\Delta E_{12})] + \exp[c^*(E_3+E_1-2E-\Delta E_{13})] + \exp[c^*(E_1+E_2+E_3-3E-\Delta E_{12}-\Delta E_{13}-\Delta E_{23})] \}$$

$$\text{Log}\left(\frac{\text{ox}}{\text{red}}\right)_1 = \frac{c^*(E-E_1)}{2.303} + \text{Log}\{ 1 + \exp[c^*(E_2-E)] + \exp[c^*(E_3-E)] + \exp[c^*(E_2+E_3-2E-\Delta E_{23})] \}$$

$$-\text{Log}\{1+\exp[c^*(E_2-E-\Delta E_{12})]+\exp[c^*(E_3-E-\Delta E_{13})]+\exp[c^*(E_2+E_3-2E-\Delta E_{12}-\Delta E_{13}-\Delta E_{23})]\}$$

Simplification:

$$\text{if } E_2=E_3=E_i$$

$$\text{Log}\left(\frac{\text{ox}}{\text{red}}\right)_1 = \frac{c^*(E-E_1)}{2.303} + \text{Log}\{1+2\exp[c^*(E_i-E)]+\exp[c^*(2E_i-2E-\Delta E_{23})]\}$$

$$-\text{Log}\{1+\exp[c^*(E_i-E-\Delta E_{12})]+\exp[c^*(E_i-E-\Delta E_{13})]+\exp[c^*(2E_i-2E-\Delta E_{12}-\Delta E_{13}-\Delta E_{23})]\}$$

Check:

$$\text{if } \Delta E_{12}=\Delta E_{13}=\Delta E_{23}=0$$

$$\text{Log}\left(\frac{\text{ox}}{\text{red}}\right)_1 = \frac{c^*(E-E_1)}{2.303} \quad \text{back to Nernst equation}$$

B) If there are 4 interaction centers, 16 redox states will occur:

$$P_1=O_1O_2O_3O_4$$

$$P_2=R_1O_2O_3O_4$$

$$P_3=O_1R_2O_3O_4$$

$$P_4=O_1O_2R_3O_4$$

$$P_5=O_1O_2O_3R_4$$

$$P_6=R_1O_2R_3O_4$$

$$P_7=R_1R_2O_3O_4$$

$$P_8=O_1R_2O_3R_4$$

$$P_9=O_1O_2R_3R_4$$

$$P_{10}=O_1R_2R_3O_4$$

$$P_{11}=R_1O_2O_3R_4$$

$$P_{12}=R_1R_2R_3O_4$$

$$P_{13}=R_1R_2O_3R_4$$

$$P_{14}=O_1R_2R_3R_4$$

$$P_{15}=R_1O_2R_3R_4$$

$$P_{16}=R_1R_2R_3R_4$$

$$P_1/P_2 = \exp[c^*(E-E_1)]$$

$$P_1/P_3 = \exp[c^*(E-E_2)]$$

$$P_1/P_4 = \exp[c^*(E-E_3)]$$

$$P_1/P_5 = \exp[c^*(E-E_4)]$$

$$P_1/P_6 = \exp[c^*(E-E_1)] * \exp[c^*(E-E_3-\Delta E_{13})]$$

$$P_1/P_7 = \exp[c^*(E-E_2)] * \exp[c^*(E-E_1-\Delta E_{12})]$$

$$P_1/P_8 = \exp[c^*(E-E_4)] * \exp[c^*(E-E_2-\Delta E_{24})]$$

$$P_1/P_9 = \exp[c^*(E-E_3)] * \exp[c^*(E-E_4-\Delta E_{34})]$$

$$P_1/P_{10} = \exp[c^*(E-E_2)] * \exp[c^*(E-E_3-\Delta E_{23})]$$

$$P_1/P_{11} = \exp[c^*(E-E_1)] * \exp[c^*(E-E_4-\Delta E_{14})]$$

$$P_1/P_{12} = \exp[c^*(E-E_1)] * \exp[c^*(E-E_3-\Delta E_{13})] * \exp[c^*(E-E_2-\Delta E_{12}-\Delta E_{23})]$$

$$P_1/P_{13} = \exp[c^*(E-E_2)] * \exp[c^*(E-E_1-\Delta E_{12})] * \exp[c^*(E-E_4-\Delta E_{14}-\Delta E_{24})]$$

$$P_1/P_{14} = \exp[c^*(E-E_4)] * \exp[c^*(E-E_2-\Delta E_{24})] * \exp[c^*(E-E_3-\Delta E_{23}-\Delta E_{34})]$$

$$P_1/P_{15} = \exp[c^*(E-E_3)] * \exp[c^*(E-E_4-\Delta E_{34})] * \exp[c^*(E-E_1-\Delta E_{13}-\Delta E_{14})]$$

$$P_1/P_{16} = \exp[c^*(E-E_3)] * \exp[c^*(E-E_4-\Delta E_{34})] * \exp[c^*(E-E_1-\Delta E_{13}-\Delta E_{14})] \\ * \exp[c^*(E-E_2-\Delta E_{12}-\Delta E_{23}-\Delta E_{24})]$$

$$\text{site 1 oxidized} \quad (P_1+P_3+P_4+P_5+P_8+P_9+P_{10}+P_{14}) / \sum_{n=1}^{16} P_n$$

$$\text{site 1 reduced} \quad (P_2+P_6+P_7+P_{11}+P_{12}+P_{13}+P_{15}+P_{16}) / \sum_{n=1}^{16} P_n$$

$$\text{Log}\left(\frac{\text{ox}}{\text{red}}\right)_1 = \frac{c^*(E-E_1)}{2.303} + \text{Log}\{1 + \exp[c^*(E_2-E)] + \exp[c^*(E_3-E)] + \exp[c^*(E_4-E)] \\ + \exp[c^*(E_2+E_4-2E-\Delta E_{24})] + \exp[c^*(E_3+E_4-2E-\Delta E_{34})] \\ + \exp[c^*(E_2+E_3-2E-\Delta E_{23})] + \exp[c^*(E_2+E_3+E_4-3E-\Delta E_{23}-\Delta E_{24})]\}$$

$$\begin{aligned}
& -\Delta E_{34})\} - \text{Log}\{1 + \exp[c^*(E_3 - E - \Delta E_{13})] + \exp[c^*(E_2 \\
& - E + \Delta E_{12})] + \exp[c^*(E_4 - E \\
& - \Delta E_{14})] + \exp[c^*(E_2 + E_3 - 2E - \Delta E_{12} - \Delta E_{13} - \Delta E_{23})] + \exp[c^*(E_2 + E_4 - 2E \\
& - \Delta E_{12} - \Delta E_{14} - \Delta E_{24})] + \exp[c^*(E_3 + E_4 - 2E - \Delta E_{13} - \Delta E_{14} - \Delta E_{34})] \\
& + \exp[c^*(E_2 + E_3 + E_4 - 3E - \Delta E_{12} - \Delta E_{13} - \Delta E_{14} - \Delta E_{23} - \Delta E_{24} - \Delta E_{34})]\}
\end{aligned}$$

C) General formula for i sites interacting with each other:

site 1:

$$\begin{aligned}
\text{Log}\left(\frac{\text{ox}}{\text{red}}\right)_1 &= \frac{c^*(E - E_1)}{2.303} + \text{Log}\left\{1 + \sum_{k=2}^i \exp[c^*(E_k - E)] \right. \\
&+ \sum_{k \geq 2}^i \sum_{j > k}^i \exp[c^*(E_k + E_j - 2E - \Delta E_{kj})] \\
&+ \left. \sum_{k \geq 2}^i \sum_{j > k}^i \sum_{l > j}^i \exp[c^*(E_k + E_j + E_l - 3E - \Delta E_{kj} - \Delta E_{jl} - \Delta E_{kl})] + \dots \right\} \\
&- \text{Log}\left\{1 + \sum_{k=2}^i \exp[c^*(E_k - E - \Delta E_{1k})] \right. \\
&+ \sum_{k \geq 2}^i \sum_{j > k}^i \exp[c^*(E_k + E_j - 2E - \Delta E_{1k} - \Delta E_{1j} - \Delta E_{jk})] \\
&+ \left. \sum_{k \geq 2}^i \sum_{j > k}^i \sum_{l > j}^i \exp[c^*(E_k + E_j + E_l - 3E - \sum_{m=1}^i \sum_{n > m}^i \Delta E_{mn})] + \dots \right\}
\end{aligned}$$